THIOREDOXIN-1 INHIBITION PROMOTES MLKL ACTIVATION:
BIOCHEMICAL INSIGHTS INTO A SUPPRESSOR OF
THE NECROPTOTIC PATHWAY

APPROVED BY SUPERVISORY COMMITTEE

Mentor: Zhigao Wang, Ph.D. _____

Chairperson: James Amatruda, M.D., Ph.D. _____

John Abrams, Ph.D. _____

Zhijian “James” Chen, Ph.D. _____

DEDICATION

This work is dedicated to my parents, Eduardo and Martha Reynoso, who through example, taught me that the road to success is predicated on sacrifice, hard work, and family.

THIOREDOXIN-1 INHIBITION PROMOTES MLKL ACTIVATION: BIOCHEMICAL INSIGHTS INTO A SUPPRESSOR OF THE NECROPTOTIC PATHWAY

by

EDUARDO REYNOSO

DISSERTATION

Presented to the Faculty of the Graduate School of Biomedical Sciences

The University of Texas Southwestern Medical Center at Dallas

In Partial Fulfillment of the Requirements

For the Degree of

DOCTOR OF PHILOSOPHY
GENETICS, DEVELOPMENT AND DISEASE

The University of Texas Southwestern Medical Center at Dallas

Dallas, Texas

August 2017

THIOREDOXIN-1 INHIBITION PROMOTES MLKL ACTIVATION:
BIOCHEMICAL INSIGHTS INTO A SUPPRESSOR OF
THE NECROPTOTIC PATHWAY

Eduardo Reynoso, Ph.D.

The University of Texas Southwestern Medical Center at Dallas, 2017

Supervising Professor: Zhigao Wang, Ph.D.

Necroptosis is an immunogenic caspase-independent cell death program. While mainly serving to defend against viral infection, dysregulated necroptotic signaling contributes to the pathology of a growing number of human diseases associated with inflammation, neurodegeneration, and ischemic injuries. Since its emergence, many key components of the mammalian necroptotic pathway have been discovered including RIP1/3 kinases and MLKL, which together, form the core of the necrosome complex. RIP3-dependent phosphorylation of MLKL promotes the formation of high molecular weight MLKL polymers that disrupt the integrity of the plasma membrane leading to cell death. However, the mechanistic details of MLKL polymerization and its precise function in executing necroptosis remain poorly understood. To gain insight into this process, the crosslinking property of the specific MLKL inhibitor Necrosulfonamide (NSA) was exploited as a strategy for identifying novel MLKL interacting proteins. Immunoprecipitation of NSA crosslinked MLKL complexes followed by mass spectrometric analysis revealed Thioredoxin-1, an essential cytosolic thiol oxidoreductase, to be a potential MLKL regulator. Based on its ability to reduce disulfide bonds on specific protein targets, it was hypothesized that Thioredoxin-1 actively maintains MLKL in a reduced monomeric state to suppress the occurrence of

spontaneous necroptosis. Therefore, genetic and pharmacological approaches were taken to perturb Thioredoxin-1 activity as a means for testing whether it would induce necroptosis in human cells. The data presented here demonstrates that inhibiting Thioreoxin-1 activity using the compound PX-12 promoted RIP3-dependent MLKL S358 phosphorylation, polymer formation, and caspase-independent necrotic cell death. Additionally, PX12-induced cell death was rescued by co-treating cells with NSA highlighting the involvement of MLKL in this cell death pathway. These results were corroborated by shRNA-mediated knockdown of Thioreoxin-1 mRNA. Altogether, these findings point to Thioredoxin-1 as a critical regulator of MLKL activity and necroptosis in human cells.

Table of Contents

PRIOR PUBLICATIONS

Gabriel Pineda, Zhouxin Shen, Claudio Ponte de Albuquerque, **Eduardo Reynoso**, Jeffrey Chen, Chi-Chiang Tu, Wingchung Tang, Steve Briggs, Huilin Zhou, Jean Y. J. Wang. (2015). Proteomics Studies of the Interactome of RNA Polymerase II C-Terminal Repeated Domain. *BMC Research Notes*. 8: 616.

Shuzhen Liu, Hua Liu, Andrea Johnston, Sarah Hanna-Addams, **Eduardo Reynoso**, Zhigao Wang. (2017). MLKL forms disulfide bond-dependent amyloid-like polymers to induce necroptosis. *PNAS* (In Revision).

Eduardo Reynoso, Hua Liu, Lin Li, Anthony L. Yuan, She Chen, and Zhigao Wang. (2017). Thioredoxin-1 negatively regulates MLKL polymerization and necroptosis by maintaining MLKL in a reduced state. *Journal of Biological Chemistry* (In Revision)

Table of Figures

Chapter 1. Introduction

Chapter 2. Thioredoxin-1 negatively regulates necroptosis by maintaining MLKL in a reduced inactive state

Chapter 3. MLKL membrane association and lysosome rupture

List of Definitions

Receptor interacting protein kinase 1 (RIP1)

Receptor interacting protein kinase 3 (RIP3)

Mixed lineage kinase domain-like protein (MLKL)

Necrosulfonamide (NSA)

Thioredoxin-1 (Trx1)

Cellular inhibitors of apoptosis (cIAPs)

TNF receptor 1 (TNFR1)

TNF-related apoptosis-inducing ligand receptor 1/2 (TRAILR1/2)

Fas ligand receptor (FasL)

Damage-associated molecular patterns (DAMPs)

High mobility group box 1 protein (HMGB1)

Cytokine response modifier A (CrmA)

Tumor necrosis factor receptor type 1-associated death domain protein (TRADD)

Z-DNA binding protein 1 (ZBP1)

Toll-like receptors 3 and 4 (TLR3/4)

FAS-associated death domain protein (FADD)

TNF receptor-associated factor 2 and 5 (TRAF2/5)

Carboxyl-terminal hydrolase (CYLD)

Death-inducing signaling complex (DISC)

Receptor homotypic interaction motif (RHIM)

TIR domain-containing adapter-inducing interferon-β (TRIF)

4-helix bundle domain (4HBD)

Phosphatidylinositol phospholipids (PIPs)

Dithiothreitol (DTT)

Beta-mercaptoethanol (βME)

Thioredoxin reductase-1 (TrxR1)

t-butyl hydroxide (TBH)

Serine/threonine protein phosphatase 5 (PGAM5)

Dynamin-like protein 1 (Drp1)

Butylated hydroxyanisole (BHA)

N-acetylcysteine (NAC)

Doxycycline (Dox)

MLKL N-terminal domain (NTD)

Semi-denaturing detergent agarose gel electrophoresis (SDD-AGE)

Apoptosis signal-regulating kinase 1 (ASK1)

Carbonyl cyanide m-chlorophenylhydrazone (CCCP)

Cathepsin L (CTSL)

Hydrophobic interacting column (HIC)

Necrostatin-1 (Nec-1)

Herpes Simplex Virus types 1 and 2 (HSV-1/2)

Influenza A Virus (IAV)

Chapter 1. Introduction

Crosstalk between apoptosis and necroptosis

Cell death plays a vital role in a variety of biological processes including embryogenesis, tissue homeostasis, wound healing, elimination of self-reactive immune cells, aging, and therefore is essential for life [1-4]. Apoptosis, for instance, is responsible for the death of billions of cells in the average human adult each day, and remains the best characterized cell death program to date [5]. Biochemical studies of apoptotic extrinsic and intrinsic pathways led to the identification of key signaling molecules such as death receptors (i.e. TNFR1/2, TRAILR1/2, FasL), Bcl-2 family members, cytochrome c, Apaf-1, and caspases, which are now used as reliable biomarkers in countless experimental models [6-10]. However, over the past several years, researchers have made significant inroads in uncovering alternative cell death modalities that are relevant to human health, particularly those that are caspase-independent. One of these forms of cell death is necroptosis. Necroptosis is a regulated form of necrosis that is involved in antiviral defense, but also contributes to a broad array of human pathological conditions [11, 12]. The emergence of necroptosis has prompted intense research efforts towards delineating molecular mechanism(s) that regulate mammalian necroptotic signaling pathways and understanding its role in disease. Thus, the thesis work presented here is aimed at providing insights into novel regulators of necroptosis and building a stronger foundation for future investigations into this cell death program.

The term “necroptosis” was coined to describe a type of cell death that shares characteristics of both necrosis and apoptosis [13]. Necroptosis morphologically resembles necrosis, whereby cells become swollen and lose the integrity of their plasma membranes [14]. This is in stark contrast to apoptosis in which cells condense, their DNA becomes fragmented, and the plasma membrane exhibits blebbing while maintaining its integrity [15]. Until recently, all forms of necrotic cell death were considered to be unregulated or passive, meaning they did not require energy or cell signaling, and were mainly caused by mechanical or physiochemical insults. However, seminal studies revealed that certain mammalian cells, such as murine L929 fibrosarcoma cells, undergo a necrotic-like death in response to TNFα, the same cytokine that triggers apoptosis [16]. Importantly, chemical inhibition of caspases (e.g. z-VAD-fmk) and in turn apoptosis, did not affect the outcome; in fact, cells became 1,000 times more sensitive to TNFα indicating that necrotic cell death is exacerbated under conditions when caspase activity is blocked [16]. This led to the realization that regulated forms of necrosis existed, and were driven by genetically hardwired programs in the cell. Furthermore, since apoptotic stimuli antagonized necrotic cell death, it was conceived that apoptosis and necroptosis shared significant crosstalk between their signaling pathways, hence “optosis” was placed in the ladder part of the term “necroptosis” [17].

Given the differences in morphology, cell death modes are also classified according to their immunogenicity. Apoptosis is considered non-immunogenic because apoptotic

cells neatly package their cellular contents into smaller apoptotic bodies that are quickly engulfed by phagocytes, and therefore does not elicit an immune response [18]. In contrast, necroptotic cells lose the integrity of their plasma membrane resulting in the release of damage-associated molecular patterns (DAMPs) into the surrounding environment [19]. These molecules serve as “alarmins” to signal cells of the innate immune system to the site of cell death. Ultimately, this causes an inflammatory response that can either be beneficial or detrimental depending on the context by which necroptosis was induced.

The role of necroptosis in antiviral defense

Until recently, the physiological role of necroptosis was unclear. Perplexingly, necroptosis was shown to be dispensable for embryogenesis and postnatal development, suggesting that necroptosis is silent under normal conditions [20, 21]. This sparked the hypothesis that necroptosis serves as an alternative “back-up” mechanism to apoptosis, that is only activated by a specific subset of death stimuli [22]. Since then, accumulating evidence has pointed to necroptosis as being a highly critical cell death mechanism for clearing organisms of viral infections [23]. Early experiments in murine cells revealed that necroptosis is stimulated by certain viruses. For example, cytokine response modifier A (CrmA), a serpin-like caspase inhibitor derived from Cowpox virus, sensitized murine L929 cells to TNFα *in vitro* [16]. This discovery corroborated similar findings using chemical caspase inhibitors [16]. More recently,

Influenza A virus (IAV) and Herpes Simplex Virus types 1 and 2 (HSV-1/2) have been added to the growing list of necroptosis-stimulating viruses [24, 25].

Interestingly, all three of these viruses trigger necroptosis in different ways. Cowpox virus and related Vaccinia virus, encoding caspase-inhibiting molecules CrmA and B13R, respectively, steer cell death signals toward pathways that favor necroptosis [26]. For IAV, elements found within specific viral RNA molecules activate a main component of the mammalian necroptotic pathway known as Z-DNA binding protein 1 (ZBP1) [25]. Genetic ablation of ZBP1 blocks cells from undergoing viral-induced necroptosis in murine and human cell lines, and causes mice to succumb to viral infection which die shortly after inoculation [25]. In general, genetically ablating core necroptotic machinery disables animals from fighting viral infection as viruses continue to propagate unfettered until overwhelming their systems [24, 25]. HSV-1/2 controls necroptotic outcomes by binding to receptor-interacting protein kinase 1 (RIP1), a serine/threonine kinase that serves as a major hub for various signaling pathways including NFκB signaling, apoptosis, and necroptosis [27, 28]. Altogether, researchers hypothesize that animals evolved necroptosis in response to selection pressures exerted by viral infections, although it remains unclear as to why some mammals express necroptotic signaling components while others do not [29].

TNFα-induced necroptotic signaling pathway

Most of our understanding of the necroptotic molecular machinery has come about

through studies of the TNFα/TNFR1 signaling pathway, although other death receptors and Toll-like receptors 3 and 4 (TLR3/4) are also involved in the necroptotic signaling [22]. In practice, *in vitro* induction of necroptosis is regularly performed by treating mammalian cells grown in culture with a cocktail comprised of TNFα, a Smac mimetic which facilitates the degradation of cellular inhibitors of apoptosis (cIAPs), and pan-caspase inhibitor, z-VAD-fmk [30]. Ligation of TNFα to TNFR1 promotes the recruitment of a multiprotein complex to the intracellular portion of the receptor near the cell surface. This complex, known as Complex I, contains adaptor proteins tumor necrosis factor receptor type 1-associated death domain protein (TRADD) and FAS-associated death domain protein (FADD), cIAP1/2, TNF receptor-associated factor 2 and 5 (TRAF2/5), and RIP1, amongst others [31]. Depending on the cell type and amount of stimuli-receptor activation, Complex I can signal for cell survival through the canonical NFκB signaling pathway [31]. Notably, Complex I is stabilized by a number of mitigating factors including RIP1-K63 polyubiquitination [32]. De-ubiquitination of RIP1 by ubiquitin carboxyl-terminal hydrolase (CYLD) destabilizes the complex, and releases RIP1 into the cytoplasm where it interacts with FADD and Caspase-8 [31, 33]. This cytosolic complex is known as Complex IIa. Once formed, Complex IIa activates initiator Caspase-8 which in turn commences to activate downstream effector caspases, Caspase-3/7, triggering apoptosis [34]. Caspase-8 has also been reported to cleave RIP1 and RIP3 to ensure that apoptosis, but not necroptosis, is activated [35].

A critical step in switching TNFα-induced apoptosis to necroptosis depends on inhibiting

caspase activity or bypassing it. Caspase inhibition, which can be achieved either chemically or through virally derived factors, drives RIP1 to interact with a closely related protein kinase, RIP3, marking the formation of the necroptotic death-inducing signaling complex (DISC), Complex IIb [22]. Alternatively, RIP1-RIP3 binding can occur as a result of increased RIP1/3 gene expression, which bypasses the threshold of basal Caspase-8 activity [36, 37]. The interaction between RIP1 and RIP3 binding is mediated by their receptor homotypic interaction motifs (RHIM), a short stretch of about 25 amino acid residues that is conserved back to fungi [38]. RHIM-domain mediated protein interactions are proven to be essential for necroptotic signal transduction. For example, viral sensing by ZBP1 requires its RHIM-domain, as does Toll-like receptor adaptor protein, TIR domain-containing adapter-inducing interferon-β (TRIF) [39, 40]. Additionally, HSV-1/2 encoded proteins, ribonucleotide reductase subunits ICP6 and ICP10, also contain RHIM-domains that regulate RIP1-RIP3 binding in infected cells [41]. Genetic deletion of either viral or host derived RHIM-domain containing proteins influences necroptotic outcomes depending of the species in question [42].

MLKL activation and its function in executing necroptosis

After a series of phosphorylation events between RIP1 and RIP3, particularly RIP3 Ser227 which is required for necroptosis, mixed lineage kinase domain-like protein (MLKL) is recruited to Complex IIb, forming the “necrosome” complex [43, 44]. Notably, MLKL is responsible for permeabilizing the plasma membrane, and potentially other cellular membranes [45]. MLKL is a pseudokinase with two important protein domains:

A N-terminal 4-helix bundle domain (4HBD) and the C-terminal kinase-like regulatory domain that is catalytically inactive [46, 47]. Under normal conditions, the C-terminal regulatory domain inhibits the 4HBD, which is the functional region of the protein responsible for executing cell death [48]. RIP3-dependent MLKL Thr357/Ser358 phosphorylation within its kinase-like domain activates the human protein, and induces a conformational shift that releases the 4HBD from the inhibitory effects of its C-terminal domain [49]. Release of the 4HBD from the C-terminal domain allows the 4HBD to associate with cellular membranes [50]. In murine cells, MLKL associates primarily with the plasma membrane while the human protein is found on the surface of mitochondria, lysosomes, and endoplasmic reticulum, suggesting that different cellular compartments may be involved in propagating necroptotic signals [51, 52]. It also suggests that necroptotic pathways may differ between species. Yet, it remains unclear whether these organelles are lysed by MLKL in response to necroptotic stimuli. Studies in *C. elegans* demonstrated that lysosome membrane integrity was lost in response to a variety of known necrotic stimuli [53-55]. Furthermore, hydrolytic lysosomal enzymes, such as the cathepsin family of proteases, were reported to be involved in necrotic cell death programs [55]. Investigations into the role of lysosomal membrane leakage in necroptosis are ongoing.

In vitro binding assays indicated that the 4HBD of MLKL interacts with a defined subset of phosphatidylinositol phospholipids (PIPs), which are found on various vesicles and organelles [52, 56]. It was also found that MLKL binds to cardiolipin, a

mitochondrial-specific lipid [52, 56]. Once associated with membranes, MLKL polymerizes into high molecular weight structures [52, 57]. MLKL activation is often determined by 1) detection of phosphorylated MLKL or 2) detection of MLKL polymers by a variety of protein resolving techniques. MLKL polymerization is thought to occur in two steps. First, MLKL forms into tetramers that feed into the second part of building larger polymers, although the mechanistic details of this process remain largely unclear [48, 58]. An even less understood process is the mechanism by which MLKL polymers execute necroptosis. In the prevailing model of MLKL-mediated membrane disruption, MLKL pierces through membranes and forms a pore that acts as a channel for various cations including sodium, calcium, magnesium, and potassium. Influx of extracellular ions causes cells to swell until they eventually burst, consequently producing the necrotic phenotype seen by electron microscopy [35, 59]. Conversely, potassium efflux has also been proposed to be involved in executing necroptosis; however, there is currently no consensus on the universal role of ion exchange during necroptosis, and therefore remains an active area of research [60]. The work presented in this thesis aims to understand the mechanism(s) that control MLKL polymerization, and the effects of MLKL polymers on membrane rupture, particularly lysosomal membranes.

Necroptosis in human disease

In terms of human health, membrane rupture caused by necroptosis is both beneficial and deleterious depending on the context of cell death induction. For fighting viral infections, membrane rupture leads to an inflammatory response that directs immune

cells to the site of infection thereby boosting an organism's ability to stop the spread of pathogens to healthy cells [61]. However, dysregulated necroptosis can lead to an excessive amount of undesired inflammation that can cause irreversible damage to surrounding healthy tissue. Since its emergence as a primary form of cell death, necroptosis has been implicated in a growing number of human pathological conditions associated with neurodegeneration, inflammatory diseases, and ischemic/reperfusion injuries [37, 62-64]. Dysregulated necroptosis is in part due to elevated levels of RIP1, RIP3, or MLKL proteins which have been detected in histological analysis of primary patient samples [37, 65, 66], leading researchers to hypothesize that changes in gene expression are the underlying cause of uncontrolled necroptosis though the causes of such changes have yet to be determined. To control the progression of necroptosis-associated diseases, efforts are currently underway to identify compounds that specifically inhibit necroptosis *in vivo*.

Regulation of MLKL polymerization by Thioredoxin-1

Insights into MLKL polymerization emerged when it was discovered that intramolecular disulfide bonds stabilized MLKL polymers [52, 58]. This was demonstrated by incubating necroptotic cell extracts containing MLKL polymers with reducing agents such as dithiothreitol (DTT) or beta-mercaptoethanol (βME), and analyzing their effects on polymer stability. The addition of reducing agents dissociated MLKL polymers, including tetramers, back to their monomeric state, suggesting that MLKL requires an oxidizing environment to execute necroptosis [52]. However, it is not known how MLKL

forms disulfide bonds given its localization within the cytoplasm, which contains two major redox-balancing systems. One is the glutathione system. Glutathione is a tripeptide (i.e. glutamate-cysteine-glycine) that serves as a highly important antioxidizing agent that reduces thiol groups on cysteine residues of protein targets [67]. The other is the cytosolic thioredoxin system [68]. A separate thioredoxin systems is found within mitochondria; however, for the purpose of this work, the emphasis will be on the cytosolic thioredoxin system, and its regulatory effects on MLKL disulfide bonds formation during polymerization [69].

The cytosolic thioredoxin system is comprised of thioredoxin-1 (Trx1), thioredoxin reductase-1 (TrxR1), and NADPH [68]. Trx1 is a highly conserved 12kDa thiol oxidoreductase involved in cellular redox balance. Genetic knockout of Trx1 or TrxR1 is embryonic lethal in mice [70]. Trx1 regulates redox balance and signaling pathways through the reduction of disulfide bonds on specific protein substrates. It does so by using two critical reactive cysteine residues located within its active site, Cys32 and Cys35 [68]. When reduced, these cysteine residues engage in dithiol exchange reactions whereby electrons from Cys32 and Cys35 are transferred to oxidized cysteine residues on the respective protein substrate, thus reducing them. In the process, Trx1's active site becomes oxidized, and can no longer reduce disulfide bonds. In order to regenerate Trx1's oxidoreductase activity, TrxR1 transfers electrons from NADPH onto Cys32 and Cys35, thus replenishing the thioredoxin system [68].

The major goal of my project was to understand the regulation of MLKL polymerization during necroptosis. We initially identified Trx1 as a potential regulator of necroptosis through the use of Necrosulfonamide (NSA), a compound that is often used to inhibit necroptosis in human cells grown in culture [71]. By covalently binding to Cys86 of MLKL, NSA blocks proper MLKL polymerization [71]. In addition to its ability to inhibit necroptosis, we demonstrate that NSA crosslinks Cys32 of Trx1 to Cys86 of MLKL. This suggested that MLKL and Trx1 may exist as a complex in nature, and therefore hypothesized that Trx1 regulates MLKL polymerization. Further analysis revealed that genetic perturbations to Trx1 via shRNA knockdown resulted in a propensity of MLKL tetramer and polymer formation, and increased sensitivity to necroptosis. Moreover, the Trx1 chemical inhibitor, PX-12, induced necroptosis in a MLKL-dependent manner [72]. Further details of these findings are presented in the following chapter.

Investigations into the necroptotic process have opened up new and exciting areas of research in the field of cell death. With the advent of specific necroptotic biomarkers, antibodies, and chemical inhibitors, researchers are now able to dissect various cell death forms that contribute to disease in a much more intricate way. The long-term goal is to further delineate mammalian necroptotic pathways in hopes of developing therapies to treat necroptosis-associated pathological conditions. Here, we are the first group to identify Trx1 as a direct regulator of MLKL function and suppressor of necroptosis, which may for instance, provide insights into the occurrence of necroptosis due to ischemia/reperfusion. Re-oxygenation of tissues results in calcium overload and

generation of ROS, which may be perturbing Trx1 activity [73]. Additionally, PX-12-induced necroptosis has implications in cancer biology. PX-12 proved to lack efficacy in a number of Phase II clinical trials; however, the data presented here suggest perhaps PX-12 treatment in tumors exhibiting elevated levels of RIP3 or MLKL may yield better results [74, 75]. In the same scenario, PX-12 efficacy may be improved if utilized in combination with other established cancer therapies.

Overall, my thesis work provides new knowledge in the regulation of MLKL activity that serves as a strong foundation for the investigation of Trx1 as a suppressor of necroptosis in *in vivo* models. The work presented in the following chapters will focus first on the regulation of MLKL polymerization by Trx1, and then the potential effect of these MLKL polymers on lysosomal membrane rupture. A model of our findings in depicted below (Figure 1.1).

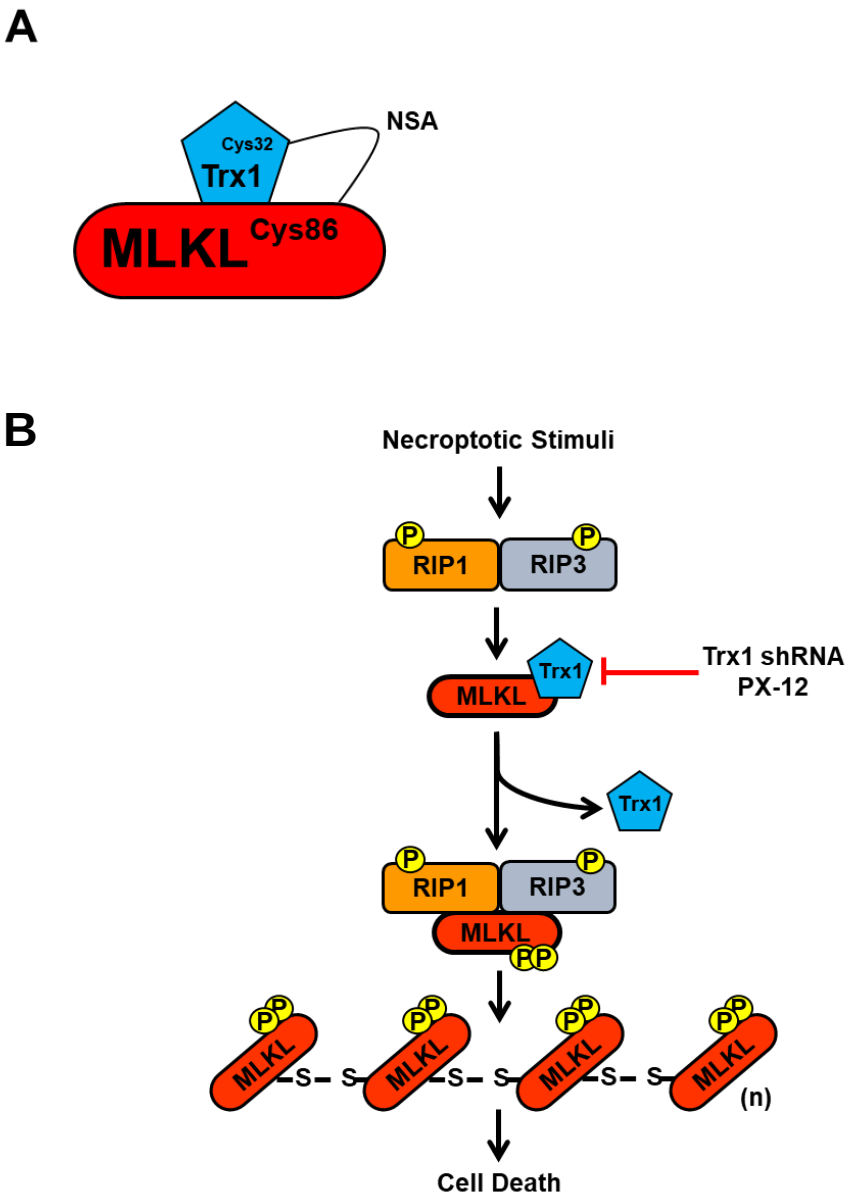

Figure 1.1 Working model Trx1-mediated suppression of necroptotic pathway
(A) NSA crosslinks Trx1 Cys32 to Cys86 of human MLKL. (B) Necroptotic stimuli (i.e. TSZ) and Trx1 inhibition promotes necrosome formation which is comprised of RIP1/RIP3/MLKL. RIP3-dependent phosphorylation of MLKL releases MLKL from the necrosome and forms high molecular weight polymers that localize to the plasma membrane. MLKL polymers actively disrupt the integrity of the plasma membrane leading to cell death and the release of DAMPs.

References

1. Abrams, J.M., et al., *Programmed cell death during Drosophila embryogenesis.* Development, 1993. **117**(1): p. 29-43.
2. Fuchs, Y. and H. Steller, *Programmed cell death in animal development and disease.* Cell, 2011. **147**(4): p. 742-58.
3. Henson, P.M. and D.A. Hume, *Apoptotic cell removal in development and tissue homeostasis.* Trends Immunol, 2006. **27**(5): p. 244-50.
4. Hartley, S.B., et al., *Elimination of self-reactive B lymphocytes proceeds in two stages: arrested development and cell death.* Cell, 1993. **72**(3): p. 325-35.
5. Arandjelovic, S. and K.S. Ravichandran, *Phagocytosis of apoptotic cells in homeostasis.* Nat Immunol, 2015. **16**(9): p. 907-17.
6. Ashkenazi, A. and V.M. Dixit, *Death receptors: signaling and modulation.* Science, 1998. **281**(5381): p. 1305-8.
7. Czabotar, P.E., et al., *Control of apoptosis by the BCL-2 protein family: implications for physiology and therapy.* Nat Rev Mol Cell Biol, 2014. **15**(1): p. 49-63.
8. Liu, X., et al., *Induction of apoptotic program in cell-free extracts: requirement for dATP and cytochrome c.* Cell, 1996. **86**(1): p. 147-57.
9. Li, P., et al., *Cytochrome c and dATP-dependent formation of Apaf-1/caspase-9 complex initiates an apoptotic protease cascade.* Cell, 1997. **91**(4): p. 479-89.
10. Julien, O. and J.A. Wells, *Caspases and their substrates.* Cell Death Differ, 2017.
11. Mocarski, E.S., H. Guo, and W.J. Kaiser, *Necroptosis: The Trojan horse in cell autonomous antiviral host defense.* Virology, 2015. **479-480**: p. 160-6.
12. Zhou, W. and J. Yuan, *Necroptosis in health and diseases.* Semin Cell Dev Biol, 2014. **35**: p. 14-23.
13. Vanden Berghe, T., et al., *Molecular crosstalk between apoptosis, necroptosis, and survival signaling.* Mol Cell Oncol, 2015. **2**(4): p. e975093.
14. Galluzzi, L. and G. Kroemer, *Necroptosis: a specialized pathway of programmed necrosis.* Cell, 2008. **135**(7): p. 1161-3.
15. Hacker, G., *The morphology of apoptosis.* Cell Tissue Res, 2000. **301**(1): p. 5-17.
16. Vercammen, D., et al., *Inhibition of caspases increases the sensitivity of L929 cells to necrosis mediated by tumor necrosis factor.* J Exp Med, 1998. **187**(9): p. 1477-85.
17. Vandenabeele, P., et al., *Molecular mechanisms of necroptosis: an ordered cellular explosion.* Nat Rev Mol Cell Biol, 2010. **11**(10): p. 700-14.
18. Hochreiter-Hufford, A. and K.S. Ravichandran, *Clearing the dead: apoptotic cell sensing, recognition, engulfment, and digestion.* Cold Spring Harb Perspect Biol, 2013. **5**(1): p. a008748.
19. Kaczmarek, A., P. Vandenabeele, and D.V. Krysko, *Necroptosis: the release of damage-associated molecular patterns and its physiological relevance.* Immunity, 2013. **38**(2): p. 209-23.

20. Weinlich, R., et al., *Necroptosis in development, inflammation and disease.* Nat Rev Mol Cell Biol, 2017. **18**(2): p. 127-136.
21. Wu, J., et al., *Mlkl knockout mice demonstrate the indispensable role of Mlkl in necroptosis.* Cell Res, 2013. **23**(8): p. 994-1006.
22. Han, J., C.Q. Zhong, and D.W. Zhang, *Programmed necrosis: backup to and competitor with apoptosis in the immune system.* Nat Immunol, 2011. **12**(12): p. 1143-9.
23. Jorgensen, I., M. Rayamajhi, and E.A. Miao, *Programmed cell death as a defence against infection.* Nat Rev Immunol, 2017. **17**(3): p. 151-164.
24. Guo, H., W.J. Kaiser, and E.S. Mocarski, *Manipulation of apoptosis and necroptosis signaling by herpesviruses.* Med Microbiol Immunol, 2015. **204**(3): p. 439-48.
25. Thapa, R.J., et al., *DAI Senses Influenza A Virus Genomic RNA and Activates RIPK3-Dependent Cell Death.* Cell Host Microbe, 2016. **20**(5): p. 674-681.
26. de Almagro, M.C. and D. Vucic, *Necroptosis: Pathway diversity and characteristics.* Semin Cell Dev Biol, 2015. **39**: p. 56-62.
27. Upton, J.W. and W.J. Kaiser, *DAI Another Way: Necroptotic Control of Viral Infection.* Cell Host Microbe, 2017. **21**(3): p. 290-293.
28. Declercq, W., T. Vanden Berghe, and P. Vandenabeele, *RIP kinases at the crossroads of cell death and survival.* Cell, 2009. **138**(2): p. 229-32.
29. Degterev, A. and J. Yuan, *Expansion and evolution of cell death programmes.* Nat Rev Mol Cell Biol, 2008. **9**(5): p. 378-90.
30. Meng, L., W. Jin, and X. Wang, *RIP3-mediated necrotic cell death accelerates systematic inflammation and mortality.* Proc Natl Acad Sci U S A, 2015. **112**(35): p. 11007-12.
31. Vanlangenakker, N., et al., *TNF-induced necroptosis in L929 cells is tightly regulated by multiple TNFR1 complex I and II members.* Cell Death Dis, 2011. **2**: p. e230.
32. de Almagro, M.C., et al., *Coordinated ubiquitination and phosphorylation of RIP1 regulates necroptotic cell death.* Cell Death Differ, 2017. **24**(1): p. 26-37.
33. Moquin, D.M., T. McQuade, and F.K. Chan, *CYLD deubiquitinates RIP1 in the TNFalpha-induced necrosome to facilitate kinase activation and programmed necrosis.* PLoS One, 2013. **8**(10): p. e76841.
34. Christofferson, D.E. and J. Yuan, *Necroptosis as an alternative form of programmed cell death.* Curr Opin Cell Biol, 2010. **22**(2): p. 263-8.
35. Ofengeim, D. and J. Yuan, *Regulation of RIP1 kinase signalling at the crossroads of inflammation and cell death.* Nat Rev Mol Cell Biol, 2013. **14**(11): p. 727-36.
36. Bailey, L.J., et al., *Augmented trophoblast cell death in preeclampsia can proceed via ceramide-mediated necroptosis.* Cell Death Dis, 2017. **8**(2): p. e2590.
37. Ito, Y., et al., *RIPK1 mediates axonal degeneration by promoting inflammation and necroptosis in ALS.* Science, 2016. **353**(6299): p. 603-8.

38. Kajava, A.V., et al., *Evolutionary link between metazoan RHIM motif and prion-forming domain of fungal heterokaryon incompatibility factor HET-s/HET-s.* Sci Rep, 2014. **4**: p. 7436.
39. Rebsamen, M., et al., *DAI/ZBP1 recruits RIP1 and RIP3 through RIP homotypic interaction motifs to activate NF-kappaB.* EMBO Rep, 2009. **10**(8): p. 916-22.
40. Kaiser, W.J., et al., *Toll-like receptor 3-mediated necrosis via TRIF, RIP3, and MLKL.* J Biol Chem, 2013. **288**(43): p. 31268-79.
41. Guo, H., et al., *Herpes simplex virus suppresses necroptosis in human cells.* Cell Host Microbe, 2015. **17**(2): p. 243-51.
42. Lin, J., et al., *RIPK1 counteracts ZBP1-mediated necroptosis to inhibit inflammation.* Nature, 2016. **540**(7631): p. 124-128.
43. Zhang, J., et al., *Necrosome core machinery: MLKL.* Cell Mol Life Sci, 2016. **73**(11-12): p. 2153-63.
44. Chan, F.K. and E.H. Baehrecke, *RIP3 finds partners in crime.* Cell, 2012. **148**(1-2): p. 17-8.
45. Linkermann, A., U. Kunzendorf, and S. Krautwald, *Phosphorylated MLKL causes plasma membrane rupture.* Mol Cell Oncol, 2014. **1**(1): p. e29915.
46. Hildebrand, J.M., et al., *Activation of the pseudokinase MLKL unleashes the four-helix bundle domain to induce membrane localization and necroptotic cell death.* Proc Natl Acad Sci U S A, 2014. **111**(42): p. 15072-7.
47. Czabotar, P.E. and J.M. Murphy, *A tale of two domains - a structural perspective of the pseudokinase, MLKL.* Febs j, 2015. **282**(22): p. 4268-78.
48. Chen, X., et al., *Translocation of mixed lineage kinase domain-like protein to plasma membrane leads to necrotic cell death.* Cell Res, 2014. **24**(1): p. 105-21.
49. Su, L., et al., *A plug release mechanism for membrane permeation by MLKL.* Structure, 2014. **22**(10): p. 1489-500.
50. Rodriguez, D.A., et al., *Characterization of RIPK3-mediated phosphorylation of the activation loop of MLKL during necroptosis.* Cell Death Differ, 2016. **23**(1): p. 76-88.
51. Cai, Z., et al., *Plasma membrane translocation of trimerized MLKL protein is required for TNF-induced necroptosis.* Nat Cell Biol, 2014. **16**(1): p. 55-65.
52. Wang, H., et al., *Mixed lineage kinase domain-like protein MLKL causes necrotic membrane disruption upon phosphorylation by RIP3.* Mol Cell, 2014. **54**(1): p. 133-46.
53. Crook, M., A. Upadhyay, and W. Hanna-Rose, *Necrosis in C. elegans.* Methods Mol Biol, 2013. **1004**: p. 171-82.
54. Artal-Sanz, M., et al., *Lysosomal biogenesis and function is critical for necrotic cell death in Caenorhabditis elegans.* J Cell Biol, 2006. **173**(2): p. 231-9.
55. Jacobson, L.S., et al., *Cathepsin-mediated necrosis controls the adaptive immune response by Th2 (T helper type 2)-associated adjuvants.* J Biol Chem, 2013. **288**(11): p. 7481-91.
56. Dondelinger, Y., et al., *MLKL compromises plasma membrane integrity by binding to phosphatidylinositol phosphates.* Cell Rep, 2014. **7**(4): p. 971-81.

57. Tanzer, M.C., et al., *Necroptosis signalling is tuned by phosphorylation of MLKL residues outside the pseudokinase domain activation loop.* Biochem J, 2015. **471**(2): p. 255-65.
58. Huang, D., et al., *The MLKL Channel in Necroptosis Is an Octamer Formed by Tetramers in a Dyadic Process.* Mol Cell Biol, 2017. **37**(5).
59. Zhang, Y. and J. Han, *Electrophysiologist shows a cation channel function of MLKL.* Cell Res, 2016. **26**(6): p. 643-4.
60. Gutierrez, K.D., et al., *MLKL Activation Triggers NLRP3-Mediated Processing and Release of IL-1beta Independently of Gasdermin-D.* J Immunol, 2017. **198**(5): p. 2156-2164.
61. Mocarski, E.S., J.W. Upton, and W.J. Kaiser, *Viral infection and the evolution of caspase 8-regulated apoptotic and necrotic death pathways.* Nat Rev Immunol, 2011. **12**(2): p. 79-88.
62. Rickard, J.A., et al., *RIPK1 regulates RIPK3-MLKL-driven systemic inflammation and emergency hematopoiesis.* Cell, 2014. **157**(5): p. 1175-88.
63. Zhao, H., et al., *Role of necroptosis in the pathogenesis of solid organ injury.* Cell Death Dis, 2015. **6**: p. e1975.
64. Pierdomenico, M., et al., *Necroptosis is active in children with inflammatory bowel disease and contributes to heighten intestinal inflammation.* Am J Gastroenterol, 2014. **109**(2): p. 279-87.
65. Seifert, L., et al., *The necrosome promotes pancreatic oncogenesis via CXCL1 and Mincle-induced immune suppression.* Nature, 2016. **532**(7598): p. 245-9.
66. Ofengeim, D., et al., *Activation of necroptosis in multiple sclerosis.* Cell Rep, 2015. **10**(11): p. 1836-49.
67. Filomeni, G., G. Rotilio, and M.R. Ciriolo, *Cell signalling and the glutathione redox system.* Biochem Pharmacol, 2002. **64**(5-6): p. 1057-64.
68. Arner, E.S. and A. Holmgren, *Physiological functions of thioredoxin and thioredoxin reductase.* Eur J Biochem, 2000. **267**(20): p. 6102-9.
69. Patenaude, A., M.R. Ven Murthy, and M.E. Mirault, *Mitochondrial thioredoxin system: effects of TrxR2 overexpression on redox balance, cell growth, and apoptosis.* J Biol Chem, 2004. **279**(26): p. 27302-14.
70. Matsui, M., et al., *Early embryonic lethality caused by targeted disruption of the mouse thioredoxin gene.* Dev Biol, 1996. **178**(1): p. 179-85.
71. Sun, L., et al., *Mixed lineage kinase domain-like protein mediates necrosis signaling downstream of RIP3 kinase.* Cell, 2012. **148**(1-2): p. 213-27.
72. Baker, A.F., et al., *The antitumor thioredoxin-1 inhibitor PX-12 (1-methylpropyl 2-imidazolyl disulfide) decreases thioredoxin-1 and VEGF levels in cancer patient plasma.* J Lab Clin Med, 2006. **147**(2): p. 83-90.
73. Gottlieb, R.A., *Cell death pathways in acute ischemia/reperfusion injury.* J Cardiovasc Pharmacol Ther, 2011. **16**(3-4): p. 233-8.
74. Ramanathan, R.K., et al., *A randomized phase II study of PX-12, an inhibitor of thioredoxin in patients with advanced cancer of the pancreas following progression after a gemcitabine-containing combination.* Cancer Chemother Pharmacol, 2011. **67**(3): p. 503-9.

75. Baker, A.F., et al., *A phase IB trial of 24-hour intravenous PX-12, a thioredoxin-1 inhibitor, in patients with advanced gastrointestinal cancers.* Invest New Drugs, 2013. **31**(3): p. 631-41.

Chapter 2. Thioredoxin-1 negatively regulates necroptosis by maintaining MLKL in a reduced state

Introduction

A considerable amount of our understanding of the necroptotic machinery has emerged through studies of the TNFα signaling pathway. These works led to the discovery of MLKL and serine/threonine kinases RIP1 and RIP3 as critical mediators of necroptosis [1-7]. Together, these proteins form the core of the necrosome complex which is central for transducing necroptotic signals. One of the most common methods for inducing necroptosis in cultured cells is by treating them with a cocktail comprised of TNFα (T), a SMAC mimetic (S), which degrades cellular inhibitors of apoptosis (cIAPs), and the pan-caspase inhibitor z-VAD-fmk (Z) [8-11]. This cocktail is commonly abbreviated as T/S/Z. The combination of a SMAC mimetic, which functions as the pro-apoptotic mitochondrial protein Smac/DIABLO, in combination with z-VAD-fmk re-directs TNFα signaling towards a pathway that triggers necroptosis. Thus, T/S/Z treatment bypasses NFκB signaling and apoptosis, and instead, drives necrosome complex formation followed by RIP3-dependent phosphorylation of MLKL Thr357 and Ser358 located within the C-terminal kinase-like domain of the human protein [11-13]. Active MLKL molecules translocate from the cytoplasm to various cellular compartments throughout the cell where they interact with a specific subset of phosphatidylinositol phospholipids and cardiolipin according to *in vitro* binding data [11, 14-16]. MLKL goes on to form membrane-piercing polymers that disrupt the integrity of cellular membranes, albeit through a process that is not fully understood. To shed light on this process, our efforts

were focused on understanding the molecular mechanism(s) that control MLKL polymerization.

Previous studies indicate that MLKL polymers are stabilized by intramolecular disulfide bonds suggesting MLKL requires an oxidative environment in order to polymerize [11, 17-19]. Mutations to critical MLKL cysteine residues disable proper polymer formation thereby compromising its ability to execute necroptosis [19]. Together, these results suggest that MLKL activity is regulated by its redox state. Interestingly, mitochondrial dysfunction and elevated ROS production have been reported in mammalian cells undergoing necroptosis [20, 21]. Furthermore, mitochondrial networks undergo fission and appear fragmented in response to necrotic stimuli such as TSZ, t-butyl hydroxide (TBH), and calcium overload [22]. This is thought to be caused in part by the action of the mitochondrial proteins serine/threonine protein phosphatase 5 (PGAM5) and Dynamin-related protein 1 (Drp1), which where were shown to interact with RIP3 in a signal-dependent manner [22]. Notably, TNFα-induced necroptosis was prevented by co-treating cells with ROS scavenging molecules butylated hydroxyanisole (BHA) and N-acetylcysteine (NAC) in murine cells [21]. More recently, mitochondrial ROS was implicated in promoting RIP1 autophosphorylation, which proved to be essential for RIP3 recruitment to the necrosome complex [20]. Thus, oxidation appears to play an important role in the necroptotic pathway. However, despite these findings, the molecular mechanism(s) that drive such oxidative events in relation to MLKL activation remains a topic of much debate.

Herein, evidence is provided to show that Thioredoxin-1 (Trx1), a 12kDa thiol oxidoreductase, suppresses necroptosis by blocking MLKL activation. Trx1 functions as an essential antioxidizing enzyme that regulates cellular redox balance. Trx1 protects cells from oxidative stress by engaging in thiol disulfide exchange reactions that results in the reduction of disulfide bonds on specific protein targets thereby modulating their activities [23, 24]. Its ability to reduce disulfide bonds is attributed to two reactive cysteine residues, Cys32 and Cys35, located within its active site. Proteins regulated by Trx1 include cell surface receptors, kinases, transcription factors, and other signaling molecules involved in a multitude of biological processes such as cell death [25-27]. In this study, we found that NSA, a small molecule inhibitor of MLKL [12], crosslinks one of two Trx1 active site cysteine residues, Cys32, to MLKL. Therefore, we tested whether genetic and pharmacological perturbations to Trx1 activity affected MLKL activation and ultimately necroptosis in HeLa cells expressing RIP3 and MLKL transgenes. As a result, we found that shRNA-mediated knockdown of Trx1 enhanced MLKL tetramer formation and subsequent assembly of larger polymers. Moreover, Trx1 knockdown cells exhibited increased sensitivity to necroptosis upon Doxycycline (Dox)-induced RIP3 and MLKL protein expression. These results were corroborated by using a commercially available Trx1 inhibitor, PX-12. PX-12, which disables the recycling of Trx1 active site cysteine residues by TrxR1 [24], promoted RIP1/RIP3/MLKL necrosome formation, RIP3-dependent MLKL S358 phosphorylation, MLKL polymerization, and ultimately caspase-independent cell death. Overall, these findings are the first to point to Trx1 as a suppressor of necroptosis that functions at the step of MLKL polymerization.

Results

NSA crosslinks Cys32 of Trx1 to Cys86 of human MLKL

NSA is a synthetic compound that is commonly used in *in vitro* studies to inhibit necroptosis in human cells. NSA contains two potential Michael acceptor moieties which covalently modify reactive cysteine residues within target proteins (Figure 2.1A) [12]. Chemical changes to either Michael acceptor renders NSA non-functional [12]. By irreversibly binding Cys86 of human MLKL protein, NSA prevents necroptosis without affecting RIP1/RIP3/MLKL necrosome complex formation or RIP3-dependent MLKL phosphorylation [12]. Initial observations demonstrated that NSA crosslinked MLKL to an endogenous protein in NTD-DmrB HeLa cells, which stably express a truncated MLKL transgene containing the N-terminal domain (NTD), also known as the 4HBD, fused to an interaction-inducible DmrB domain (Figure 1.1B). The NTD-DmrB transgene is under the control of a Dox-inducible promoter as illustrated in Figure 2.1B. Western blot analysis revealed that NSA, but not a NSA derivative (NSA-D1) produced a prominent extra protein band that migrated near 55kDa (Figure 1.1B), which is about 12-15kDa larger than NTD-DmrB itself. This indicated that NSA requires two cysteine-reactive Michael acceptor moieties for successful crosslinking to occur. As expected, NSA crosslinking occurred at Cys86 of MLKL which is a known targeting site for NSA (Figure 2.1C) [12].

Next, we set out to determine the identity of the protein crosslinked to NTD-DmrB by NSA. MLKL-NSA-protein complexes were isolated from whole cell extracts by FLAG-tag

affinity purification, and subjected to SDS-PAGE for silver staining (Figure 2.1D). The 55kDa gel band of interest was excised and subjected to LC/MS analysis to determine its protein composition. The list of candidate proteins was narrowed down to those with a molecular weight between 12-15kDa. One of the proteins that fit this criterion was Trx1, which is a small cytosolic oxidoreductase that catalyzes the reduction of disulfide bonds on specific protein substrates [24]. To verify that NSA crosslinks Trx1 was crosslinked to MLKL, we ectopically expressed either wild-type or a C86S mutant HA-FLAG-MLKL full-length protein in HEK293T cells, and treated these cells with NSA for 16 hours. Anti-Trx1 Western blotting of the FLAG-tag immunopurified product confirmed that Trx1 was crosslinked by NSA to wild-type MLKL, but not the C86S mutant (Figure 2.1E, lane 2 versus lane 4). MLKL-NSA-Trx1 crosslinking was also confirmed by performing the same analysis using ectopically expressed HA-tagged Trx1 in GFP-RIP3: MLKL-HA-FLAG HeLa cells. GFP-RIP3 and MLKL-HA-FLAG transgenes are stably integrated into the HeLa genome, and are under the control of a Dox-inducible promoter as illustrated in Figure 2.1F. In cells expressing HA-Trx1, NSA crosslinked MLKL to both endogenous Trx1 and HA-Trx1, producing two crosslinked products that differ slightly in size due to the HA-tag on Trx1 (Figure 2.1F, lane 4).

To determine which Trx1 cysteine reacts with NSA, Trx1 active site cysteines Cys32 and Cys35 were substituted for serine residues individually or in combination, and tested whether NSA was still capable of crosslinking Trx1 to MLKL. Western blot analysis of immunopurified NSA-crosslinked MLKL complexes revealed that Cys32S,

but not Cys35S, was required for successful crosslinking. Altogether, these results suggest that MLKL and Trx1 form a complex under normal conditions, and that the catalytic region of Trx1 either mediates or stabilizes the interaction with MLKL (Figure 2.1G).

Trx1 has a higher binding affinity to inactive MLKL

Given that NSA crosslinks Trx1 to MLKL, we tested whether Trx1 directly binds MLKL in cells. However, attempts to verify their interaction by standard MLKL or Trx1 immunoprecipitation assays were not successful. To overcome this challenge, we first immobilized recombinant HA-Trx1-6xHis purified from BL21 bacteria cells to nickel-agarose beads, and incubated them with cell extracts prepared from GFP-RIPK3: MLKL-HA-FLAG cells. Nickel beads containing wild-type Trx1 were able to pulldown MLKL (Figure 2.2A, lane 2), which was not the case with beads containing Trx1 C32S-C35S (CS2) double mutant (Figure 2.2A, lane 3). In a similar experiment, immobilized Trx1 nickel beads were incubated with either control or T/S/Z-induced necroptotic cell extracts prepared from HT-29 human colorectal adenocarcinoma cells (Figure 2.2B). This experiment was conducted to gain insights into binding affinities between Trx1 and active MLKL species. Both wild-type Trx1 and the C35S mutant bound MLKL (Figure 2.2C, lane 3 and lane 5), but not the CS2 double mutant. Interestingly, Trx1 bound more MLKL in control extracts than those prepared from T/S/Z treated cells, suggesting that Trx1 preferentially associates with monomeric MLKL molecules under normal condition (Figure 2.2C, lane 7). This fits our model (Figure 1.1B) in which Trx1 is released from

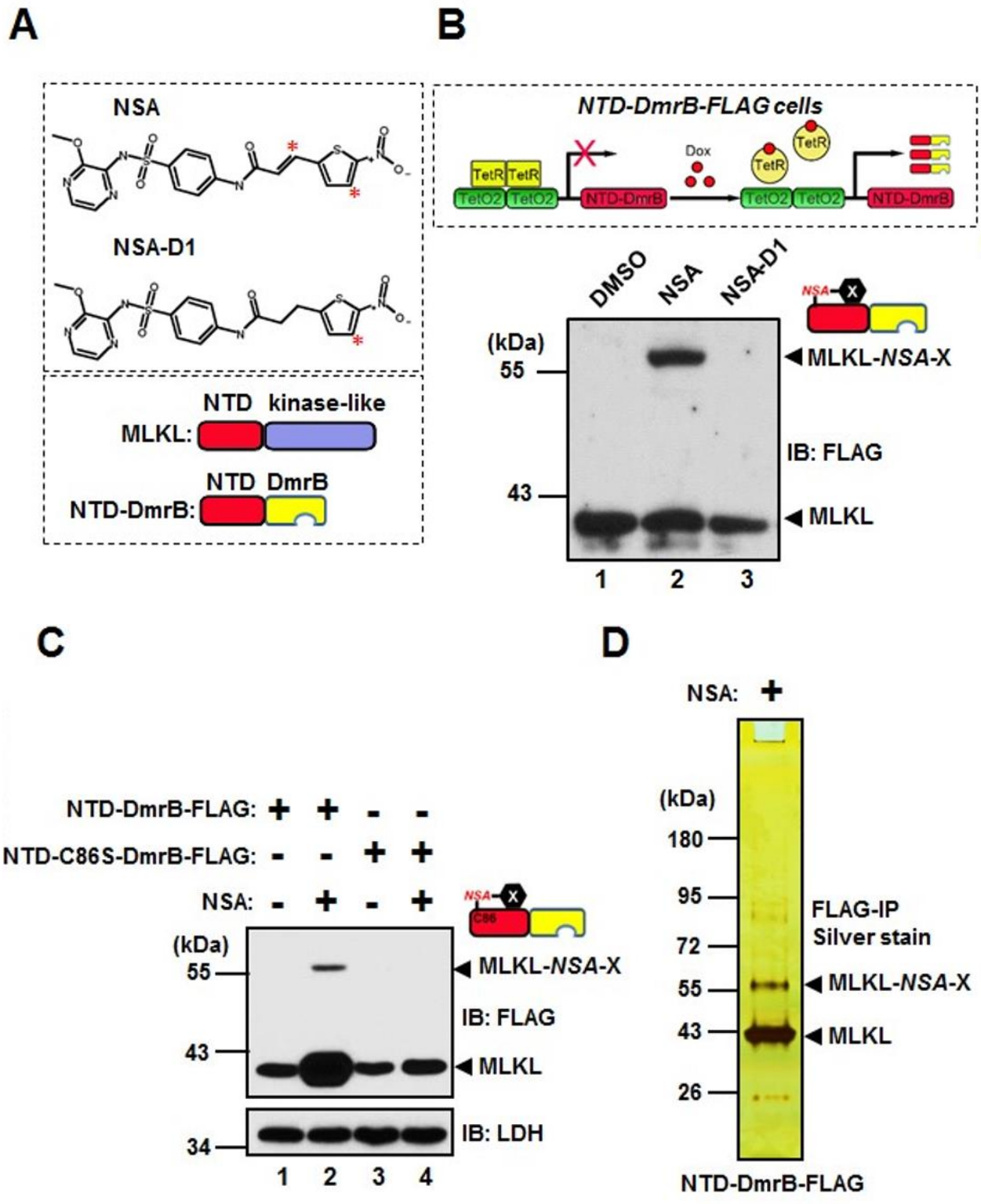
A
B
NSA
NSA-D1
NTD kinase-like
MLKL:
NTD DmrB
NTD-DmrB:
NTD-DmrB-FLAG cells
TetR TetR
TetO2 TetO2
NTD-DmrB
Dox
TetR
TetR
TetO2 TetO2
NTD-DmrB
DMSO
NSA
NSA-D1
(kDa)
55
43
MLKL-NSA-X
IB: FLAG
MLKL
1 2 3
C
D
NTD-DmrB-FLAG: + + - -
NTD-C86S-DmrB-FLAG: - - + +
NSA: - + - +
(kDa)
55
43
34
MLKL-NSA-X
IB: FLAG
MLKL
IB: LDH
1 2 3 4
NSA: +
(kDa)
180
95
72
55
43
26
FLAG-IP
Silver stain
MLKL-NSA-X
MLKL
NTD-DmrB-FLAG

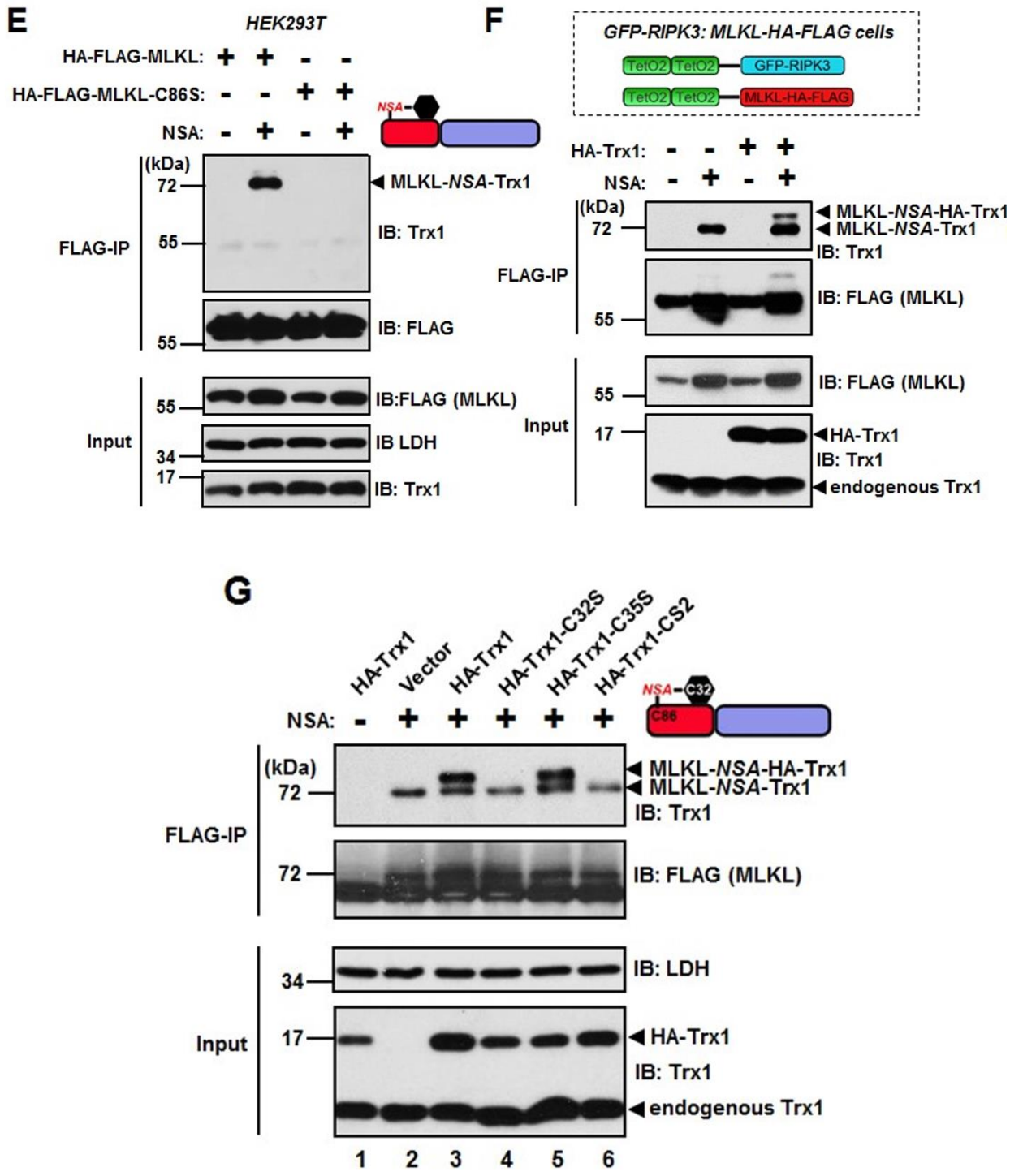

Figure 2.1 NSA crosslinks Cys32 of Trx1 to Cys86 of human MLKL
(A) Upper panel, chemical structures of NSA and a NSA variant, NSA-D1 (red asterisks denote Michael acceptor moieties needed for cysteine conjugation). Lower panel, domain structures of MLKL and NTD-DmrB. NTD, N-terminal domain; DmrB,

dimerization domain. (B) HeLa cells stably expressing Dox inducible NTD-DmrB-FLAG were treated with 5μM NSA or NSA-D1 for 16 hours followed by anti-FLAG Western blotting of whole cell extracts. Arrowhead at about 55kDa points to NSA crosslinked MLKL product. Upper panel depicts Dox-inducible NTD-DmrB expression. In this HeLa cell line, Tet repressor (TetR) is constitutively expressed. Endogenous MLKL is inactivated with CRISPR-Cas9 and NTD-DmrB-FLAG protein was stably expressed under Dox-inducible promoter TetO2. Dox, doxycycline. (C) NTD-DmrB-FLAG or NTD-C86S-DmrB-FLAG proteins were ectopically expressed in HEK293T cells and treated with NSA, then followed by anti-FLAG Western blotting. (D) MLKL complexes were isolated from NTD-DmrB-FLAG cells by FLAG-tag affinity purification (FLAG-IP) and subjected to SDS-PAGE and silver staining. The 55kDa band was excised and sent for mass spec analysis and Trx1 peptides were identified. (E) Full length MLKL or MLKL-C86S mutant proteins were ectopically expressed in HEK293T cells and treated with NSA. MLKL complexes were purified by FLAG-IP and analyzed by Western blotting. Arrowhead at 72kDa points to NSA crosslinked full length MLKL and endogenous Trx1. (F) HA-tagged Trx1 was ectopically expressed in GFP-RIPK3: MLKL-HA-FLAG cells. In this HeLa cell line, Tet repressor (TetR) is constitutively expressed. Endogenous MLKL is inactivated with CRISPR-Cas9 and GFP-RIPK3 and MLKL-HA-FLAG proteins were stably expressed under Dox-inducible promoter. Cells were treated with NSA for 16 hours prior to performing FLAG-IP. Isolated MLKL complexes were analyzed by Western blotting. (G) A panel of HA-tagged mutant Trx1 proteins were ectopically expressed in GFP-RIPK3: MLKL-HA-FLAG cells followed by NSA treatment. FLAG-IP products were analyzed by Western blotting.

MLKL under necroptotic conditions thereby allowing MLKL to polymerize through the formation of intramolecular disulfide bonds.

Trx1 inhibits MLKL polymerization *in vitro*

Trx1 reduces disulfide bonds on specific target proteins, thereby maintaining the reducing environment of the cytoplasm, preventing undesired protein aggregation, and regulating redox signaling pathways [27-30]. As previously stated, MLKL tetramers are stabilized by intermolecular disulfide bonds as are larger MLKL polymers [12, 18, 19]. As shown in Figure 2.3A, T/S/Z treatment induced MLKL phosphorylation in GFP-RIPK3: MLKL-HA-FLAG cells. Phosphorylated MLKL was mainly found in tetramers

revealed by non-reducing SDS-PAGE (Figure 2.3B, lane 2). It was determined that MLKL tetramers were stabilized by disulfide bonds since incubation with 5mM βME reduced tetramers back to their monomeric state (Figure 2.3B, lane 4). Similar analysis was performed on larger MLKL polymers by semi-denaturing detergent agarose gel electrophoresis (SDD-AGE). T/S/Z treatment resulted in MLKL polymer formation (Figure 2.3C, lane 2), which were dissociated after incubation with 5mM DTT (Figure 2.3C, lane 4). Altogether, these results confirm that active MLKL tetramers and polymers are stabilized by disulfide bonds.

To address the mechanism by which Trx1 regulates MLKL function, we developed a cell-free system to assess the effects of Trx1 on MLKL polymerization. Recombinant GST-NTD-FLAG protein was purified from BL21 bacteria cells. Overnight incubation of GST-NTD-FLAG at 37°C resulted in MLKL polymer formation (Figure 2.3D, lane 2). Importantly, GST-NTD incubated at 4°C did not polymerize suggest that the process is temperature sensitive (Figure 2.3D, lane 1). Moreover, polymers that were incubated with DTT also failed to polymerize (Figure 2.3D, lane 3), confirming the importance of disulfide bond formation for *in vitro* polymerization. To test the effect of Trx1 in this system, 5μM GST-NTD-FLAG protein was incubated with increasing amounts of Trx1 (3μM, 10μM, and 30μM) overnight at 37°C. Wild-type Trx1 inhibited MLKL tetramer formation (Figure 2.3E, lanes 2-4) while the CS2 mutant did not (Figure 2.3E, lane 5-7).

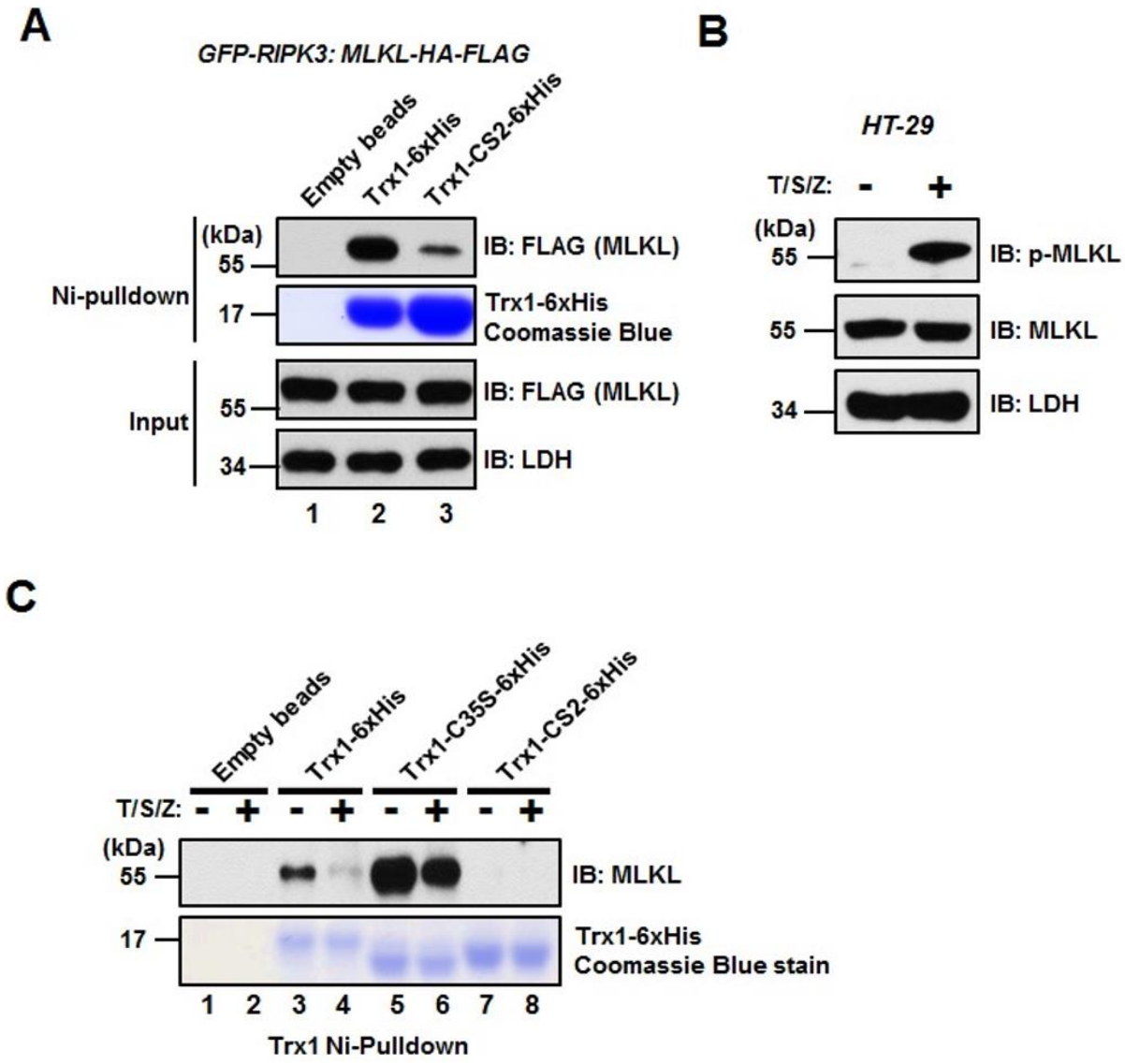

Figure 2.2 Trx1 has a higher binding affinity to inactive MLKL
(A) Purified HA-Trx1-6XHis was immobilized to nickel-agarose beads and incubated with whole cell extracts from GFP-RIPK3: MLKL-HA-FLAG cells. MLKL binding was analyzed by anti-FLAG Western blotting. (B) Western blot analysis of DMSO or T/S/Z treated whole cell extracts from HT-29 cells. TNFα (T), Smac-mimetic (S), z-VAD-fmk (Z). (C) Trx1 mutant proteins were immobilized to nickel beads, and then incubated with DMSO or T/S/Z treated HT-29 whole cell extracts. MLKL binding was analyzed by anti-MLKL Western blotting. In CS2 mutant, both Cys32 and Cys35 are mutated to serine residues.

Similar results were obtained when analyzing larger MLKL polymers (Figure 2.3F, upper panel), indicating that Trx1's oxidoreductase activity is required for maintaining MLKL in a monomeric state. Protein amounts of recombinant GST-NTD-FLAG and HA-Trx1-6xHis used in these experiments were visualized by Coomassie Blue staining (Figure 2.3F, lower panel). These results confirm that MLKL is a substrate of Trx1 which can be reduced by Trx1 *in vitro*.

shRNA-mediated Trx1 knockdown promotes MLKL polymerization and sensitizes cells to necroptosis

Trx1 is an essential gene, and thus cannot be successfully knocked out in cells [31]. Therefore, in order to test whether Trx1 suppresses MLKL activation, we stably introduced a Dox-inducible Trx1 shRNA cassette into the genome of HeLa GFP-RIPK3: MLKL-HA-FLAG cells by lentiviral transduction (Figure 2.4A). Cells that survived hygromycin selection grew at similar rates as parental cells, and exhibited normal morphology (data not shown). After 72 hours of Dox treatment, whole cell extracts were prepared to analyze Trx1/RIP3/MLKL protein levels by Western blotting. Trx1 expression was significantly reduced in shTrx1 cells. Notably, Trx1 protein levels were also reduced without Dox (Figure 2.4A, lane 3), suggesting the occurrence of leaky shRNA expression. Importantly, inhibition of Trx1 is known to trigger apoptosis by activating apoptosis signal regulating kinase 1 (ASK1) [27, 28]. Therefore, to eliminate the possibility of apoptosis in shTrx1 cells, z-VAD-fmk was included in all experiments. Next, cell extracts were subjected to non-reducing SDS-PAGE and SDD-AGE analysis

to test whether Trx1 knockdown promoted MLKL polymer formation. Indeed, cells with diminished levels of Trx1 exhibited a propensity for forming MLKL tetramers (Figure 2.4B, lane 4). MLKL polymers were also detected by SDD-AGE in Trx1 knockdown samples (Figure 2.4C, lane 4). Lastly, cell death measurement indicated that reduction of Trx1 protein resulted in higher sensitivity to necroptosis (Figure 2.4D, column 2 and 4). These results suggest that Trx1 maintains MLKL in a reduced state to suppress MLKL polymerization (Figure 2.4E).

To address the possibility that the crosslinking product MLKL-NSA-Trx1 might contribute to NSA's ability to block cell death, we tested the effect of NSA in shTrx1 cells. In these cells, MLKL-NSA-Trx1 crosslinked complex was not detected (Figure 2.4F, lane 4); however, NSA was fully capable of blocking T/S/Z-induced cell death (Figure 2.4G, column 5 and 6), suggesting that NSA-mediated MLKL-Trx1 crosslinking is not required for NSA to block necroptosis. The ability of NSA to inhibit necroptosis is solely dependent on interacting with C86S of MLKL, and not Trx1 crosslinking.

PX-12 induces necroptosis in GFP-RIPK3: MLKL-HA-FLAG cells

Since shRNA-mediated Trx1 knockdown sensitized cells to necroptosis, we tested whether chemical inhibition of Trx1 activity also exhibited the same effect. To perform these experiments, we utilized a commercially available Trx1 inhibitor known as PX-12, which irreversibly binds to Cys73 of Trx1, and prevents its two active site cysteines from being reduced by thioredoxin reductase [32, 33]. We first tested PX-12 in GFP-RIPK3:

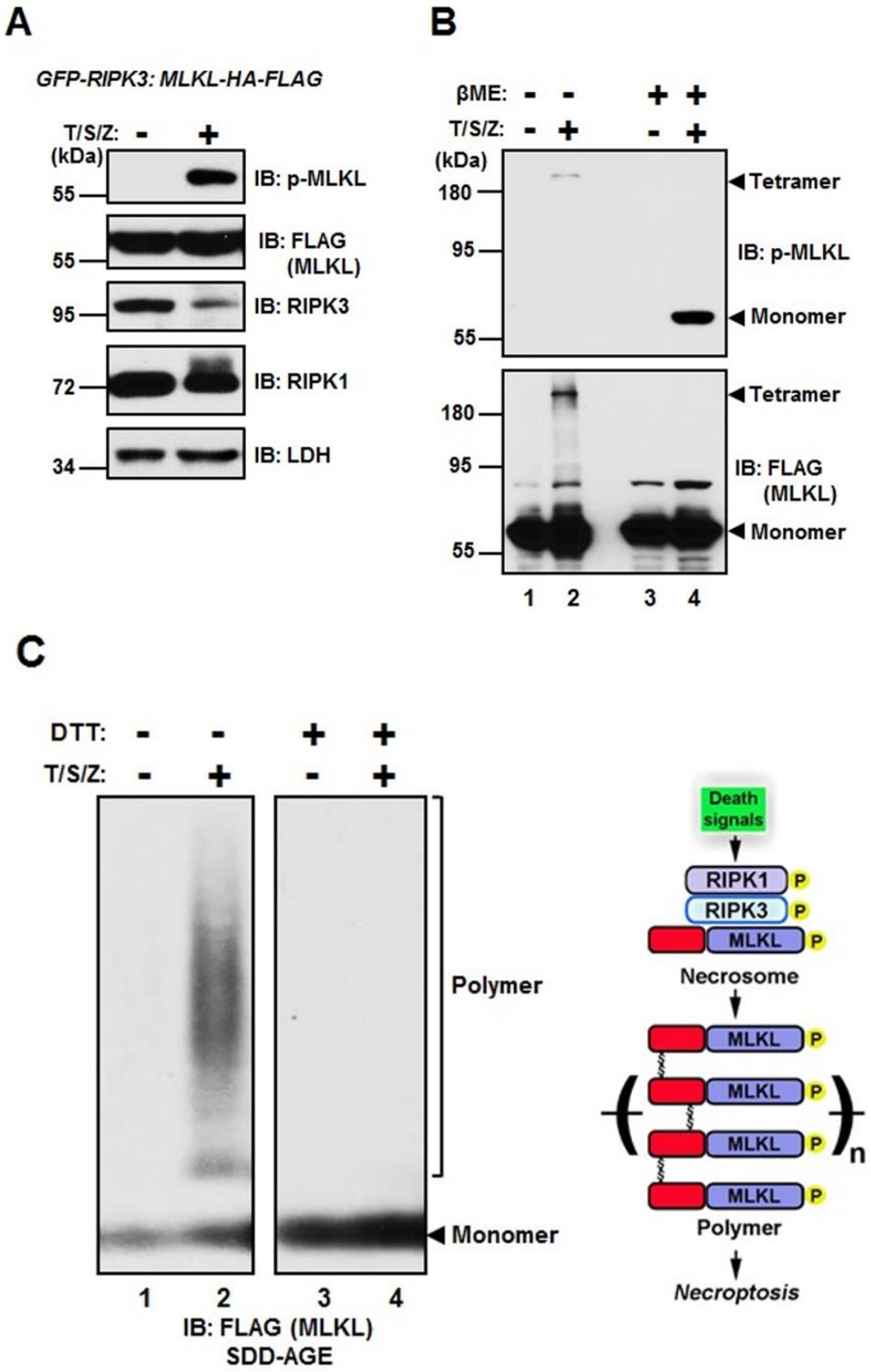
A
GFP-RIPK3: MLKL-HA-FLAG
T/S/Z: - +
(kDa)
55
IB: p-MLKL
55
IB: FLAG (MLKL)
95
IB: RIPK3
72
IB: RIPK1
34
IB: LDH
B
βME: - - + +
T/S/Z: - + - +
(kDa)
180
95
55
Tetramer
IB: p-MLKL
Monomer
180
95
55
Tetramer
IB: FLAG (MLKL)
Monomer
1 2 3 4
C
DTT: - - + +
T/S/Z: - + - +
Polymer
Monomer
1 2 3 4
IB: FLAG (MLKL)
SDD-AGE
Death signals
RIPK1 P
RIPK3 P
MLKL P
Necrosome
MLKL P
MLKL P
MLKL P
MLKL P
n
Polymer
Necroptosis

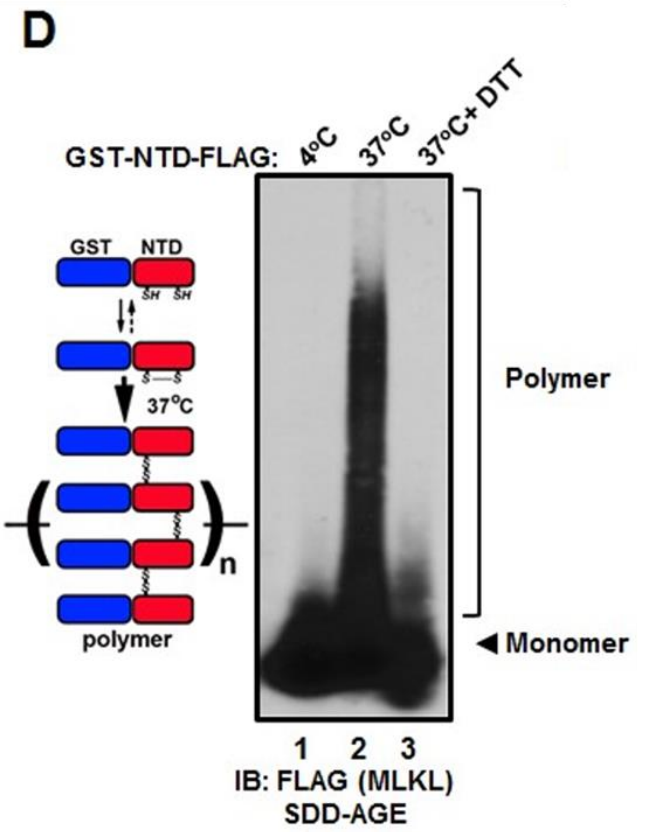
D
GST-NTD-FLAG:
4°C
37°C
37°C+ DTT
GST
NTD
SH SH
S—S
37°C
n
polymer
Polymer
Monomer
1 2 3
IB: FLAG (MLKL)
SDD-AGE

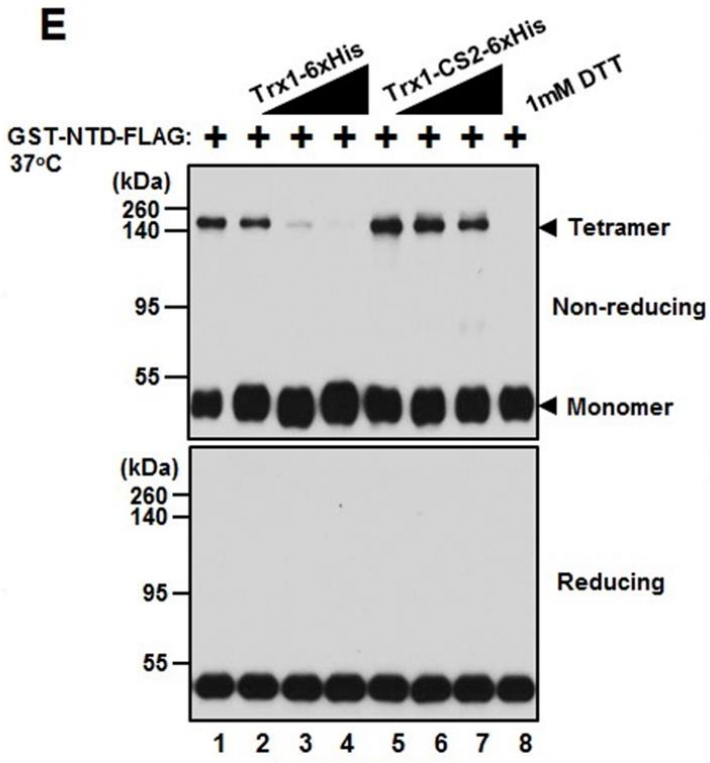
E
Trx1-6xHis
Trx1-CS2-6xHis
1mM DTT
GST-NTD-FLAG: + + + + + + + +
37°C
(kDa)
260
140
95
55
Tetramer
Non-reducing
Monomer
(kDa)
260
140
95
55
Reducing
1 2 3 4 5 6 7 8

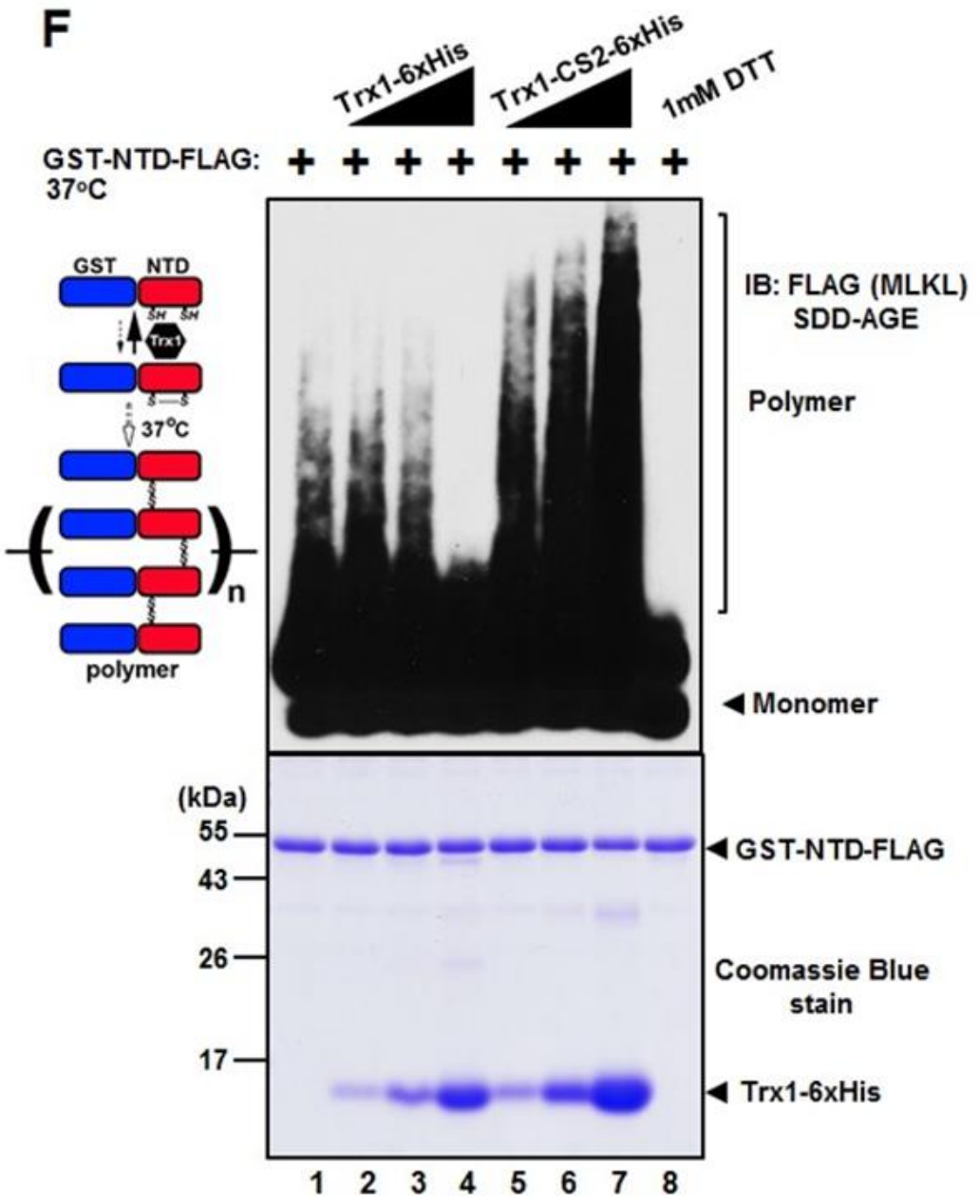

Figure 2.3 Trx1 inhibits MLKL polymerization *in vitro*

(A) Whole cell extracts were prepared from GFP-RIPK3: MLKL-HA-FLAG cells and Western blotting was performed with indicated antibodies. (B) Detection of MLKL tetramers by non-reducing SDS-PAGE. Reduction of MLKL tetramers was performed by incubating samples in 10mM β-mercaptoethanol (βME) at 30°C for 30 minutes. Western blotting was performed with antibodies against p-S358 of MLKL (upper panel) or FLAG-tag (lower panel). (C) Resolution of MLKL polymers by semi-denaturing detergent agarose gel electrophoresis (SDD-AGE). MLKL polymers were reduced by incubating

samples in 5mM dithiothreitol (DTT) at 30°C for 30 minutes. (D) *In vitro* MLKL polymerization assay. Recombinant GST-NTD protein was incubated at 4°C (Lane 1) or 37°C (lane 2) for 16 hours. Half of the 37°C sample was then incubated with 5mM DTT at 30°C for 30 minutes (lane 3). (E) Increasing amounts of Trx1 or CS2 mutant (3μM, 10μM and 30μM) were mixed with 5μM recombinant GST-NTD-FLAG, and incubated at 37°C to induce MLKL polymerization. The samples were separated by non-reducing SDS-PAGE (upper panel) or regular SDS-PAGE (lower panel). (F) Samples were prepared as in (E). MLKL polymers were resolved by SDD-AGE (upper panel), and protein loading was visualized with Coomassie Blue staining (lower panel).

MLKL-HA-FLAG cells. Cells were treated with or without Dox for 24 hours followed by increasing amounts of PX-12 ranging from 3μM to 30μM for an additional 16 hours. Again, z-VAD-fmk was given to all experimental samples to eliminate the possibility of PX-12-induced apoptosis. Dox-treated cells, which express GFP-RIP3 and MLKL-HA-FLAG, exhibited an increased sensitivity to PX-12 treatment than cells given DMSO (control) (Figure 2.5A). Importantly, co-treatment with NSA blocked PX-12-induced cell death, confirming that PX-12 induced MLKL-dependent necroptosis as opposed to other cell death types (Figure 2.5A). Cells were also stained with the cell-impermeable DNA dye Sytox Green to confirm that cells exhibited a necrotic-like phenotype [34]. Our findings confirmed that the observed cell death type was due to necroptosis and not apoptosis (Figure 2.5B).

After determining that RIP3-MLKL expression sensitized cells to PX-12-induced cell death, we evaluated the status of canonical biomarkers of necroptosis. PX-12 treatment induced MLKL phosphorylation at a putative RIP3-specific phosphorylation site, S358, indicating that RIP3 kinase activity was stimulated during PX-12-induced cell death (Figure 2.5C) [35]. Moreover, MLKL FLAG-IP assays determined that RIP1, RIP3, and

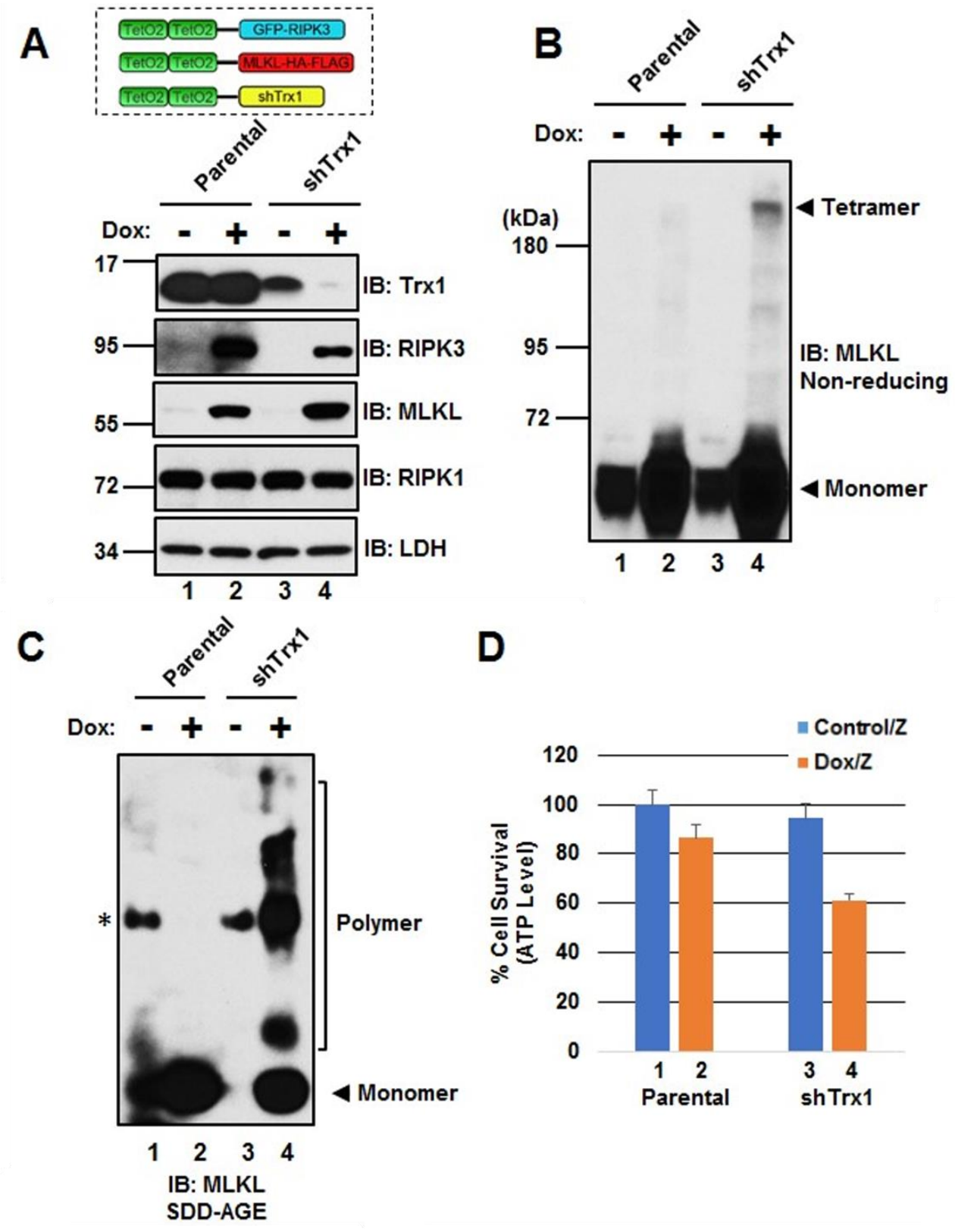
A
TetO2 TetO2 GFP-RIPK3
TetO2 TetO2 MLKL-HA-FLAG
TetO2 TetO2 shTrx1
Parental
shTrx1
Dox: - + - +
17
IB: Trx1
95
IB: RIPK3
55
IB: MLKL
72
IB: RIPK1
34
IB: LDH
1 2 3 4
B
Parental
shTrx1
Dox: - + - +
(kDa)
180
95
72
Tetramer
IB: MLKL
Non-reducing
Monomer
1 2 3 4
C
Parental
shTrx1
Dox: - + - +
*
Polymer
Monomer
1 2 3 4
IB: MLKL
SDD-AGE
D
Control/Z
Dox/Z
120
100
80
60
40
20
0
% Cell Survival
(ATP Level)
1 2
Parental
3 4
shTrx1

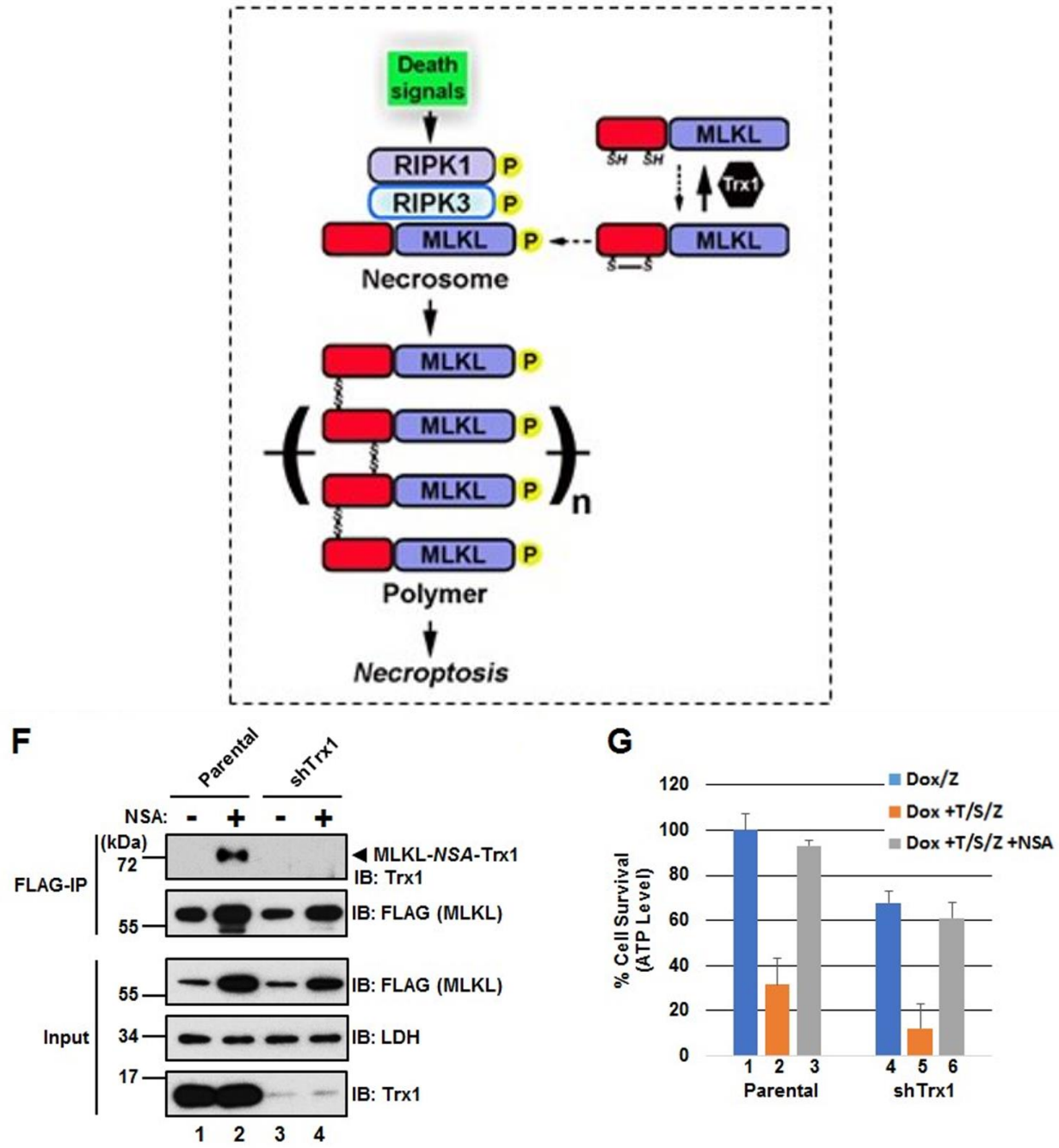

Figure 2.4 shRNA Trx1 knockdown promotes MLKL polymerization and sensitizes cells to necroptosis

(A) Lentiviruses encoding Dox-inducible shRNA against Trx1 were transduced into GFP-RIPK3: MLKL-HA-FLAG cells. Western blotting was performed to compare Trx1, RIPK3, and MLKL protein levels in parental cells versus lenti-shTrx1 cells. Cells were treated with Dox for 72 hours prior to preparation of whole cell extracts. (B) Cells were

treated with or without Dox for 72 hours. MLKL tetramers were examined by non-reducing SDS-PAGE. (C) Cells were treated with or without Dox for 72 hours, and MLKL polymers were examined by SDD-AGE. Asterisk denotes a non-specific signal. (D) Cells were treated with or without Dox for 72 hours and cell survival was measured by CellTiter Glo assay. z-VAD-fmk was added the whole time to protect against apoptosis. (E) Working model. Trx1 interacts with MLKL and keeps MLKL in a reducing state which prevents it from spontaneous disulfide bond formation and being recruited into the necrosome. (F) Parental or shTrx1 cells were treated with Dox for 24 hours before 5μM NSA addition for another 16 hours. MLKL complexes were purified by FLAG-IP and analyzed by Western blotting with antibodies against Trx1 or FLAG tag. Arrowhead points to NSA crosslinked MLKL and Trx1. (G) Cells were treated as indicated and cell survival was measured by CellTiter Glo assay.

MLKL were recruited to the necrosome complex in response to PX-12 treatment (Figure 2.5C). Lastly, PX-12 induced MLKL tetramer formation and polymerization demonstrated by non-reducing SDS-PAGE and SDD-AGE, respectively (Figure 2.5D and 2.5E). Taken together, Trx1 inhibition by PX-12 induced canonical biomarkers of necroptosis in GFP-RIPK3: MLKL-HA-FLAG cells (Figure 2.5F).

PX-12 induces RIPK3-independent necroptosis in MLKL NTD-DmrB cells

To test whether PX-12 could kill cells in a RIP3-independent manner, we tested PX-12 in NTD-DmrB cells, which were originally generated from HeLa cells which do not express RIP3 or endogenous MLKL [36]. In these cells, endogenous MLKL was knocked out with CRIPSR-Cas9 technology. As noted before, expression of NTD-DmrB is under the control of a Dox-inducible promoter (Figure 2.6A). The addition of Dimerizer forces the interaction of the DmrB domain, and induces MLKL polymerization and necroptosis [37]. To test whether the expression of NTD-DmrB sensitized cells to necroptosis after PX-12 treatment, we treated cells with or without Dox for 24 hours

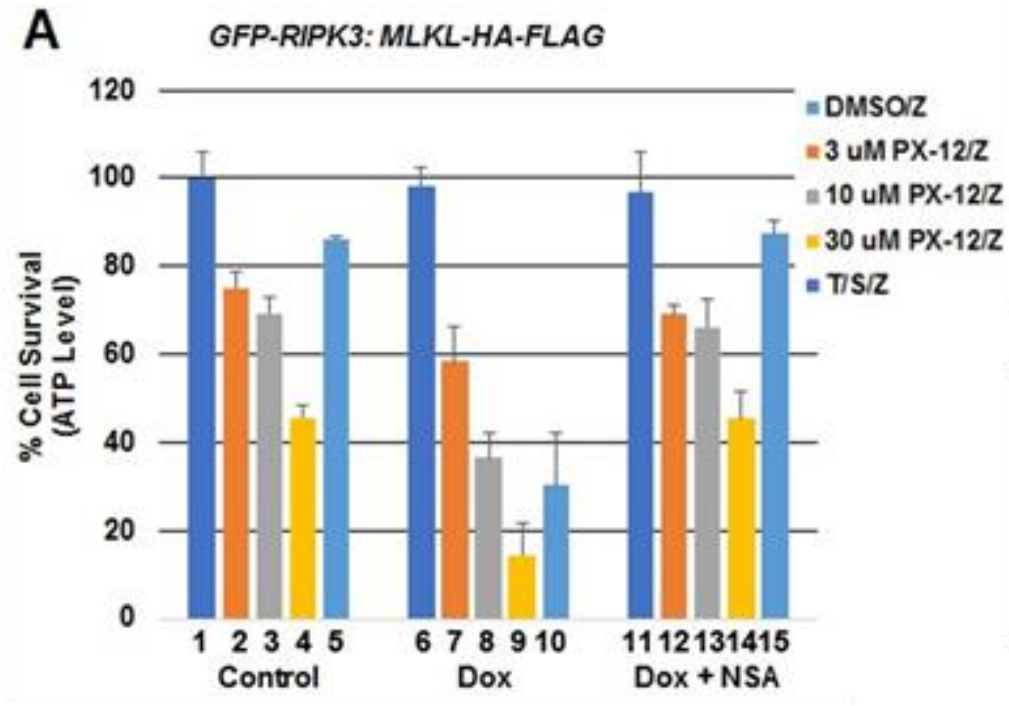
A
GFP-RIPK3: MLKL-HA-FLAG
% Cell Survival (ATP Level)
120
100
80
60
40
20
0
DMSO/Z
3 uM PX-12/Z
10 uM PX-12/Z
30 uM PX-12/Z
T/S/Z
1 2 3 4 5
Control
6 7 8 9 10
Dox
11 12 13 14 15
Dox + NSA

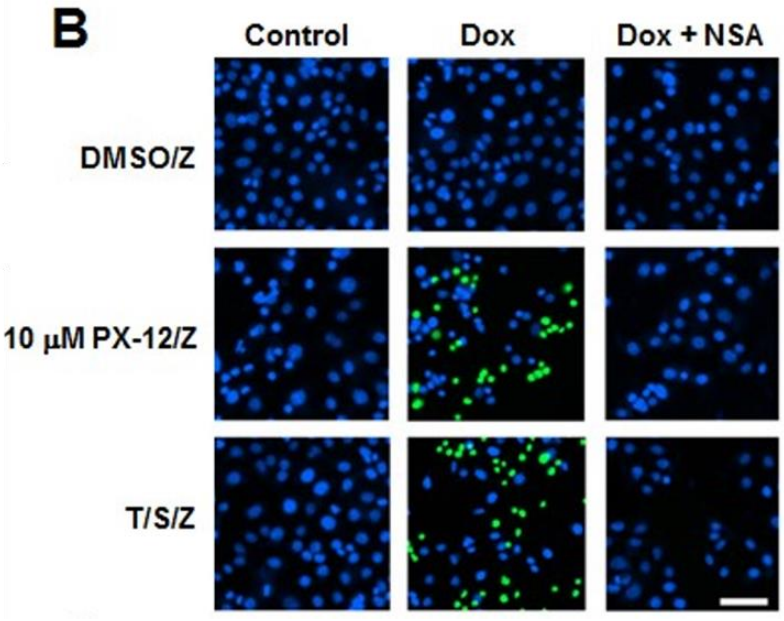
B
Control
Dox
Dox + NSA
DMSO/Z
10 μM PX-12/Z
T/S/Z

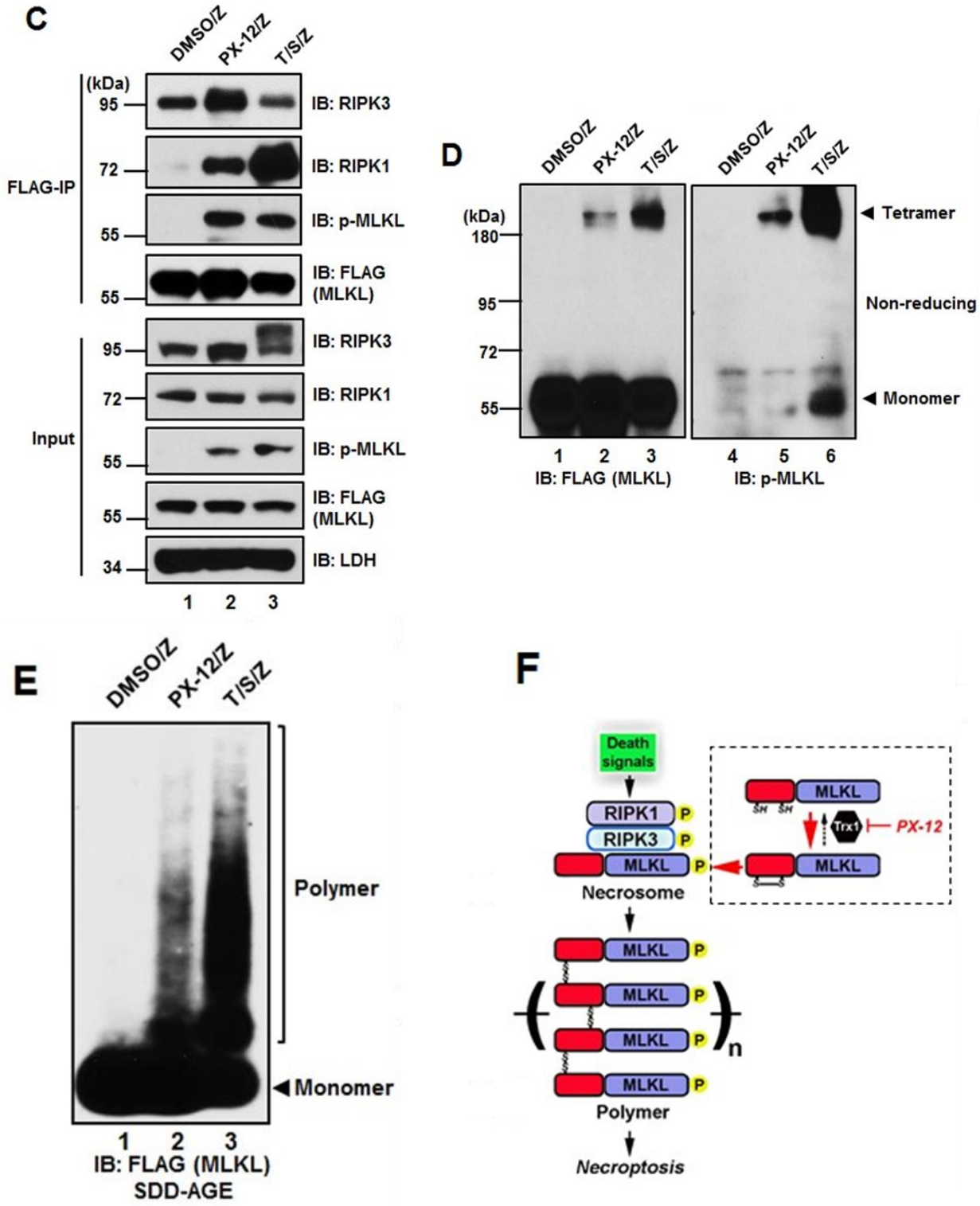
C
DMSO/Z
PX-12/Z
T/S/Z
(kDa)
95
72
55
55
FLAG-IP
IB: RIPK3
IB: RIPK1
IB: p-MLKL
IB: FLAG (MLKL)
95
72
55
55
34
Input
IB: RIPK3
IB: RIPK1
IB: p-MLKL
IB: FLAG (MLKL)
IB: LDH
1 2 3
D
DMSO/Z
PX-12/Z
T/S/Z
DMSO/Z
PX-12/Z
T/S/Z
(kDa)
180
95
72
55
Tetramer
Non-reducing
Monomer
1 2 3
IB: FLAG (MLKL)
4 5 6
IB: p-MLKL
E
DMSO/Z
PX-12/Z
T/S/Z
Polymer
Monomer
1 2 3
IB: FLAG (MLKL)
SDD-AGE
F
Death signals
RIPK1
RIPK3
MLKL
P
Necrosome
MLKL
Trx1
PX-12
MLKL
MLKL
MLKL
MLKL
n
Polymer
Necroptosis

Figure 2.5 PX-12 induces necrosome formation and necroptosis in GFP-RIPK3: MLKL-HA-FLAG cells
(A) CellTiter Glo cell survival assay following PX-12 titration (3-30μM). GFP-RIPK3: MLKL-HA-FLAG cells were treated with or without Dox for 24 hours followed by PX-12 or T/S/Z treatment for an additional 16 hours. z-VAD-fmk (20μM) was included in all treatments to prevent apoptosis. (B) Sytox Green and Hoechst staining of live cells. Scale bar represents 20μm. (C) GFP-RIPK3: MLKL-HA-FLAG cells were induced with Dox for 24 hours and then treated with 10μM PX-12 or T/S/Z for 6 hours. Whole cell extracts were subjected to FLAG-IP, followed by Western blotting with indicated antibodies. (D) Cells were treated as in (C) and whole cell extracts were separated by non-reducing SDS-PAGE. Western blotting was performed with anti-FLAG (left panel) or anti-pS358 MLKL antibody (right panel). (E) Cells were treated as in (C) and whole cell extracts were separated by SDD-AGE. (F) Working model. Trx1 interacts with MLKL under normal conditions to prevent MLKL polymerization. Trx1 inhibition increases MLKL disulfide bond formation, and promotes its recruitment into the necrosome complex to trigger necroptosis.

followed by increasing concentrations of PX-12 (1μM-10μM) in combination with z-VAD-fmk for an additional 16 hours. Cell death was measured by cell survival by CellTiter Glo assay. Cells expressing NTD-DmrB were significantly sensitized to PX-12-induced cell death, which could be blocked by co-treatment with NSA (Figure 2.6B, column 4, 9 and 14). Cell death was confirmed to be necrotic in nature by Sytox Green staining (Figure 2.6C). PX-12 also appeared to stabilize NTD-DmrB, and promoted the formation of MLKL tetramers and high molecular weight polymers (Figure 2.6D and 2.6E). These results suggest that inhibition of Trx1 can promote necroptosis in a RIPK3-independent manner by promoting MLKL polymerization directly, and thus has implications in cancer biology (Figure 2.6F, right panel). In fact, PX-12 has been tested in Phase II clinical trials; however, it proved to be ineffective for the treatment of advanced pancreatic and gastrointestinal cancers [38, 39]. Therefore, it is conceivable that cells with elevated MLKL expression may be more susceptible to PX-12 treatment. Further investigation

will need to be conducted to determine whether PX-12 can induce necroptosis *in vivo* models, and if so, does it do so in a RIP3-dependent or independent manner as depicted in Figure 2.6F.

Discussion

Necroptosis has garnered increasing attention over the past several years for its implications in host immune defense and human disease. At the heart of the necroptotic pathway is RIP1, RIP3 and MLKL, the major components of the necrosome complex. In mammalian cells, RIP3-dependent MLKL activation leads to the formation of toxic MLKL polymers [37]. Current models of necroptosis indicate that MLKL polymers are responsible for disrupting the integrity of the plasma membrane. MLKL polymers were previously shown to be stabilized by intermolecular disulfide bonds as reducing agents such as dithiothreitol and β-mercaptoethanol readily dissociate polymers *in vitro* [11, 37]. Yet, the mechanistic details as to how these polymers are formed remains unresolved. We identified Trx1, a thiol oxidoreductase, as a MLKL binding partner. As previously illustrated, Trx1 interacts with MLKL under normal conditions, and actively maintains it in a reduced inactive state. However, when Trx1 activity is perturbed, MLKL is incorporated into the necrosome complex, thus enabling MLKL to assemble into high molecular weight polymers that are necessary for executing necroptosis. Whether oxidation plays a role in activating MLKL polymerization though remains an open question in the field.

Interestingly, mitochondrial dysfunction and ROS production has been observed during

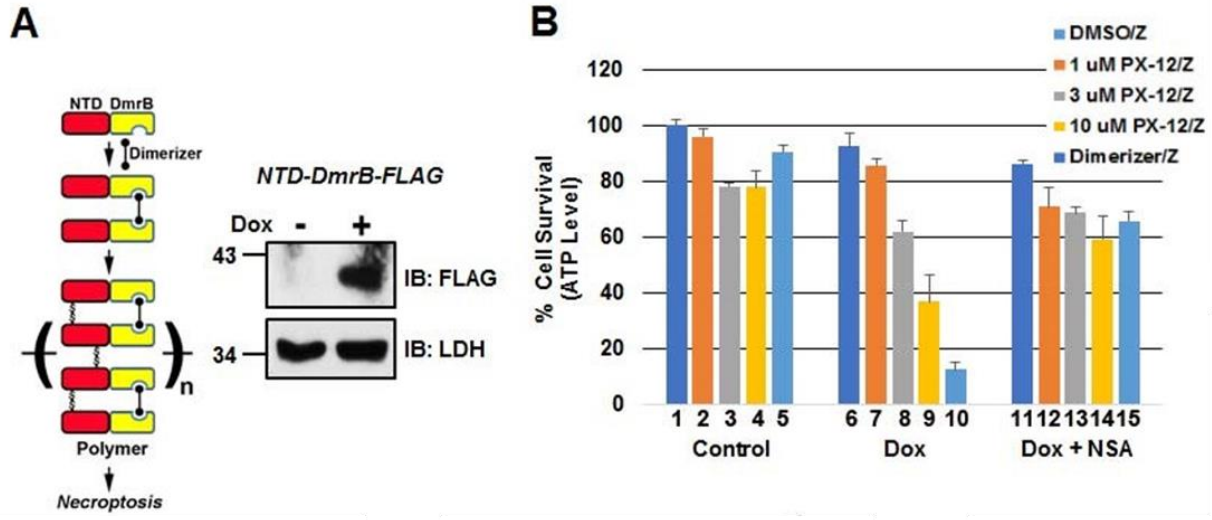
A
NTD DmrB
Dimerizer
Polymer
Necroptosis
NTD-DmrB-FLAG
Dox - +
43
IB: FLAG
34
IB: LDH
B
DMSO/Z
1 uM PX-12/Z
3 uM PX-12/Z
10 uM PX-12/Z
Dimerizer/Z
% Cell Survival (ATP Level)
120
100
80
60
40
20
0
1 2 3 4 5
6 7 8 9 10
11 12 13 14 15
Control
Dox
Dox + NSA

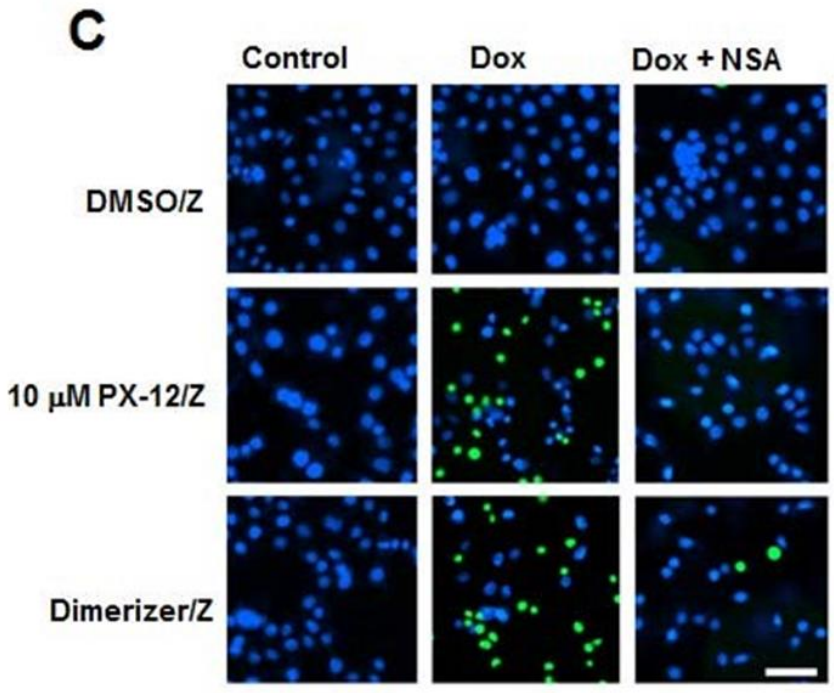
C
Control
Dox
Dox + NSA
DMSO/Z
10 μM PX-12/Z
Dimerizer/Z

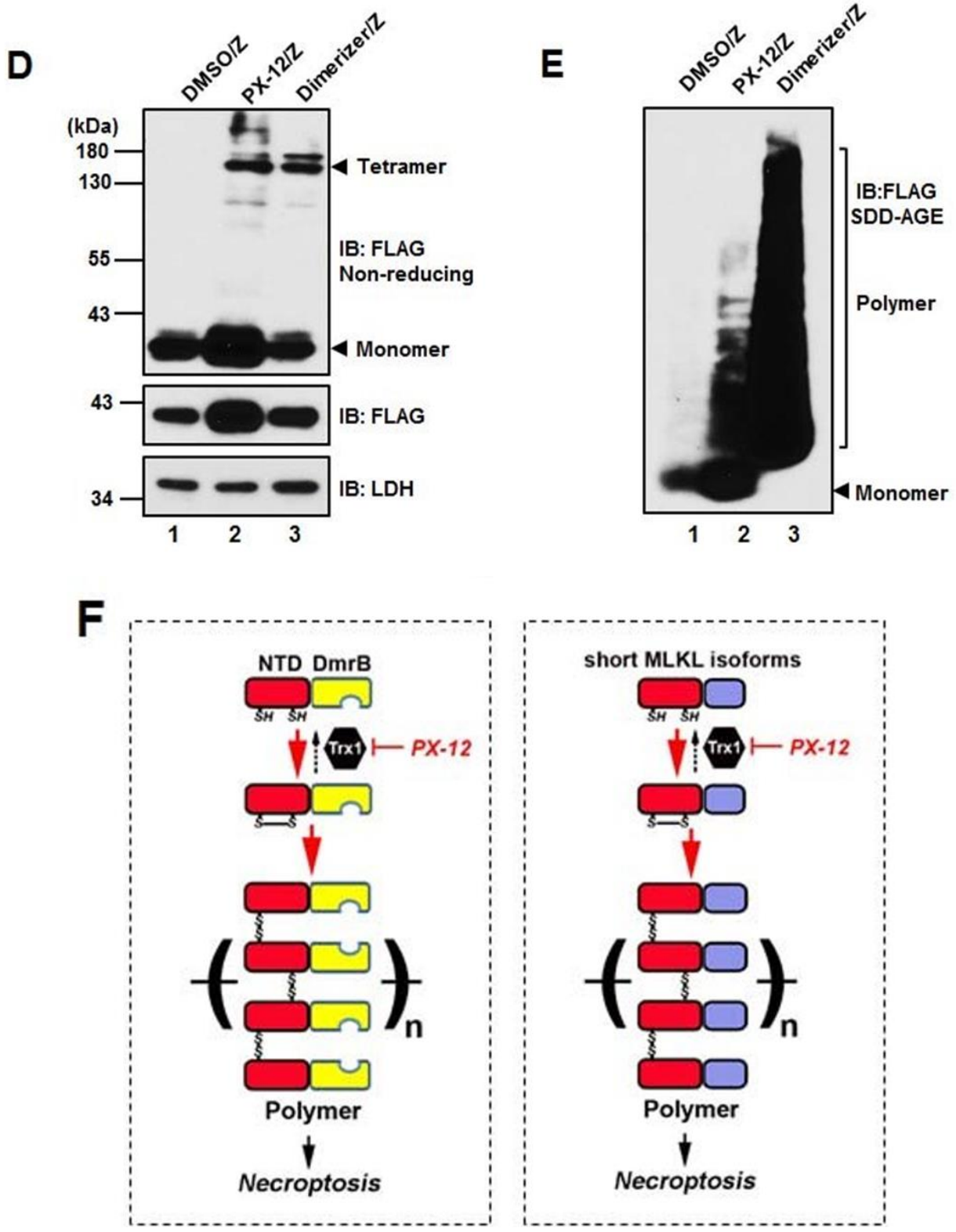
D
DMSO/Z
PX-12/Z
Dimerizer/Z
(kDa)
180
130
55
43
43
34
Tetramer
IB: FLAG
Non-reducing
Monomer
IB: FLAG
IB: LDH
1
2
3
E
DMSO/Z
PX-12/Z
Dimerizer/Z
IB:FLAG
SDD-AGE
Polymer
Monomer
1
2
3
F
NTD DmrB
SH SH
Trx1
PX-12
Polymer
Necroptosis
short MLKL isoforms
SH SH
Trx1
PX-12
Polymer
Necroptosis

Figure 2.6 PX-12 induces RIPK3-independent MLKL polymerization in NTD-DmrB cells
(A) Western blot characterization of Dox-inducible NTD-DmrB expression. With Dimerizer, NTD-DmrB forms disulfide bond-dependent polymers to trigger necroptosis. (B) CellTiter Glo cell survival assay following PX-12 titration (1-10μM). NTD-DmrB-FLAG cells were treated with or without Dox for 24 hours followed by PX-12 or Dimerizer treatment for an additional 16 hours. z-VAD-fmk (20μM) was included in all treatments to prevent apoptosis. (C) Sytox Green and Hoechst staining of live cells. Scale bar represents 20μm. (D-E) Assessment of MLKL tetramer and oligomer formation by non-reducing SDS-PAGE and SDD-AGE, respectively. (F) Working model. (Left panel) Trx1 inhibition promotes necrosome formation and RIP3-dependent MLKL activation and polymerization. (Right panel) Trx1 inhibition may also directly induce disulfide bond-dependent MLKL polymer formation to promote necroptosis.

necroptosis leading researchers to hypothesize that oxidation plays an important role during necroptosis [40-42]. Moreover, RIP1 was recently shown to be activated by ROS generated during TNFα-induced necroptosis in L929 murine cells [20]. Here, we propose that Trx1 may be directly exerting its oxidoreductase activity on MLKL to suppress necroptosis. It is conceivable that elevated ROS levels may perturb Trx1 activity, although this idea has not been thoroughly investigated. This is supported by our findings which show that genetic and pharmacological inhibition of Trx1 enhanced MLKL activation as seen by polymer formation, resulting in higher sensitivity to necroptosis. Interestingly, RIP3, a major component of the necrosome, was dispensable for executing necroptosis as a result of Trx1 inhibition (Figure 2.6), supporting the notion that Trx1 activates MLKL directly. However, the presence of RIP3 may still facilitate MLKL activation in this context given that MLKL S358 phosphorylation and RIP1/3 necrosome recruitment was detected when Trx1 activity was inhibited (Figure 2.5).

Markedly, only a fraction of total MLKL was crosslinked to Trx1, suggesting that the majority of MLKL is not associated to Trx1 at any given time. One explanation for this result is that the interaction between Trx1 and MLKL may be transient, which is common among an enzyme and its substrates. Previous reports indicate that the associations between Trx1 and its substrates are relatively weak and short-lived, particularly during oxidative stress. For example, Trx1 maintains apoptosis signal-regulating kinase 1 (ASK1) in a reduced, inactive state under normal conditions; however, increase in oxidative-stress dissociates Trx1-ASK1 and induces apoptosis [25, 27]. We hypothesize that Trx1 may be regulating MLKL in a similar manner. Therefore, NSA may be primarily trapping Trx1 molecules that come into contact with MLKL intermittently, which may explain why we were not able to co-immunopurify Trx1 with MLKL using standard IP assays. As shown in Figure 2.2, this problem was overcome by increasing the amount of available Trx1 using recombinant protein. Trx1 immobilized nickel beads were able to pulldown endogenous MLKL from HT29 cell extracts. Notably, Trx1 preferentially bound monomeric MLKL suggesting that active MLKL polymers have a lower affinity for Trx1 binding (Figure 2.2C). Thus, alterations in MLKL conformation that occur during necroptosis, potentially via RIP3-dependent phosphorylation, may lead to Trx1-MLKL dissociation. To better understand this phenomenon, further analysis is required to determine the precise conformational changes in MLKL that affect Trx1 binding.

Overall, these findings provide a deeper understanding of the regulatory networks that control MLKL activation. This is the first line of evidence to implicate Trx1 as a binding partner and suppressor of MLKL in cells. Future studies will be directed towards *in vivo* validation of Trx-1-MLKL interaction, and whether Trx1 inhibition induces necroptosis in tissues. Lastly, reports linking Trx1-inhibition to apoptosis in cells is well established [33, 43, 44], however, our results expand cell death outcomes induced by Trx1 inhibition to necroptosis. The notion that inhibition of Trx1 with PX-12 sensitizes cells to necroptosis could have significant implication in cancer therapy. PX-12 has been employed in cancer clinical trials without obvious efficacy [38, 39]. However, our data suggest that PX-12-induced necroptosis depends on elevated levels of MLKL expression (Figure 2.5 and Figure 2.6). Identifying cancer patients with high MLKL expressing tumors will potentially result in better outcomes with PX-12 treatment.

References

1. Degterev, A., et al., *Identification of RIP1 kinase as a specific cellular target of necrostatins.* Nat Chem Biol, 2008. **4**(5): p. 313-21.
2. Kaiser, W.J., et al., *RIP3 mediates the embryonic lethality of caspase-8-deficient mice.* Nature, 2011. **471**(7338): p. 368-72.
3. Moujalled, D.M., et al., *TNF can activate RIPK3 and cause programmed necrosis in the absence of RIPK1.* Cell Death Dis, 2013. **4**: p. e465.
4. Murphy, J.M., et al., *The pseudokinase MLKL mediates necroptosis via a molecular switch mechanism.* Immunity, 2013. **39**(3): p. 443-53.
5. Remijsen, Q., et al., *Depletion of RIPK3 or MLKL blocks TNF-driven necroptosis and switches towards a delayed RIPK1 kinase-dependent apoptosis.* Cell Death Dis, 2014. **5**: p. e1004.
6. Vanlangenakker, N., et al., *TNF-induced necroptosis in L929 cells is tightly regulated by multiple TNFR1 complex I and II members.* Cell Death Dis, 2011. **2**: p. e230.
7. Wu, J., et al., *Mlkl knockout mice demonstrate the indispensable role of Mlkl in necroptosis.* Cell Res, 2013. **23**(8): p. 994-1006.

8. McComb, S., et al., *cIAP1 and cIAP2 limit macrophage necroptosis by inhibiting Rip1 and Rip3 activation.* Cell Death Differ, 2012. **19**(11): p. 1791-801.
9. Moquin, D.M., T. McQuade, and F.K. Chan, *CYLD deubiquitinates RIP1 in the TNFalpha-induced necrosome to facilitate kinase activation and programmed necrosis.* PLoS One, 2013. **8**(10): p. e76841.
10. Wu, Y.T., et al., *zVAD-induced necroptosis in L929 cells depends on autocrine production of TNFalpha mediated by the PKC-MAPKs-AP-1 pathway.* Cell Death Differ, 2011. **18**(1): p. 26-37.
11. Wang, H., et al., *Mixed lineage kinase domain-like protein MLKL causes necrotic membrane disruption upon phosphorylation by RIP3.* Mol Cell, 2014. **54**(1): p. 133-46.
12. Sun, L., et al., *Mixed lineage kinase domain-like protein mediates necrosis signaling downstream of RIP3 kinase.* Cell, 2012. **148**(1-2): p. 213-27.
13. Zhao, J., et al., *Mixed lineage kinase domain-like is a key receptor interacting protein 3 downstream component of TNF-induced necrosis.* Proc Natl Acad Sci U S A, 2012. **109**(14): p. 5322-7.
14. Chen, X., et al., *Translocation of mixed lineage kinase domain-like protein to plasma membrane leads to necrotic cell death.* Cell Res, 2014. **24**(1): p. 105-21.
15. Dondelinger, Y., et al., *MLKL compromises plasma membrane integrity by binding to phosphatidylinositol phosphates.* Cell Rep, 2014. **7**(4): p. 971-81.
16. Quarato, G., et al., *Sequential Engagement of Distinct MLKL Phosphatidylinositol-Binding Sites Executes Necroptosis.* Mol Cell, 2016. **61**(4): p. 589-601.
17. Cai, Z., et al., *Plasma membrane translocation of trimerized MLKL protein is required for TNF-induced necroptosis.* Nat Cell Biol, 2014. **16**(1): p. 55-65.
18. Su, L., et al., *A plug release mechanism for membrane permeation by MLKL.* Structure, 2014. **22**(10): p. 1489-500.
19. Huang, D., et al., *The MLKL Channel in Necroptosis Is an Octamer Formed by Tetramers in a Dyadic Process.* Mol Cell Biol, 2017. **37**(5).
20. Zhang, Y., et al., *RIP1 autophosphorylation is promoted by mitochondrial ROS and is essential for RIP3 recruitment into necrosome.* Nat Commun, 2017. **8**: p. 14329.
21. Shindo, R., et al., *Critical contribution of oxidative stress to TNFalpha-induced necroptosis downstream of RIPK1 activation.* Biochem Biophys Res Commun, 2013. **436**(2): p. 212-6.
22. Wang, Z., et al., *The mitochondrial phosphatase PGAM5 functions at the convergence point of multiple necrotic death pathways.* Cell, 2012. **148**(1-2): p. 228-43.
23. Du, Y., et al., *Thioredoxin 1 is inactivated due to oxidation induced by peroxiredoxin under oxidative stress and reactivated by the glutaredoxin system.* J Biol Chem, 2013. **288**(45): p. 32241-7.
24. Arner, E.S. and A. Holmgren, *Physiological functions of thioredoxin and thioredoxin reductase.* Eur J Biochem, 2000. **267**(20): p. 6102-9.

25. Jin, R., et al., *Trx1/TrxR1 system regulates post-selected DP thymocytes survival by modulating ASK1-JNK/p38 MAPK activities.* Immunol Cell Biol, 2015. **93**(8): p. 744-52.
26. Sueblinvong, V., et al., *Nuclear Thioredoxin-1 Overexpression Attenuates Alcohol-Mediated Nrf2 Signaling and Lung Fibrosis.* Alcohol Clin Exp Res, 2016. **40**(9): p. 1846-56.
27. Wu, X., et al., *Inhibition of thioredoxin-1 with siRNA exacerbates apoptosis by activating the ASK1-JNK/p38 pathway in brain of a stroke model rats.* Brain Res, 2015. **1599**: p. 20-31.
28. Saitoh, M., et al., *Mammalian thioredoxin is a direct inhibitor of apoptosis signal-regulating kinase (ASK) 1.* Embo j, 1998. **17**(9): p. 2596-606.
29. Rand, J.D. and C.M. Grant, *The thioredoxin system protects ribosomes against stress-induced aggregation.* Mol Biol Cell, 2006. **17**(1): p. 387-401.
30. Lopez-Mirabal, H.R. and J.R. Winther, *Redox characteristics of the eukaryotic cytosol.* Biochim Biophys Acta, 2008. **1783**(4): p. 629-40.
31. Matsui, M., et al., *Early embryonic lethality caused by targeted disruption of the mouse thioredoxin gene.* Dev Biol, 1996. **178**(1): p. 179-85.
32. Baker, A.F., et al., *The antitumor thioredoxin-1 inhibitor PX-12 (1-methylpropyl 2-imidazolyl disulfide) decreases thioredoxin-1 and VEGF levels in cancer patient plasma.* J Lab Clin Med, 2006. **147**(2): p. 83-90.
33. Tan, Y., et al., *Thioredoxin-1 inhibitor PX-12 induces human acute myeloid leukemia cell apoptosis and enhances the sensitivity of cells to arsenic trioxide.* Int J Clin Exp Pathol, 2014. **7**(8): p. 4765-73.
34. Grootjans, S., et al., *A real-time fluorometric method for the simultaneous detection of cell death type and rate.* Nat Protoc, 2016. **11**(8): p. 1444-54.
35. Rodriguez, D.A., et al., *Characterization of RIPK3-mediated phosphorylation of the activation loop of MLKL during necroptosis.* Cell Death Differ, 2016. **23**(1): p. 76-88.
36. Moriwaki, K., et al., *Differential roles of RIPK1 and RIPK3 in TNF-induced necroptosis and chemotherapeutic agent-induced cell death.* Cell Death Dis, 2015. **6**: p. e1636.
37. Hildebrand, J.M., et al., *Activation of the pseudokinase MLKL unleashes the four-helix bundle domain to induce membrane localization and necroptotic cell death.* Proc Natl Acad Sci U S A, 2014. **111**(42): p. 15072-7.
38. Baker, A.F., et al., *A phase IB trial of 24-hour intravenous PX-12, a thioredoxin-1 inhibitor, in patients with advanced gastrointestinal cancers.* Invest New Drugs, 2013. **31**(3): p. 631-41.
39. Ramanathan, R.K., et al., *A randomized phase II study of PX-12, an inhibitor of thioredoxin in patients with advanced cancer of the pancreas following progression after a gemcitabine-containing combination.* Cancer Chemother Pharmacol, 2011. **67**(3): p. 503-9.
40. Ma, Y.M., et al., *Novel CHOP activator LGH00168 induces necroptosis in A549 human lung cancer cells via ROS-mediated ER stress and NF-kappaB inhibition.* Acta Pharmacol Sin, 2016. **37**(10): p. 1381-1390.

41. Qu, Y., et al., *MLKL inhibition attenuates hypoxia-ischemia induced neuronal damage in developing brain.* Exp Neurol, 2016. **279**: p. 223-31.
42. Fulda, S., *Regulation of necroptosis signaling and cell death by reactive oxygen species.* Biol Chem, 2016. **397**(7): p. 657-60.
43. Schroeder, A., et al., *Targeting Thioredoxin-1 by dimethyl fumarate induces ripoptosome-mediated cell death.* Sci Rep, 2017. **7**: p. 43168.
44. You, B.R., et al., *PX-12 induces apoptosis in Calu-6 cells in an oxidative stress-dependent manner.* Tumour Biol, 2015. **36**(3): p. 2087-95.

Chapter 3. MLKL membrane association and lysosome rupture

Introduction

A defining morphological feature of necroptosis is the disintegration of cellular membranes. Breakdown of membranous structures, in particular the plasma membrane, distinguishes necroptosis from non-immunogenic cell death programs such as apoptosis, and is the preeminent factor attributed with its pro-inflammatory nature [1]. Previously described as an “ordered cellular explosion”, necroptosis-associated membrane rupture causes cells to release their contents into the surrounding tissue thereby signaling an inflammatory response [2]. As a result, membrane rupture presents serious consequences for human health. Excessive necroptotic cell death and subsequent inflammation contributes to a wide array of human pathophysiological conditions [3-5]. Given these outcomes, cells have evolved several regulatory measures to tightly control necroptosis and prevent undesired cell death from occurring, many of which also control apoptosis [6-8]. In effect, necroptosis is regularly suppressed in cells, and is only triggered under very specific conditions. This is best exemplified by previous experiments showing that genetic ablation of RIP3 or MLKL, core components of the necrosome complex, had no physical effects at any stage during mouse embryogenesis or further developmental processes throughout adulthood [8]. Therefore, the contribution of necroptosis in human disease is thought to be acquired from dysregulated necroptotic signaling molecules, particularly RIP1, RIP3, or MLKL [3, 9, 10]. Upregulated expression of central necroptotic genes sensitizes cells to death

stimuli by surpassing the inhibitory threshold of the aforementioned regulatory networks. In order to find methods for preventing the negative effects of unchecked necroptosis, researchers have focused their efforts in understanding the final stages of the necroptotic pathway which encompasses MLKL-mediated membrane rupture.

Conversely, necroptotic cellular membrane rupture is a critical mechanism for host immune defense against microbial infection, particularly those manifested by viruses. A growing number of viruses including HSV-1/2 and IAV have been shown to modulate necroptotic cell death signaling in mammalian cells [11, 12]. Cells equipped with the appropriate necroptotic machinery sense certain viral components (e.g. viral RNA and DNA) during an infection, and transduce necroptotic signals through RHIM-domain mediated protein interactions (i.e. TRIF, ZBP1, and RIP1/3) [13, 14]. Consequently, membrane rupture serves as a beneficial barrier against viral propagation by mounting a two-prong immune response. First, necroptosis eliminates infected cells, thus hindering the spread of infection to other healthy cells [15]. Secondly, the release of damage-associated molecular patterns that simultaneously alert nearby cells of the innate immune system to the site of infection [16, 17]. The combination of cell death and activation of the host's antiviral immune response coordinates efficient clearance of viral particles. Although this approach appears potentially harmful, necroptosis is evolutionarily advantageous as it serves as an insurance policy that protects organisms against invading pathogens in times when apoptosis is not sufficient for clearing the infection [18, 19]. This is bolstered by several *in vivo* findings showing that RIP3

knockout mice succumb to viral infection and die shortly after being inoculated [11, 12, 20].

Altogether, membrane rupture is a critical step in executing necroptosis, and is caused in part by the direct action of MLKL [21]. Under necroptotic conditions, MLKL is recruited to the necrosome, a multi-protein complex central for transducing necroptotic signals that contains serine/threonine kinases, RIP1 and RIP3 [22]. RIP3-dependent phosphorylation of MLKL's C-terminal kinase-like domain promotes the formation of high molecular weight MLKL polymers that localize to the surface of various cellular compartments [23-25]. Early biochemical studies indicated that activated forms of MLKL translocated to membrane-rich fractions which was determined by subjecting cellular extracts to differential centrifugation [23, 26]. Moreover, cell-free assays using recombinant MLKL protein revealed that its ability to associate with membranes was attributed to its N-terminal 4HBD [27, 28]. Overexpression of MLKL's 4HBD is sufficient for executing necroptosis, and was shown to interact with various subtypes cellular compartments [23, 29]. These results were corroborated using immunofluorescent MLKL staining which demonstrated that MLKL formed distinct punctae that were enriched primarily at the plasma membrane in murine cells while human MLKL was detected with mitochondria, endoplasmic reticulum, and lysosomes, in addition to the plasma membrane suggesting that executing necroptosis differs slightly between species [23, 30, 31].

Once membrane bound, MLKL polymers disrupt the integrity of their target membranes ultimately causing cell death. Yet many outstanding questions regarding this process remain unanswered such as 1.) What is the precise molecular mechanism by which MLKL disrupts membranous structures? 2.) Is MLKL solely responsible for membrane rupture, or are other factors involved? 3.) Is MLKL-mediated membrane permeabilization non-selective, or are specific organelles preferentially targeted in order to execute cell death? 4.) Is membrane rupturing the final step of necroptosis, or do molecules leaked from permeabilized organelles play a role in downstream signaling events? By better understanding MLKL-mediated membrane rupture and subsequent consequences, strategies for developing therapeutic approaches for modulating necroptosis *in vivo* are expected to emerge.

So far, a class of small molecule inhibitors known as necrostatins, which target upstream RIP1 kinase activity, along with a few RIP3 inhibitors have been successfully utilized for blocking necroptosis in cells grown in culture and in mice [32-35]. However, given their effects on other important signaling pathways, primarily those involved in apoptosis and inflammatory cytokine production, these compounds pose significant problems in terms of undesired side-effects [36, 37]. Another well-known compound, NSA, was discovered to be a direct inhibitor of MLKL [38]. NSA covalently modifies Cys86 of the human MLKL protein, and blocks proper MLKL polymer formation [38]. Unfortunately, given that it reacts with cysteine residues found on other proteins, NSA has proven to be impractical for *in vivo* use. Nonetheless, *in vitro* use of NSA has

provided a proof of principle indicating that MLKL inhibition, and perhaps downstream events, is a better route for blocking necroptosis. Therefore, identifying compounds that inhibit necroptosis at the level of MLKL provides a more stringent approach for treating necroptosis-associated human diseases in a more effective and specific manner.

As previously mentioned, various cellular organelles are targeted by MLKL, and thus implicated in being involved in the necroptotic pathway. In murine cells, MLKL localizes predominantly at the cell surface, which is largely in agreement with the prevailing model of necroptosis that depicts the rupturing of the plasma membrane as the final step in executing cell death. The morphological features of plasma membrane rupture if often shown through images taken by an electron microscope (EM) [2, 39]. EM images show necroptotic cells with a discontinuous plasma membrane indicating that rupture had occurred. The same was not detected in cells undergoing apoptosis. Furthermore, rupturing of the plasma membrane is necessary for the release of intracellular DAMPs. Over the past several years, the list of DAMPs has grown with the most cited molecules being nucleotides (i.e. ATP), nucleic acids, and HMGB1 [40]. Overall, studies of necroptosis in murine cells has shed light on the mechanism of MLKL-mediated plasma membrane rupture, although the same cannot be said about human cells.

In human cells, activated MLKL localizes to various cellular organelles with varying degrees of enrichment [23]. For instance, MLKL and RIP3 were shown to interact with mitochondrial serine/threonine-protein phosphatase PGAM5 providing a line of evidence

that mitochondria play a significant role during necroptosis in human cells [30, 41]. This is bolstered by in vitro binding data which suggested that MLKL interacts with cardiolipin [23]. Moreover, mitochondrial networks were shown to be fragmented after TSZ treatment [41]. In line with these findings, increase in ROS production was detected in a variety of cell types further suggesting that mitochondrial dysfunction and perturbations in oxidative phosphorylation occurred in response to necroptotic stimuli [42-44]. However, recent studies have challenged the notion of mitochondrial involvement in necroptosis. In one study, ablation of mitochondria by means of carbonyl cyanide m-chlorophenylhydrazone (CCCP)-induced mitophagy, did not affect the sensitivity of cells to TSZ [45]. Other studies indicate that deletion of PGAM5 and Drp1 also had no effect on apoptosis or necroptosis, and thus are dispensable for these cell death programs [30, 46]. Currently, it remains unclear whether necroptotic signals converge on the mitochondria. However, the possibility that mitochondria plays a role during necroptosis in specific cell types, or in a context-dependent manner cannot be ruled out. Therefore, further investigations are needed to determine whether mitochondria or other organelles are involved in the necroptotic process.

To this end, we decided to focus our efforts on the role of lysosomes in the human necroptotic pathway. Promising results produced in *C. elegans* and RIP3-expressing HeLa cells lines suggested the involvement of lysosome membrane rupture and lysosomal proteases in executing necroptosis [47-49]. Moreover, hydrolytic lysosomal enzymes, particularly the cathepsin family of proteases, have been implicated in

mediating necrotic cell death [49, 50]. Thus, this chapter will highlight experiments aimed at investigating the mechanism of lysosomal membrane leakage.

Results

Lysosomal membrane rupture occurs during necroptosis in human cells

Previous data indicate that lysosomal membrane rupture occurs in response to various necrotic stimuli in *C. elegans* [47, 51]. In accordance with these findings, our preliminary data suggested that lysosomes were also affected in human cells. Live-cell imaging indicated that lysosomal membranes were compromised in HT-29 cells after TSZ treatment (Figure 3.1). To detect this phenomenon, cells were pre-loaded with 10,000 MW FITC-labeled dextran beads. Dextran beads are endocytosed by the cells, and eventually stored in lysosomes [52]. Dextran bead-loaded lysosomes were observed as bright green punctae under a fluorescent microscope (Left panel Figure 3.1A). Under necroptotic conditions, the fluorescent green signal dispersed throughout the cytoplasm indicating that the dextran beads were no longer restricted within lysosomes due to lysosomal membrane permeabilization (Right panel, Figure 3.1B). However, whether lysosome membrane rupture is necessary for executing necroptosis, or merely a consequence of cell death remained an open question.

Given that dextran beads were released from lysosomes during necroptosis, presumably hydrolytic lysosomal enzymes would also be leaked into the cytoplasm. Indeed, preliminary data shows that cathepsin A, B, C, K were released into the

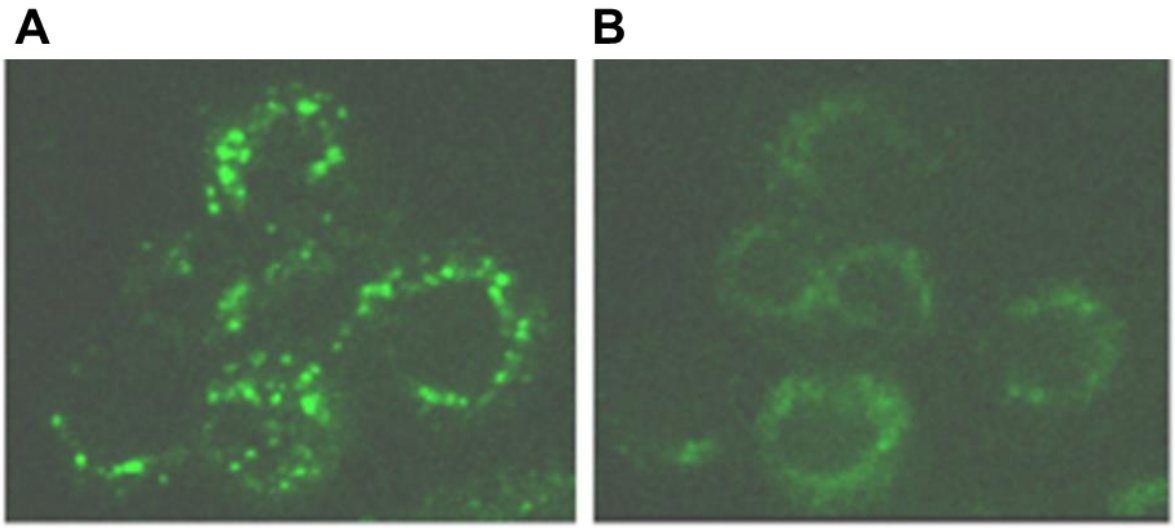

Figure 3.1 Lysosomes rupture during necroptosis in HT-29 cells. Lysosomes were labeled with 10,000 MW FITC-labeled dextran beads prior to TNFα-induced necroptosis induction. **(A)** Fluorescent green dextran lysosome labeling prior to necroptosis. **(B)** Fluorescent green dextran lysosome labeling after TSZ treatment.

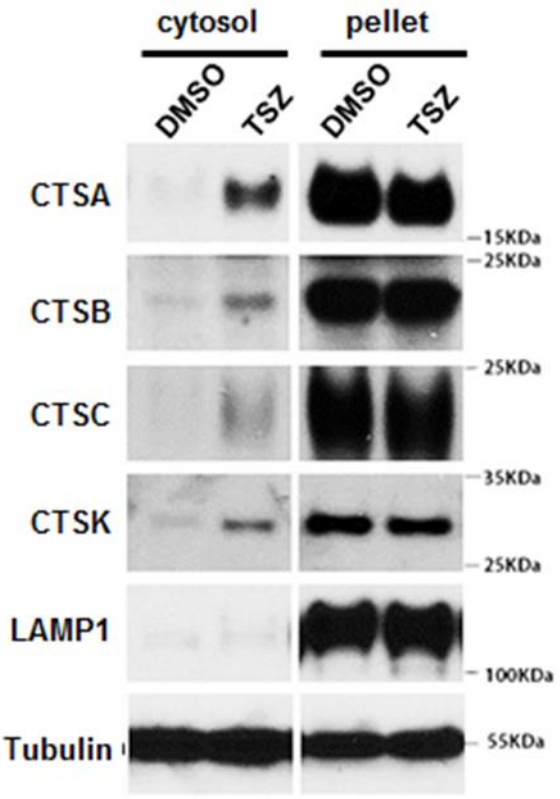

Figure 3.2 Cathepsin proteases are released into the cytosolic fraction after TSZ treatment. Cytosolic (S20) and crude membrane fractions (P20) of HT-29 cells treated with a vehicle control (DMSO) or TSZ were separated by centrifugation, and analyzed by Western blotting.

cytosolic fraction in response to TSZ treatment as detected by Western blotting (Figure 3.2). To test whether lysosomal enzymes contributed to cell death, cell survival was measured after co-treating RIP3-expressing HeLa cells with a cathepsin B inhibitor, CA-074Me [53]. Cathepsin B belongs to a family of lysosomal cysteine proteases involved in the degradation of protein substrates [54]. Importantly, cathepsins have been implicated in inducing necrotic forms of cells death [49, 53, 55]. CA-074Me partially protected cells from TSZ-induced necroptosis suggesting cell death is driven through a proteolytic process in which cathepsin B is involved (Figure 3.3). Altogether, lysosomal membrane rupture and subsequent release of luminal enzymes appears to play a significant role in executing necroptosis in human cells; however, their importance in *in vivo* models of necroptosis has yet to be determined. Additionally, the identity of factors involved in directly disrupting lysosomal membranes, which include RIP3 and MLKL, remained undetermined.

Establishment of *in vitro* cathepsin L leakage assay

Due to a lack of tools for studying lysosome rupture, it was necessary to develop a biochemical assay as a means for identifying factors involved in this process. Ideally, the assay would be able to detect active leakage of luminal lysosome enzymes in an unbiased manner. In theory, lysosomal leakage factors would be found in cytosolic cell

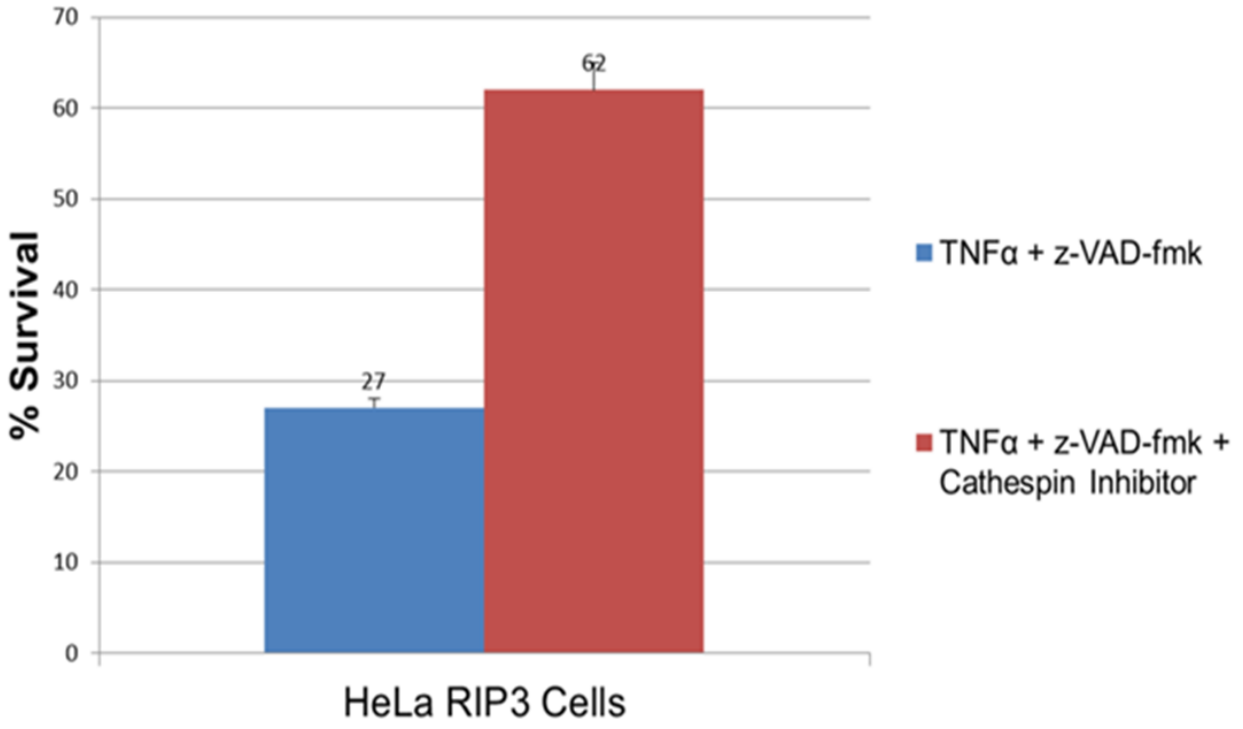

Figure 3.3 Cathepsin B CA-074Me blocks TSZ-induced necroptosis in RIP3-expressing HeLa cells. Cells were co-treated with TSZ and 1mM CA-074Me for 16 hours in a 96-well format. CellTiter Glo assay was used to measure cell death.

extracts. Therefore, the assay was designed in a way that cathepsin leakage emanating from crude lysosomal membrane fractions could be detected after incubation with necrotic cytosolic cell extracts. To this end, RIP3-expressing HeLa cells were stably transfected with a FLAG-tagged version of the lysosomal enzyme, Cathepsin L (CTSL). Crude membrane fractions (P20) were prepared from these cells, and subsequently incubated with cytosolic cell extracts (S20) from TSZ treated necroptotic cells. If CatL-FLAG was released, it would be detected in the soluble fraction either by enzymatic activity using a specific fluorescent cathepsin L substrate, Z-Phe-Arg-AMC, or by SDS-PAGE anti-FLAG immunoblotting. By probing against the FLAG epitope, the detection

of leaked CatL-FLAG is made highly sensitive, diminishing any unwanted background that may arise from endogenous cytosolic or membrane portions found within the system. Initial data showed that CatL-FLAG was released from P20 fractions after a 3-hour incubation at 30°C incubation suggesting that the assay was functioning as expected (Figure 3.4). Interestingly, CatL-FLAG leakage activity was found in both healthy and necroptotic cytosolic extracts. Moreover, CatL-FLAG leakage happened in a dose-dependent manner (Figure 3.5). However, it was unclear whether the leakage of CatL-FLAG was due to protein(s) activity or small molecules.

Induction of Cathepsin L leakage by NTD-DmrB polymers

As an alternative approach to test CatL-FLAG leakage, rather than using whole cell extracts derived from HT-29 cells, cytosolic S20 extracts from MLKL NTD-DmrB were utilized to determine whether MLKL polymers could lyse lysosomes within the P20 membrane fraction. To accomplish this, we set out to induce NTD-DmrB polymerization *in vitro* by adding DmrB dimerizing agent to the S20/P20 mixture and then examine CatL-FLAG release as previously described. However, we were unable to detect NTD-DmrB polymerization regardless of extract, Dimerizer, or incubation time tested (data not shown). A positive readout of proper *in vitro* polymerization would have to be comparable to NTD-DmrB polymers produced in cells prior to lysis as seen by Blue-Native PAGE Western blot analysis (Figure 3.6).

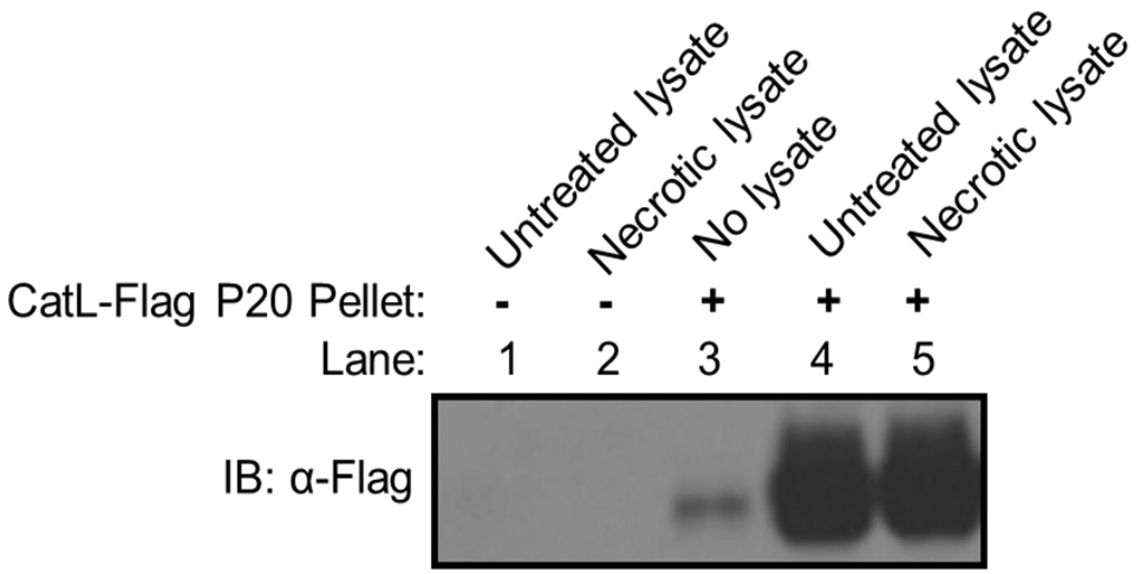

Figure 3.4 Cathepsin L (CatL-FLAG) lysosomal leakage assay. Cytosolic extracts (S100) from healthy and TSZ treated HeLa cells were tested for lysosome CatL-FLAG leakage activity. P20 crude lysosomal extracts containing recombinant FLAG-tag cathepsin L were incubated with S100 extracts to induce the release of CatL-FLAG into the soluble fraction. Anti-FLAG Western blotting was used to confirm CatL-FLAG leakage.

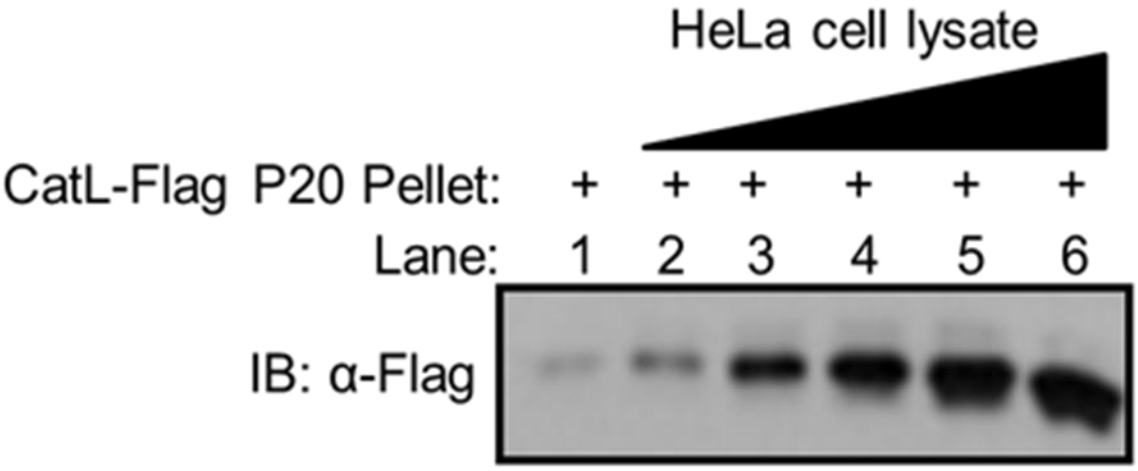

Figure 3.5 Cathepsin L leakage occurs in a dose-dependent manner. Increasing amounts of cytosolic S100 extract was incubated with P20 membrane fractions. Cathepsin L leakage was analyzed by anti-FLAG Western blotting.

Unfortunately, under the several conditions tested, we were unable to detect generation of NTD-DmrB polymers. As with any cell-free assay, there are several reasons that may explain why polymerization could not be achieved in S20 extracts. First, it is conceivable that cellular membranes facilitate or are required for MLKL polymerization, thus removal of the P20 fractions may have undermined the design of the experiment. However, supplementing the reaction with P20 or using whole cell extract also did not render positive results. Altogether, MLKL association with lysosomal membranes may rely on the architecture of an intact cell which would allow for proper membrane trafficking to lysosomes. It is also possible that the DmrB-domain simply is not accessible after cell lysis. The structure of NTD-DmrB may be altered, or non-specific protein binding may sterically hinder the DmrB-domain. Lastly, certain parameters needed for polymerization may not have been met. For instance, NTD-DmrB may need to meet a critical concentration barrier, perhaps in a specific cellular compartment or vesicle in order to polymerize. In our assay, NTD-DmrB may have been too dilute to successfully polymerize. All of these concerns may have contributed to the failure of this part of the project. Perhaps a better approach would be to test purified NTD-DmrB. NTD-DmrB could be purified either by immunoprecipitation, liquid chromatography, or from a human protein expression system like HEK293 cells. However, isolating recombinant MLKL poses problems in terms of it self-polymerizing during the purification process. It is possible that MLKL can be truncated further to find species that are stable and soluble in monomeric forms. The effect of truncated MLKL proteins would have to be tested in a cell death assay to confirm that they still retain their necroptosis executing function.

Verification of the cathepsin L leakage assay

To verify that the source of CatL-FLAG activity was coming from proteins, we used a protein spin column with a 5kDa molecular weight cutoff to separate small molecules from proteins in S100 cytosolic extracts. It is important to note that healthy extract was used since it exhibited the same activity as necroptotic extract. Small molecules pass through the protein column (flow through) while proteins larger than 5kDa were retained in the column. Both fractions were then applied to the CatL-FLAG leakage assay to determine whether the observed outcome was due to a small molecule or protein(s). CatL-FLAG leakage activity remained in the retained fraction indicating that proteins were responsible for the observed result (Figure 3.7).

As a secondary approach, cytosolic extracts were heat-treated at 65°C for different times as way of eliminating the lysosomal leakage activity. Under these conditions, most protein activity would be lost while small molecules would be left unaffected. As seen in Figure 3.8, heat-inactivation significantly reduced CatL-FLAG leakage activity. Again, lysosomal leakage was attributed to the action of proteins and not small molecules. Lastly, to identify the proteins responsible for CatL-FLAG leakage, cytosolic extracts were fractionated using a hydrophobic interacting column (HIC) via fast protein liquid chromatography (FPLC). Proteins possessing CatL-FLAG leakage activity bound to the HIC column, which eluted in fractions 7 and 8 as indicated by the anti-FLAG immunoblots and the resulting FPLC chromatogram (Figure 3.9). This was the first step in purifying the protein(s) responsible for lysosomal leakage. Through additional

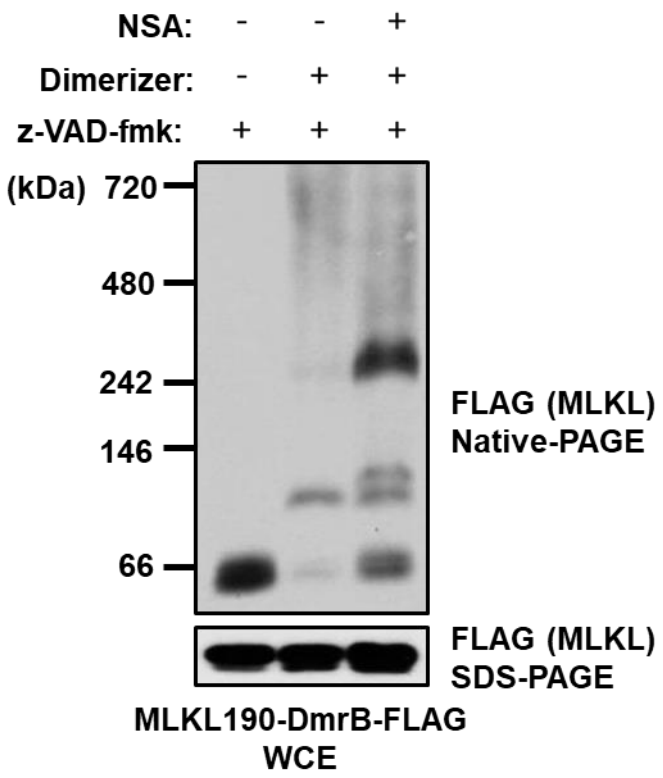

Figure 3.6 MLKL NTD-DmrB polymers resolved by Blue-Native PAGE. Whole cell extracts from NTD-DmrB cells were resolved on a 4-12% gradient Blue-Native PAGE gels. Cells were treated with Dimerizer and NSA for 16 hours. Anti-FLAG Western blotting was performed to visualize MLKL polymers.

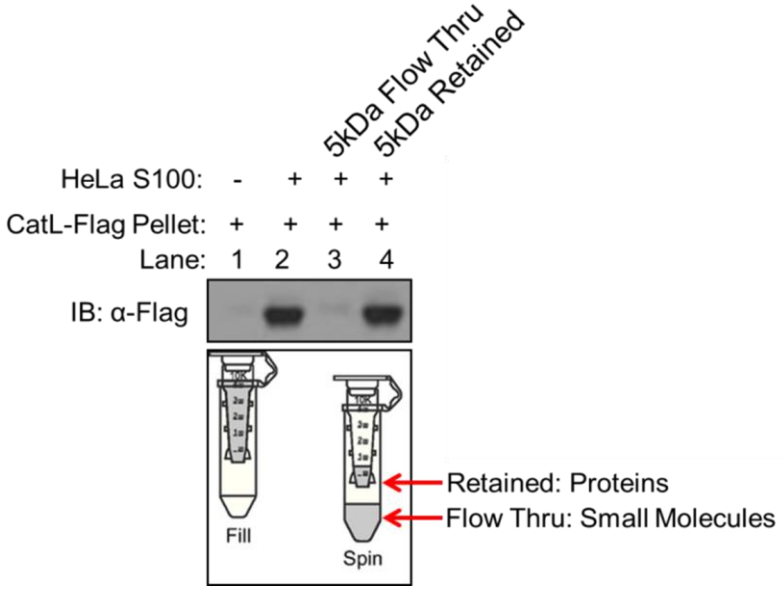

Figure 3.7 Lysosomal leakage activity in cytosolic cell extracts is retained in protein fraction. HeLa S100 extract was passed through a 5kDa protein spin column to determine whether the lysosomal leakage activity was emanating from a protein or small molecule. The retained fraction and flow through were applied to the cathepsin L leakage assay.

purification steps, it would be possible to track lysosomal leakage activity in S100 cytosolic extracts to the point that proteins could be identified by mass spectrometry. Unfortunately, at this point, the direction of this project changed due to challenges outlined in the discussion section below.

Discussion

Lysosome membrane rupture is observed during the final stages of the human necroptotic pathway, and therefore may be a critical step for executing cell death. Breakdown of lysosomal membranes causes cell death through the release of hydrolytic enzymes, such as cathepsin cysteine proteases, into the cytoplasm where they degrade vital cellular components needed for survival. However, the molecular mechanism(s) controlling lysosomal membrane disruption has remained elusive due to a lack of tools and reagents needed for studying this process. Therefore, we established an *in vitro* cathepsin L lysosomal leakage assay for identifying endogenous proteins involved in directly disrupting lysosome membrane integrity. This assay would allow us to track protein activity as we further fractionate cytosolic extracts to purify leakage factors using various biochemical techniques.

Once the identity of the proteins is discovered by mass spectrometry, cell-based loss-of-

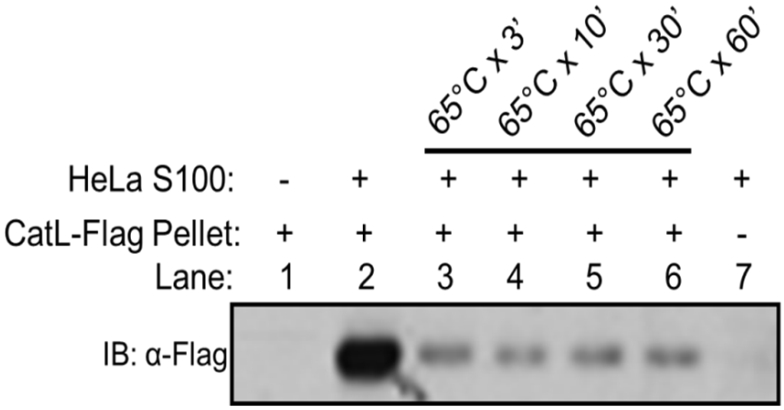

Figure 3.8 Heat treatment of cytosolic extracts decreases lysosomal leakage activity. S100 extracts were heat-treated at 65°C for the corresponding length of time, and incubated with crude P20 membrane fractions. CatL-FLAG leakage was analyzed by anti-FLAG Western blotting.

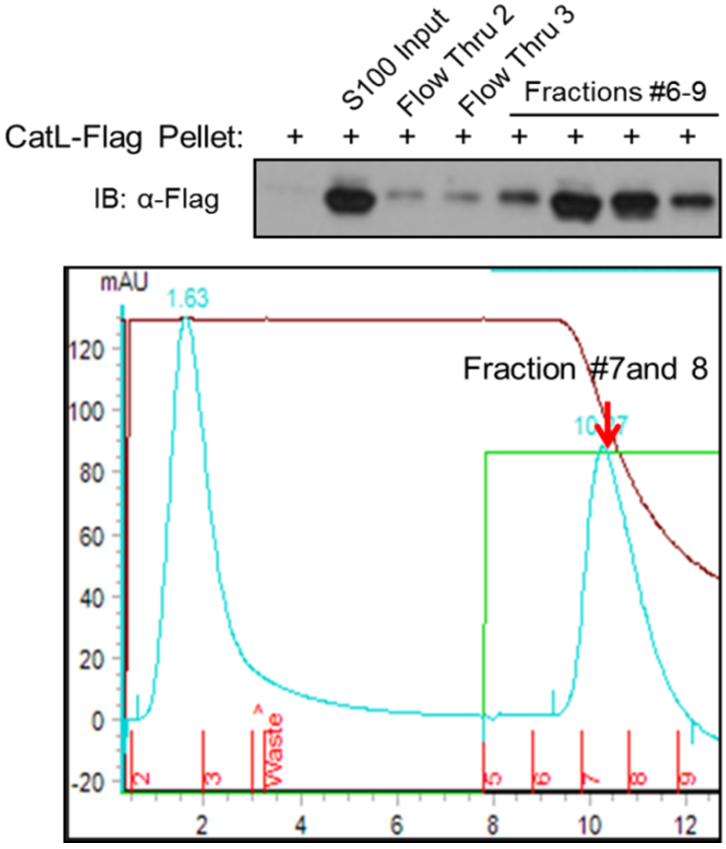

Figure 3.9 Active lysosomal leakage proteins bound to a hydrophobic interaction column (HIC). Cytosolic S100 HeLa cell extract was fractionated via a HIC column by FPLC. Eluted fractions were tested for lysosomal leakage activity using the cathepsin L

leakage assay. (Above) Anti-Flag western blot analysis of the leakage assay. (Below) HIC chromatogram of fractionated S100 cell extract.

function (i.e. siRNA-mediated knockdown) and gain-of-function (i.e. overexpression) experiments would be conducted to verify the involvement of candidate proteins in necroptosis. Unfortunately, further analysis determined that the observed leakage of CatL-FLAG was an artifact. First, lysosomal leakage activity was not specific to necroptotic cell extracts. This meant that the activity we were tracking was most likely not associated with necroptosis. More importantly, MLKL knockout extracts did not affect CatL-FLAG release which was one of the main reasons why the lysosomal leakage assay was established (data not shown). Secondly, CatL-FLAG leakage occurred almost instantly on ice indicating a lack of enzymatic activity. Lastly, stable expression of CatL-FLAG did not produce mature protease products which are attributed with proper protein processing, maturation and lysosome localization [56]. Therefore, we were unable to conclude that CatL-FLAG was leaking from lysosomes. Given these drawbacks, this project was discontinued.

References

1. Fink, S.L. and B.T. Cookson, *Apoptosis, pyroptosis, and necrosis: mechanistic description of dead and dying eukaryotic cells.* Infect Immun, 2005. **73**(4): p. 1907-16.
2. Vandenabeele, P., et al., *Molecular mechanisms of necroptosis: an ordered cellular explosion.* Nat Rev Mol Cell Biol, 2010. **11**(10): p. 700-14.
3. Ito, Y., et al., *RIPK1 mediates axonal degeneration by promoting inflammation and necroptosis in ALS.* Science, 2016. **353**(6299): p. 603-8.
4. Zhao, Q., et al., *RIPK3 Mediates Necroptosis during Embryonic Development and Postnatal Inflammation in Fadd-Deficient Mice.* Cell Rep, 2017. **19**(4): p. 798-808.

5. Zhang, T., et al., *CaMKII is a RIP3 substrate mediating ischemia- and oxidative stress-induced myocardial necroptosis.* Nat Med, 2016. **22**(2): p. 175-82.
6. Tummers, B. and D.R. Green, *Caspase-8: regulating life and death.* Immunol Rev, 2017. **277**(1): p. 76-89.
7. Feoktistova, M., et al., *cIAPs block Ripoptosome formation, a RIP1/caspase-8 containing intracellular cell death complex differentially regulated by cFLIP isoforms.* Mol Cell, 2011. **43**(3): p. 449-63.
8. Dowling, J.P., A. Nair, and J. Zhang, *A novel function of RIP1 in postnatal development and immune homeostasis by protecting against RIP3-dependent necroptosis and FADD-mediated apoptosis.* Front Cell Dev Biol, 2015. **3**: p. 12.
9. Kim, S.K., et al., *Upregulated RIP3 Expression Potentiates MLKL Phosphorylation-Mediated Programmed Necrosis in Toxic Epidermal Necrolysis.* J Invest Dermatol, 2015. **135**(8): p. 2021-30.
10. Ofengeim, D., et al., *Activation of necroptosis in multiple sclerosis.* Cell Rep, 2015. **10**(11): p. 1836-49.
11. Huang, Z., et al., *RIP1/RIP3 binding to HSV-1 ICP6 initiates necroptosis to restrict virus propagation in mice.* Cell Host Microbe, 2015. **17**(2): p. 229-42.
12. Nogusa, S., et al., *RIPK3 Activates Parallel Pathways of MLKL-Driven Necroptosis and FADD-Mediated Apoptosis to Protect against Influenza A Virus.* Cell Host Microbe, 2016. **20**(1): p. 13-24.
13. Thapa, R.J., et al., *DAI Senses Influenza A Virus Genomic RNA and Activates RIPK3-Dependent Cell Death.* Cell Host Microbe, 2016. **20**(5): p. 674-681.
14. Wang, X., et al., *Direct activation of RIP3/MLKL-dependent necrosis by herpes simplex virus 1 (HSV-1) protein ICP6 triggers host antiviral defense.* Proc Natl Acad Sci U S A, 2014. **111**(43): p. 15438-43.
15. Upton, J.W., M. Shubina, and S. Balachandran, *RIPK3-driven cell death during virus infections.* Immunol Rev, 2017. **277**(1): p. 90-101.
16. Kearney, C.J. and S.J. Martin, *An Inflammatory Perspective on Necroptosis.* Mol Cell, 2017. **65**(6): p. 965-973.
17. Kaczmarek, A., P. Vandenabeele, and D.V. Krysko, *Necroptosis: the release of damage-associated molecular patterns and its physiological relevance.* Immunity, 2013. **38**(2): p. 209-23.
18. Han, J., C.Q. Zhong, and D.W. Zhang, *Programmed necrosis: backup to and competitor with apoptosis in the immune system.* Nat Immunol, 2011. **12**(12): p. 1143-9.
19. Mocarski, E.S., J.W. Upton, and W.J. Kaiser, *Viral infection and the evolution of caspase 8-regulated apoptotic and necrotic death pathways.* Nat Rev Immunol, 2011. **12**(2): p. 79-88.
20. Cho, Y.S., et al., *Phosphorylation-driven assembly of the RIP1-RIP3 complex regulates programmed necrosis and virus-induced inflammation.* Cell, 2009. **137**(6): p. 1112-23.
21. Zhang, J., et al., *Necrosome core machinery: MLKL.* Cell Mol Life Sci, 2016. **73**(11-12): p. 2153-63.

22. Li, J., et al., *The RIP1/RIP3 necrosome forms a functional amyloid signaling complex required for programmed necrosis.* Cell, 2012. **150**(2): p. 339-50.
23. Wang, H., et al., *Mixed lineage kinase domain-like protein MLKL causes necrotic membrane disruption upon phosphorylation by RIP3.* Mol Cell, 2014. **54**(1): p. 133-46.
24. Huang, D., et al., *The MLKL Channel in Necroptosis Is an Octamer Formed by Tetramers in a Dyadic Process.* Mol Cell Biol, 2017. **37**(5).
25. Cai, Z., et al., *Plasma membrane translocation of trimerized MLKL protein is required for TNF-induced necroptosis.* Nat Cell Biol, 2014. **16**(1): p. 55-65.
26. Tanzer, M.C., et al., *Necroptosis signalling is tuned by phosphorylation of MLKL residues outside the pseudokinase domain activation loop.* Biochem J, 2015. **471**(2): p. 255-65.
27. Hildebrand, J.M., et al., *Activation of the pseudokinase MLKL unleashes the four-helix bundle domain to induce membrane localization and necroptotic cell death.* Proc Natl Acad Sci U S A, 2014. **111**(42): p. 15072-7.
28. Su, L., et al., *A plug release mechanism for membrane permeation by MLKL.* Structure, 2014. **22**(10): p. 1489-500.
29. Dondelinger, Y., et al., *MLKL compromises plasma membrane integrity by binding to phosphatidylinositol phosphates.* Cell Rep, 2014. **7**(4): p. 971-81.
30. Lu, W., et al., *Mitochondrial Protein PGAM5 Regulates Mitophagic Protection against Cell Necroptosis.* PLoS One, 2016. **11**(1): p. e0147792.
31. Chen, X., et al., *Translocation of mixed lineage kinase domain-like protein to plasma membrane leads to necrotic cell death.* Cell Res, 2014. **24**(1): p. 105-21.
32. Su, X., et al., *Necrostatin-1 ameliorates intracerebral hemorrhage-induced brain injury in mice through inhibiting RIP1/RIP3 pathway.* Neurochem Res, 2015. **40**(4): p. 643-50.
33. Duprez, L., et al., *RIP kinase-dependent necrosis drives lethal systemic inflammatory response syndrome.* Immunity, 2011. **35**(6): p. 908-18.
34. Duprez, L., et al., *Intermediate domain of receptor-interacting protein kinase 1 (RIPK1) determines switch between necroptosis and RIPK1 kinase-dependent apoptosis.* J Biol Chem, 2012. **287**(18): p. 14863-72.
35. Kaiser, W.J., et al., *Toll-like receptor 3-mediated necrosis via TRIF, RIP3, and MLKL.* J Biol Chem, 2013. **288**(43): p. 31268-79.
36. Moriwaki, K. and F.K. Chan, *Necrosis-dependent and independent signaling of the RIP kinases in inflammation.* Cytokine Growth Factor Rev, 2014. **25**(2): p. 167-74.
37. Cho, Y., et al., *RIP1-dependent and independent effects of necrostatin-1 in necrosis and T cell activation.* PLoS One, 2011. **6**(8): p. e23209.
38. Sun, L., et al., *Mixed lineage kinase domain-like protein mediates necrosis signaling downstream of RIP3 kinase.* Cell, 2012. **148**(1-2): p. 213-27.
39. Fortes, G.B., et al., *Heme induces programmed necrosis on macrophages through autocrine TNF and ROS production.* Blood, 2012. **119**(10): p. 2368-75.

40. Srikrishna, G. and H.H. Freeze, *Endogenous damage-associated molecular pattern molecules at the crossroads of inflammation and cancer.* Neoplasia, 2009. **11**(7): p. 615-28.
41. Wang, Z., et al., *The mitochondrial phosphatase PGAM5 functions at the convergence point of multiple necrotic death pathways.* Cell, 2012. **148**(1-2): p. 228-43.
42. Sun, W., et al., *Cytosolic calcium mediates RIP1/RIP3 complex-dependent necroptosis through JNK activation and mitochondrial ROS production in human colon cancer cells.* Free Radic Biol Med, 2017. **108**: p. 433-444.
43. Basit, F., et al., *Mitochondrial complex I inhibition triggers a mitophagy-dependent ROS increase leading to necroptosis and ferroptosis in melanoma cells.* Cell Death Dis, 2017. **8**(3): p. e2716.
44. Zhang, Y., et al., *RIP1 autophosphorylation is promoted by mitochondrial ROS and is essential for RIP3 recruitment into necrosome.* Nat Commun, 2017. **8**: p. 14329.
45. Tait, S.W., et al., *Widespread mitochondrial depletion via mitophagy does not compromise necroptosis.* Cell Rep, 2013. **5**(4): p. 878-85.
46. Moriwaki, K., et al., *The Mitochondrial Phosphatase PGAM5 Is Dispensable for Necroptosis but Promotes Inflammasome Activation in Macrophages.* J Immunol, 2016. **196**(1): p. 407-15.
47. Artal-Sanz, M., et al., *Lysosomal biogenesis and function is critical for necrotic cell death in Caenorhabditis elegans.* J Cell Biol, 2006. **173**(2): p. 231-9.
48. Tu, H.C., et al., *The p53-cathepsin axis cooperates with ROS to activate programmed necrotic death upon DNA damage.* Proc Natl Acad Sci U S A, 2009. **106**(4): p. 1093-8.
49. Jacobson, L.S., et al., *Cathepsin-mediated necrosis controls the adaptive immune response by Th2 (T helper type 2)-associated adjuvants.* J Biol Chem, 2013. **288**(11): p. 7481-91.
50. Brojatsch, J., et al., *Distinct cathepsins control necrotic cell death mediated by pyroptosis inducers and lysosome-destabilizing agents.* Cell Cycle, 2015. **14**(7): p. 964-72.
51. Luke, C.J., et al., *An intracellular serpin regulates necrosis by inhibiting the induction and sequelae of lysosomal injury.* Cell, 2007. **130**(6): p. 1108-19.
52. Wilson, R., et al., *Squalestatin alters the intracellular trafficking of a neurotoxic prion peptide.* BMC Neurosci, 2007. **8**: p. 99.
53. Xu, Y., et al., *Protective mechanisms of CA074-me (other than cathepsin-B inhibition) against programmed necrosis induced by global cerebral ischemia/reperfusion injury in rats.* Brain Res Bull, 2016. **120**: p. 97-105.
54. Turk, V., et al., *Cysteine cathepsins: from structure, function and regulation to new frontiers.* Biochim Biophys Acta, 2012. **1824**(1): p. 68-88.
55. Moriwaki, K., et al., *Differential roles of RIPK1 and RIPK3 in TNF-induced necroptosis and chemotherapeutic agent-induced cell death.* Cell Death Dis, 2015. **6**: p. e1636.

56. Katunuma, N., *Posttranslational processing and modification of cathepsins and cystatins.* J Signal Transduct, 2010. **2010**: p. 375345.

Chapter 4. Discussion

The relevance of necroptosis in human health has been demonstrated in a variety of *in vitro* and *in vivo* model systems [1-3]. Over the past several years, it has become increasingly clear that the primary physiological role of necroptosis is to defend against invading pathogens, and therefore necessary for survival [4, 5]. Viruses, in particular, trigger necroptosis, which clears infection in host organisms by destroying infected cells, and eliciting an inflammatory response through the release of DAMPs [6, 7]. Some viruses inhibit necroptosis as a way of evading detections and clearance [8]. Thus far, Vaccinia virus, Cytomegalovirus, Herpes Simplex Virus types 1 and 2, Influenza A virus, and Human Immunodeficiency Virus Type-1 have all been implicated in modulating necroptosis in murine and/or human experimental models [9-14]. The list of pathogens capable of controlling necroptosis is likely to grow as investigations into viral-related cell death mechanisms continues to advance. In fact, early evidence suggests that programmed forms of necrosis are triggered in response to Zika virus, a highly infectious virus that threatens the health of millions of people worldwide [15].

Efforts aimed at unraveling the molecular mechanisms that regulate necroptosis led to the identification of death receptors, TLR3/4, and RHIM-domain containing proteins TRIF, ZBP1, RIP1, and RIP3 as proteins necessary for sensing microbial-derived factors and transducing death signals in mammalian cells [6, 16-21]. These signals converge through RIP3 kinase-dependent activation of pseudokinase, MLKL, which is responsible for disrupting the plasma membrane, and remains the most reliable

necroptotic biomarker known to date [22, 23]. Mice lacking RIP3 kinase activity or MLKL are susceptible to microbial infection and die shortly after viral challenge, highlighting the importance of necroptosis in host antiviral response [1, 24]. Apart from the TNFα-induced necroptosis model (i.e. TSZ), the use of viruses will be key to uncovering novel necroptotic regulators. Viruses provide a more reliable system for studying necroptosis since they are naturally occurring infectious particles that requires no additional supplements, such as pan-caspase inhibitors (i.e. z-VAD-fmk) or Smac mimetics, to kill cells. The use of these additives is widely accepted in the field, and has helped to identify several other components of the necroptotic pathway(s); however, treatments like TSZ create an artificial scenario that does not reflect necroptosis in nature, thus giving viral-driven studies an edge in producing high impact discoveries.

However, unlike apoptosis, necroptosis is not required for proper development or tissue homeostasis [25, 26]. RIP3 or MLKL knockout mice mature to adulthood without any obvious defects. This indicates that necroptosis is held in a perpetual state of inhibition, and is only triggered in highly specific circumstances (e.g. viral infection) as to prevent excessive inflammation and tissue damage. Thus, numerous necroptotic regulatory networks have been identified, most of which also regulate apoptosis, including cIAP1/2, FADD, and caspases, particularly Caspase-8, which at basal levels, actively cleaves RIP1 and RIP3 to suppress necroptosis [27-29]. As a result, pan-caspase inhibitors are often used in combination with death-inducing stimuli to drive necroptosis *in vitro*. Certain viruses also encode caspase inhibitors to modulate necroptosis [30].

Caspase-8 or FADD knockout confers embryonic lethality in mice due to excessive necroptosis [31]. To prove that necroptosis was involved in the death of these mice, researchers were able to rescue the phenotype by genetically co-ablating RIP3 or MLKL [1, 28]. Given these findings, necroptosis remains relatively “quiet” under sterile conditions, which led to the “back-up” cell death theory. Only in situations when apoptosis fails, is bypassed, or inhibited, are alternative forms of cell death like necroptosis activated. Thus, necroptosis is thought to serve as a “back-up” to apoptosis when absolutely needed like during a viral infection. However, there are exceptions to the rule. For example, in murine L929 fibroblast cells, TNFα preferentially induces necroptosis over apoptosis [32]. Therefore, it is possible that certain cell types can undergo necroptosis more readily than others, and thus are more susceptible to death signals. Moving forward, it will be important to determine whether there is a subset of human cells that exhibit the same phenotype as L929 cells.

Although having the requisite molecular machinery for undergoing necroptosis is advantageous in fighting infection, the potential of it becoming dysregulated constantly looms in the background. Upregulated expression of RIP1, RIP3, or MLKL is thought to be a major contributing factor in the pathogenesis and progression of a broad array of human diseases, though the causes leading to these changes in gene expression are not known [33-35]. Yet, the number of necroptosis-associated diseases continues to grow with the advent of anti-phospho-RIP3/MLKL antibodies, which allow for histological studies of primary patient samples. In effect, necroptosis has been linked to

neurodegenerative diseases, inflammatory diseases, and ischemic/reperfusion injuries [25, 36, 37].

To curb the progression of these diseases, efforts have been made to identify compounds that specifically inhibit necroptosis. To this end, researchers found a class of small molecule RIP1 inhibitors known as necrostatins [38]. Nec-1 inhibits RIP1 kinase activity, and blocks necroptosis in mammalian cells grown in culture [39]. In addition to Necrostatins, there are also RIP3 kinases inhibitors (e.g. dabrafenib, GSK'872) [40, 41]. However, given that RIP1 and RIP3 play important roles in other pathways such as in NFκB signaling, inflammasome activation, and apoptosis, these compounds carry inherent risks in terms of undesired off-target effects [42-44]. Therefore, to best target necroptosis, inhibitors against MLKL should, in theory, be much more specific. This led to the discovery of NSA [45]. However, given NSA's reactivity to reactive cysteine residues, it is conceivable that it targets other proteins, and therefore may present unforeseen off-target effects. Additionally, murine MLKL lacks Cys86, so NSA cannot be tested in *in vivo* mouse models which is a considerable limitation. Other than Nec-1, effective methods for inducing or inhibiting necroptosis *in vivo* continues to be a major focus in the cell death field. Therefore, it is critical to further investigate properties of MLKL like polymer formation, its binding partners, and downstream cellular events in order to discover additional necroptotic biomarkers and potential novel therapeutic targets.

A major portion of my thesis work was focused on identifying MLKL binding partners and evaluating their effect on MLKL activity. Our research efforts led to the identification of Trx1 as a suppressor of MLKL polymerization. MLKL polymer formation is a necessary step in executing necroptosis [46]. In mammalian cells, RIP3-dependent MLKL phosphorylation leads to the formation of SDS-resistant MLKL polymers that may possess amyloid-like characteristics according to our SDD-AGE data in Chapter 2. Current models of necroptosis indicate that MLKL polymers are responsible for disrupting the integrity of the plasma membrane, and perhaps other membranous compartments as well [47]. As previously stated, membrane rupture is a major facet of the necroptotic pro-inflammatory response needed to clear invading pathogens. However, the precise mechanism by which MLKL polymers disrupt cellular membranes in not fully understood. Recent findings suggest that these polymers form pores that pierce through membranes, and act as channels that allow for an acute influx of extracellular cations, which ultimately causes cells lysis [48]. Studies show that calcium ion chelation protects certain cell types against necroptosis [49]. Alternatively, potassium ion efflux has also been proposed as an event needed for MLKL-mediated NLRP3 inflammasome activation and IL-1β pro-inflammatory cytokine processing [50]. However, there is still much debate surrounding these findings, as this appears to be a context-dependent event.

Interestingly, MLKL polymers are stabilized by intermolecular disulfide bonds, as reducing agents such as DTT and βME readily dissociate polymers *in vitro* suggesting

that MLKL requires an oxidative environment to execute necroptosis [46]. In practice, non-reducing SDS-PAGE Western blotting is often used for detecting MLKL tetramers [46]. For resolving larger megadalton size MLKL polymers, techniques such as semi-denaturing detergent agarose gel electrophoresis (SDD-AGE) provide a qualitative output for determining the occurrence of MLKL polymers in a given sample. Given that MLKL polymers are held together by intramolecular disulfide bonds, it is conceivable that MLKL is a Trx1 substrate, as Trx1 can readily reduce MLKL to block the induction of spontaneous necroptosis from occurring. Yet, the mechanistic details as to how these polymers are formed, and the role of cellular oxidation in necroptosis is not fully understood.

As stated before, ROS production has been reported during necroptotic cell death leading researchers to hypothesize that oxidation plays an important role during necroptosis [51, 52]. Given these findings, we proposed that Trx1 protects cells from undergoing necroptosis by directly exerting its oxidoreductase activity on MLKL. This is supported by our findings which demonstrate that genetic and pharmacological inhibition of Trx1 enhanced MLKL activation, as seen by polymer formation and increased sensitivity to cell death in two independent HeLa cell line model of necroptosis (NTD-DmrB and GFP-RIP3: MLKL-HA-FLAG). Surprisingly, RIP3 was dispensable for inducing necroptosis after Trx1 inhibition in NTD-DmrB expressing cells supporting the notion that Trx1 inhibition leads to direct MLKL activation. However, the presence of RIP3 may facilitate MLKL activation given that MLKL S358 phosphorylation

and RIPK1/3 necrosome recruitment was detected when Trx1 activity was inhibited by PX-12. Therefore, future studies should test whether Trx1 and MLKL directly interact with one another, and whether their interaction changes depending on the polymer status of MLKL.

As shown in Figure 2.1, insights into the nature of MLKL-Trx1 interactions emerged from NSA crosslinking experiments. NSA crosslinking Trx1 Cys32 which is located within its active site suggesting that the functional region of Trx1 mediates the interaction between MLKL. Moreover, *in vitro* HA-Trx1-6xHis binding data revealed that mutations to Trx1's active site cysteines significantly reduced its ability to bind MLKL (Figure 2.2A). Previous reports indicate that the associations between Trx1 and its substrates are relatively weak in the presence of oxidative stress [53]. It is possible that increased ROS may deactivate Trx1 activity while simultaneously promoting disulfide-bond dependent MLKL polymerization. Such an acute increase in ROS would most likely affect the glutathione system; however, given that Trx1 is an enzyme with a specific cohort of target proteins, deactivation of Trx1 would have increasingly higher consequences than those caused by perturbations to GSH. This is bolstered by the finding that MLKL is a substrate of Trx1 which preferentially interacts with monomeric MLKL suggesting that active MLKL polymers have a lower affinity for Trx1 binding, and thus lead to Trx1-MLKL dissociation as illustrated in Figure 1.1B. To better understand this phenomenon, further analysis is required to determine the precise conformational changes in MLKL that affect Trx1 binding.

Overall, these findings provide a deeper understanding of the regulatory networks that control MLKL activation. This is the first line of evidence to implicate Txr1 as a binding partner and suppressor of MLKL. Future studies will be directed towards *in vivo* validation of Trx1-MLKL interaction, and whether Trx1 inhibition induces necroptosis in tissues. Reports linking Trx1-inhibition to apoptosis in cells is well established; however, our results expand cell death outcomes induced by Trx1 inhibition to necroptosis. Furthermore, the notion that inhibition of Trx1 with PX-12 sensitizes cells to necroptosis could have significant implication in cancer therapy. PX-12 has been employed in cancer clinical trials without obvious efficacy [54]. However, our data suggest that PX-12-induced necroptosis depends on elevated levels of MLKL expression. Thus, tumors with high MLKL levels may potentially have increased sensitivity to PX-12 treatment.

Despite the advances in our understanding of necroptosis, many critical questions still remain such as 1) Is Trx1 activity suppressed in tissues marked by necroptosis? 2) Which specific ROS species and/or source of ROS is responsible for the inhibitory effect of Trx1 on MLKL? 3) Do other components of the Trx1 system such as TrxR1, or mitochondrial Trx2 or TrxR2 affect necroptotic outcomes? 4) Are other factors involved in executing necroptosis downstream of MLKL? 5) Which organelles are specifically targeted by MLKL to propagate necroptosis? In Chapter 3, we explored the possibility of lysosomes as being the targeted organelle. We detected lysosomal membrane rupture in HT-29 cells after TSZ treatment. Moreover, a cathepsin-B inhibitor, CA-074Me, partially protected cells from necroptosis, suggesting that lysosomal hydrolytic enzymes

play a role in executing cell death. However, our pursuit of establishing an *in vitro* MLKL-mediated lysosomal leakage assay was unsuccessful as we were unable to detect cathepsin leakage in a signal-dependent manner. Although our approach initially failed, we cannot rule out lysosomal leakage as a critical step in the necroptotic pathway. An alternative strategy for determining whether lysosomes are involved could be to perform a siRNA or CRISPR screen against known lysosomal enzymes and measuring the effect on necroptotic cell death. Moreover, evaluating the potential co-localization of MLKL on lysosomes by immunostaining would also be informative. In reflection upon this work, performing these experiments may yield to more conclusive results.

The goal of my thesis work was to further understand the mechanistic details that control necroptosis. Overall, this work has provided new insights into the regulation of MLKL activity and the subsequent effects on necroptosis. Our experiments have uncovered Trx1 as a negative regulator of MLKL polymerization and suppressor of necroptosis in our *in vitro* system. This research has created a foundation for future studies into the role of Trx1 in necroptosis.

References

1. Wu, J., et al., *Mlkl knockout mice demonstrate the indispensable role of Mlkl in necroptosis.* Cell Res, 2013. **23**(8): p. 994-1006.
2. Afonso, M.B., et al., *Necroptosis is a key pathogenic event in human and experimental murine models of non-alcoholic steatohepatitis.* Clin Sci (Lond), 2015. **129**(8): p. 721-39.
3. Zhou, W. and J. Yuan, *Necroptosis in health and diseases.* Semin Cell Dev Biol, 2014. **35**: p. 14-23.

4. Robinson, N., et al., *Type I interferon induces necroptosis in macrophages during infection with Salmonella enterica serovar Typhimurium.* Nat Immunol, 2012. **13**(10): p. 954-62.
5. Lamkanfi, M. and V.M. Dixit, *Manipulation of host cell death pathways during microbial infections.* Cell Host Microbe, 2010. **8**(1): p. 44-54.
6. Upton, J.W. and W.J. Kaiser, *DAI Another Way: Necroptotic Control of Viral Infection.* Cell Host Microbe, 2017. **21**(3): p. 290-293.
7. Kaczmarek, A., P. Vandenabeele, and D.V. Krysko, *Necroptosis: the release of damage-associated molecular patterns and its physiological relevance.* Immunity, 2013. **38**(2): p. 209-23.
8. Guo, H., et al., *Herpes simplex virus suppresses necroptosis in human cells.* Cell Host Microbe, 2015. **17**(2): p. 243-51.
9. Veyer, D.L., et al., *Vaccinia virus evasion of regulated cell death.* Immunol Lett, 2017. **186**: p. 68-80.
10. Omoto, S., et al., *Suppression of RIP3-dependent necroptosis by human cytomegalovirus.* J Biol Chem, 2015. **290**(18): p. 11635-48.
11. Huang, Z., et al., *RIP1/RIP3 binding to HSV-1 ICP6 initiates necroptosis to restrict virus propagation in mice.* Cell Host Microbe, 2015. **17**(2): p. 229-42.
12. Yu, X., et al., *Herpes Simplex Virus 1 (HSV-1) and HSV-2 Mediate Species-Specific Modulations of Programmed Necrosis through the Viral Ribonucleotide Reductase Large Subunit R1.* J Virol, 2015. **90**(2): p. 1088-95.
13. Xu, Y.L., et al., *RIP3 deficiency ameliorates inflammatory response in mice infected with influenza H7N9 virus infection.* Oncotarget, 2017. **8**(17): p. 27715-27724.
14. Pan, T., et al., *Necroptosis takes place in human immunodeficiency virus type-1 (HIV-1)-infected CD4+ T lymphocytes.* PLoS One, 2014. **9**(4): p. e93944.
15. Cugola, F.R., et al., *The Brazilian Zika virus strain causes birth defects in experimental models.* Nature, 2016. **534**(7606): p. 267-71.
16. Dondelinger, Y., et al., *Poly-ubiquitination in TNFR1-mediated necroptosis.* Cell Mol Life Sci, 2016. **73**(11-12): p. 2165-76.
17. Jouan-Lanhouet, S., et al., *TRAIL induces necroptosis involving RIPK1/RIPK3-dependent PARP-1 activation.* Cell Death Differ, 2012. **19**(12): p. 2003-14.
18. LaRocca, T.J., et al., *CD59 signaling and membrane pores drive Syk-dependent erythrocyte necroptosis.* Cell Death Dis, 2015. **6**: p. e1773.
19. Kearney, C.J., et al., *Necroptosis suppresses inflammation via termination of TNF- or LPS-induced cytokine and chemokine production.* Cell Death Differ, 2015. **22**(8): p. 1313-27.
20. Takemura, R., et al., *PolyI:C-Induced, TLR3/RIP3-Dependent Necroptosis Backs Up Immune Effector-Mediated Tumor Elimination In Vivo.* Cancer Immunol Res, 2015. **3**(8): p. 902-14.
21. Kaiser, W.J., et al., *Toll-like receptor 3-mediated necrosis via TRIF, RIP3, and MLKL.* J Biol Chem, 2013. **288**(43): p. 31268-79.
22. He, S., S. Huang, and Z. Shen, *Biomarkers for the detection of necroptosis.* Cell Mol Life Sci, 2016. **73**(11-12): p. 2177-81.

23. Zhang, J., et al., *Necrosome core machinery: MLKL.* Cell Mol Life Sci, 2016. **73**(11-12): p. 2153-63.
24. Wang, X., et al., *Direct activation of RIP3/MLKL-dependent necrosis by herpes simplex virus 1 (HSV-1) protein ICP6 triggers host antiviral defense.* Proc Natl Acad Sci U S A, 2014. **111**(43): p. 15438-43.
25. Weinlich, R., et al., *Necroptosis in development, inflammation and disease.* Nat Rev Mol Cell Biol, 2017. **18**(2): p. 127-136.
26. Rickard, J.A., et al., *RIPK1 regulates RIPK3-MLKL-driven systemic inflammation and emergency hematopoiesis.* Cell, 2014. **157**(5): p. 1175-88.
27. McComb, S., et al., *cIAP1 and cIAP2 limit macrophage necroptosis by inhibiting Rip1 and Rip3 activation.* Cell Death Differ, 2012. **19**(11): p. 1791-801.
28. Zhao, Q., et al., *RIPK3 Mediates Necroptosis during Embryonic Development and Postnatal Inflammation in Fadd-Deficient Mice.* Cell Rep, 2017. **19**(4): p. 798-808.
29. Tummers, B. and D.R. Green, *Caspase-8: regulating life and death.* Immunol Rev, 2017. **277**(1): p. 76-89.
30. Moriwaki, K. and F.K. Chan, *RIP3: a molecular switch for necrosis and inflammation.* Genes Dev, 2013. **27**(15): p. 1640-9.
31. Liu, Y., et al., *RIP1 kinase activity-dependent roles in embryonic development of Fadd-deficient mice.* Cell Death Differ, 2017.
32. Vanlangenakker, N., et al., *TNF-induced necroptosis in L929 cells is tightly regulated by multiple TNFR1 complex I and II members.* Cell Death Dis, 2011. **2**: p. e230.
33. Pierdomenico, M., et al., *Necroptosis is active in children with inflammatory bowel disease and contributes to heighten intestinal inflammation.* Am J Gastroenterol, 2014. **109**(2): p. 279-87.
34. Ito, Y., et al., *RIPK1 mediates axonal degeneration by promoting inflammation and necroptosis in ALS.* Science, 2016. **353**(6299): p. 603-8.
35. Kim, S.K., et al., *Upregulated RIP3 Expression Potentiates MLKL Phosphorylation-Mediated Programmed Necrosis in Toxic Epidermal Necrolysis.* J Invest Dermatol, 2015. **135**(8): p. 2021-30.
36. Zhao, H., et al., *Role of necroptosis in the pathogenesis of solid organ injury.* Cell Death Dis, 2015. **6**: p. e1975.
37. Liu, S., et al., *Necroptosis mediates TNF-induced toxicity of hippocampal neurons.* Biomed Res Int, 2014. **2014**: p. 290182.
38. Degterev, A., et al., *Identification of RIP1 kinase as a specific cellular target of necrostatins.* Nat Chem Biol, 2008. **4**(5): p. 313-21.
39. Xie, T., et al., *Structural basis of RIP1 inhibition by necrostatins.* Structure, 2013. **21**(3): p. 493-9.
40. Li, J.X., et al., *The B-Raf(V600E) inhibitor dabrafenib selectively inhibits RIP3 and alleviates acetaminophen-induced liver injury.* Cell Death Dis, 2014. **5**: p. e1278.
41. Mandal, P., et al., *RIP3 induces apoptosis independent of pronecrotic kinase activity.* Mol Cell, 2014. **56**(4): p. 481-95.

42. Meylan, E., et al., *RIP1 is an essential mediator of Toll-like receptor 3-induced NF-kappa B activation.* Nat Immunol, 2004. **5**(5): p. 503-7.
43. Wang, X., et al., *RNA viruses promote activation of the NLRP3 inflammasome through a RIP1-RIP3-DRP1 signaling pathway.* Nat Immunol, 2014. **15**(12): p. 1126-33.
44. Ofengeim, D. and J. Yuan, *Regulation of RIP1 kinase signalling at the crossroads of inflammation and cell death.* Nat Rev Mol Cell Biol, 2013. **14**(11): p. 727-36.
45. Sun, L., et al., *Mixed lineage kinase domain-like protein mediates necrosis signaling downstream of RIP3 kinase.* Cell, 2012. **148**(1-2): p. 213-27.
46. Huang, D., et al., *The MLKL Channel in Necroptosis Is an Octamer Formed by Tetramers in a Dyadic Process.* Mol Cell Biol, 2017. **37**(5).
47. Wang, H., et al., *Mixed lineage kinase domain-like protein MLKL causes necrotic membrane disruption upon phosphorylation by RIP3.* Mol Cell, 2014. **54**(1): p. 133-46.
48. Cai, Z. and Z.G. Liu, *Execution of RIPK3-regulated necrosis.* Mol Cell Oncol, 2014. **1**(2): p. e960759.
49. Sun, W., et al., *Cytosolic calcium mediates RIP1/RIP3 complex-dependent necroptosis through JNK activation and mitochondrial ROS production in human colon cancer cells.* Free Radic Biol Med, 2017. **108**: p. 433-444.
50. Conos, S.A., et al., *Active MLKL triggers the NLRP3 inflammasome in a cell-intrinsic manner.* Proc Natl Acad Sci U S A, 2017. **114**(6): p. E961-e969.
51. Fulda, S., *Regulation of necroptosis signaling and cell death by reactive oxygen species.* Biol Chem, 2016. **397**(7): p. 657-60.
52. Zhang, Y., et al., *RIP1 autophosphorylation is promoted by mitochondrial ROS and is essential for RIP3 recruitment into necrosome.* Nat Commun, 2017. **8**: p. 14329.
53. Arner, E.S. and A. Holmgren, *Physiological functions of thioredoxin and thioredoxin reductase.* Eur J Biochem, 2000. **267**(20): p. 6102-9.
54. Baker, A.F., et al., *A phase IB trial of 24-hour intravenous PX-12, a thioredoxin-1 inhibitor, in patients with advanced gastrointestinal cancers.*

Materials and Methods

Reagents

Recombinant human TNFα, Smac-mimetic and anti-human RIPK3 antibody were prepared as previously described (He et al., 2009). The following reagents and antibodies were used: z-VAD-fmk (ApexBio), CA-074me (Calbiochem), Necrostatin-1 (Calbiochem), Necrosulfonamide (Millipore), Dimerizer (Clontech, 635058), Anti-Flag M2 antibody and affinity gel (Sigma), Anti-human MLKL (Genetex, GTX107538), Anti-mouse MLKL (Aviva Systems Biology, OAAB10571), Anti-phospho-MLKL S358 (Abcam, ab187091), Anti-RIPK1 (BD, 551042), Anti-LDH (Abcam, ab53292). Reagent concentrations for T/S/Z-induced necroptosis: 2ng/ml TNF, 10nM Smac-mimetic, and 20μM z-VAD-FMK. Concentrations for Dimerizer-induced necroptosis: 20nM Dimerizer and 20 μM z-VAD-FMK. Compound concentrations: 10μM Necrostatin-1, 5μM Necrosulfonamide, 1mM CA-074me. Cells were generally treated for 16 hours prior to cell death analysis.

Cell Culture and Stable Cell Lines

HT-29 and HeLa cells were cultured in DMEM (high glucose) supplemented with 10% fetal bovine serum and 1% Penicillin/Streptomycin. All HeLa stable lines were generated in previously reported HeLa-TetR cells which express Tet repressor (TetR) [1]. (1) *MLKL KO* HeLa line. *MLKL KO* cells were established in a HeLa-TetR background according to the protocol described in Cong et al., 2013 [2]. Briefly, oligo

targeting human MLKL with the sequence GCTGCCCTGGAGGAGGCTAATGG was cloned into the gRNA vector. gRNA vector was co-transfected with a Cas9 expressing vector in HeLa-TetR cells. MLKL knockout was confirmed by Western blotting and sequencing. (2) NTD-DmrB-FLAG cells. NTD-DmrB contains amino acids 1-190 of human MLKL fused to a DmrB domain with a C-terminal 3XFlag. NTD-DmrB is driven by a doxycycline inducible promoter. This construct was stably expressed in the MLKL knockout HeLa cells. (3) GFP-RIPK3: MLKL-HA-FLAG line. Doxycycline-inducible GFP-RIPK3 and MLKL-HA-3XFlag were stably expressed in the MLKL knockout HeLa cells. Protein expression was achieved through the addition of 50ng/mL doxycycline for 24 hours.

Mass spectrometric analysis

Mass spectrometric analysis was performed as previously described [1]. Briefly, protein band was excised, de-stained, and reduced followed by in gel trypsin digestion. The peptides were extracted and analyzed by a QSTAR XL mass spectrometer (AB Sciex, CA, USA).

Plasmid DNA Transfection

Cells were seeded in 10 cm dishes with complete media at a final confluency of ~60-70% 24 hours before performing the transfection. Plasmid DNA and Polyjet In Vitro Transfection Reagent (SignaGen Laboratories) were incubated in Dulbecco's Modified Eagle's Medium (DMEM) at a ratio of 3:1 as recommended in the manufacturer's

protocol. Culture media was replaced with fresh complete media the following day. Cells were harvested 72 hours post-transfection.

Protein Extraction and Western blotting

Cells were scraped and washed in ice-cold PBS prior to lysing them in Protein Extraction Buffer (PEB) comprised of 20mM Tris pH7.4, 150mM NaCl, 0.5% Triton X-100, 10% glycerol, and freshly added protease and phosphatase inhibitors. Cells were rotated at 4°C for 15 minutes before being centrifuged at 20,000xg for 20 minutes to clear out insoluble debris. Protein concentrations were determined by Coomassie Plus Protein Assay Reagent (Thermo Scientific). Samples were boiled in 5X SDS sample buffer (250mM Tris pH6.8, 5% beta-mercaptoethanol, 0.02% bromophenol Blue, 30% glycerol, 10% SDS) for 5 minutes, resolved by SDS-PAGE, and transferred onto PVDF membranes (Bio-Rad). Membranes were incubated in 5% Blotting-Grade Blocker (Bio-Rad) reconstituted in phosphate buffered saline (PBS) solution with 0.1% Tween-20 (PBS-T). Primary and secondary HRP antibodies were also diluted in 5% PBS-T milk solution.

Immunoprecipitation assay

Protein samples were diluted to a final concentration of 1mg/mL in 1mL of PEB containing freshly added protease and phosphate inhibitors. Samples were incubated with 10µL FLAG(M2)-agarose beads (Sigma-Aldrich), and rotated overnight at 4°C. M2-beads were washed with 1mL ice-cold extraction buffer 3 times, and directly boiled in

1X SDS sample buffer. Isolated protein complexes were resolved by SDS-PAGE Western blotting. Silver staining was performed using ProteoSilver Plus Silver Stain kit (Sigma Aldrich).

Cell Survival Assay

Cell survival was measured using CellTiter-Glo Luminescent Cell Viability Assay according to the manufacturer's protocol (Promega). Cells were seeded at $1x10^3$ cells/well in white flat-bottom 96-well plates (Corning) 24 hours prior to treatment. Luminescence was measured using a BioTek Synergy 2 plate reader.

Semi-Denaturing Detergent Agarose Gel Electrophoresis (SDD-AGE)

SDD-AGE gels were made using TAE buffer (40mM Tris pH8.6, 20mM acetate, 1mM EDTA) containing 1% agarose (Denville Scientific Inc.) and 0.1% SDS (Bio-Rad). Protein samples were mixed with 4X sample buffer (2X TAE buffer, 20% glycerol, 8% SDS) at room temperature, and run at a constant 60V for 5 hours in TAE buffer containing 0.1% SDS. Proteins were transferred onto PVDF membranes by capillary action using TBS buffer (20mM Tris pH7.4, 150mM NaCl). Membranes were treated in accordance with the Western blotting procedure.

Protein Purification

Recombinant proteins were purified from Rosetta DE3 bacterial cells grown in LB media (0.5L culture volume). Cultures were grown to an O.D.600 of 0.6 at 37°C prior to IPTG

induction (0.1mM IPTG final concentration). Cultures were shifted to a temperature of 18°C, and allowed to grow for 16 hours. The bacteria were pelleted by centrifugation at 3,000xg for 10 minutes, washed once in ice-cold PBS and re-pelleted before being resuspended in 40mL binding buffer. For HA-Trx1-6xHis, binding buffer contained 20mM Tris pH8.0, 150mM NaCl, 0.1% Triton X-100, 10% glycerol, 20mM imidazole, 10mM beta-mercaptoethanol, 1mM PMSF, EDTA-free protease inhibitor cocktail. Cells were lysed by sonication pulsing 15 times for 30 seconds each time. Lysates were centrifuged at 10,000xg for 20 minutes and filtered before incubation with 100µL Ni-NTA agarose beads (Qiagen). Binding was performed at 4°C for 30 minutes. Nickel beads were washed 3 times in binding buffer lacking beta-mercaptoethanol. To elute HA-Trx1-6xHis, 250mM imidazole was added to the binding buffer. 100uL fractions were collected, and dialyzed against PBS.

For recombinant GST-NTD-FLAG, 100uL Glutathione agarose beads (Pierce) were used following the previously stated procedure with binding buffer containing 20mM Tris pH7.4, 150mM NaCl, 0.1% Triton X-100, 10% glycerol, 5mM DTT, 1mM PMSF, EDTA-free protease inhibitor cocktail. GST-NTD-FLAG was eluted in 100uL fractions with binding buffer containing 10mM reduced L-glutathione at pH8.0. Positive GST-NTD-FLAG fractions were consolidated and dialyzed against PBS.

Cell staining

HeLa NTD-DmrB and GFP-RIPK3: MLKL-HA-FLAG cells were seeded at $1x10^5$

cells/well in a 12-well plate (Cellstar). Sytox Green and Hoechst dyes were added directly to culture media at 1 µM and incubated for 10 minutes prior to imaging. A BioTek Cytation 3 plate reader was used to capture images at 40X magnification.

In vitro GST-NTD-FLAG polymerization assay

Recombinant GST-NTD-FLAG was used at a final concentration of 5 µM in 20µL of PBS. To induce polymerization, samples were incubated at 37°C for 16 hours. 50 ng of GST-NTD-FLAG was used for anti-FLAG SDD-AGE immunoblotting. HA-Trx1-6xHis was used at a final concentration of 3 µM, 10 µM, and 30 µM. 1mM DTT was used as a positive control.

Trx1 shRNA knockdown

Trx1 shRNA lentivirus was produced by transfecting HEK293T cells with pTY-Trx1shRNA-EF1a-HygromycinB-2A-IRES-GFP-3XFLAG (ADDGENE), pMD2.G, and psPAX2 vectors in a 10cm plate. The Trx1 shRNA sense strand primer sequence is as following:

GATCCCCGTGTGAAGTCAAATGCATGTTCAAGAGACATGCATTTGACTTCACACTT TTTA. The Trx1 anti-sense strand is: AGCTTAAAAAGTGTGAAGTCAAATGCATGTCTCTTGAACATGCATTTGACTTCACAC GGG. Lentiviral media was collected at 48 hours and 72 hours post-transfection, filtered through a 0.45 µm sterile filter, and stored at -80°C. Lentiviral transduction of GFP-RIPK3: MLKL-HA-FLAG cells was performed by seeding cells at $1x10^5$ cells/well in a 6-

well plate. Cells were provided with 1 mL complete media with 1 mL of lentiviral media supplemented with 5 µg/mL polybrene. The following day, cells were trypsinized and seeded at $1x10^5$ cells/well in a 6-well plate with media containing 0.2 µg/mL Hygromycin B. Surviving cells were thereafter expanded, and utilized for downstream experiments after validating Trx1 knockdown.

In vitro NTD-DmrB oligomerization assay

Cytosolic S100 extracts were prepared form NTD-DmrB-FLAG expressing cells using the protocol described in the CatL-FLAG lysosome leakage section. To induce DmrB-mediated NTD polymerization, S100 extracts were spiked with 10nM Dimerizer followed by a 3-hour incubation at 30°C. Samples were then mixed with sample buffer, and subjected to Blue-Native PAGE (BN-PAGE) anti-FLAG Western blotting. Proteins were resolved on a 4-12% BN-PAGE gradient gel. All buffer and reagents used were prepared in accordance with the Blue-Native-PAGE protocol described in Fiala et al, 2011 [3].

Cathepsin L-FLAG lysosome leakage assay

Assay substrate: Crude membrane fraction (P20) prepared from HeLa cells stably expressing a FLAG-tagged cathepsin-L transgene (CatL-FLAG). Cells harvested from a confluent 10cm plate were resuspended in ice-cold hypotonic buffer (20mM Tris Ph7.4, 10mM $MgCl_2$, 250mM sucrose, 1mM EDTA) for 30 minutes on ice. Cells lysis was performed by passing cells through a 22G needle 20 times. Lysates were subjected to a

5-minute 500xg centrifugation step to clear out unbroken cells. The supernatant containing the lysosomal fraction were then re-spun at 20,000xg for 30 minutes. The supernatant was removed, and the remaining P20 fraction was washed 3 times before being resuspended in ice-cold isotonic buffer (20mM Tris Ph7.4, 150mM NaCl, 250mM sucrose, 1mM EDTA). P20 fractions were uses immediately after the final resuspension step.

Active/Experimental fraction: Cytosolic fraction (S100) from HT-29 cells. Cells were resuspended and lysed in ice-cold hypotonic buffer as described above. Lysates were centrifuged at 100,000xg for 30 minutes, and the supernatant was taken for use in the assay.

Assay setup: 5µg of the CatL-FLAG P20 fraction was mixed with 50µg of S100 fraction in a final volume of 20µL. Samples were incubated at 30°C for 3 hours to allow for lysosome membrane breakdown. CatL-FLAG release was monitored by subjecting the soluble fraction to SDS-PAGE Western blotting probed against the FLAG epitope.

References

1. Wang, Z., et al., *The mitochondrial phosphatase PGAM5 functions at the convergence point of multiple necrotic death pathways.* Cell, 2012. **148**(1-2): p. 228-43.
2. Cong, L., et al., *Multiplex genome engineering using CRISPR/Cas systems.* Science, 2013. **339**(6121): p. 819-23.
3. Fiala, G.J., W.W. Schamel, and B. Blumenthal, *Blue native polyacrylamide gel electrophoresis (BN-PAGE) for analysis of multiprotein complexes from cellular lysates.* J Vis Exp, 2011(48).

Acknowledgements

First and foremost, I would like to thank my thesis mentor, Dr. Zhigao Wang, for all the support and one-on-one training you provided over the past four years. I truly appreciate you allowing me to follow my own lines of scientific investigations, and giving me, the level of independence needed for me to grow as a researcher. It was a pleasure working under your direction. I am confident that whatever career path I take in the future, I will be successful due in large part to your mentorship, and for that, I am incredibly grateful.

I also want to thank the rest of the Wang lab members, Dr. Shuzhen Liu, Dr. Yougui Xiang, Dr. Hua Liu, Hong Yu, Andrea Johnston, and Sarah Addams, for being such helpful and pleasant people to work with. I think we all realized after a while that necroptosis research was not going to be easy, but we hung in there, fought hard, and made it happen to the best of our abilities. All of you were so easy to work with which made doing research in the Wang lab such an enjoyable experience.

I want to thank my committee members, Drs. John Abrams, James Amatruda, and Zhijian “James” Chen, for all of your scientific input, recommendation letters, and ultimately helping me drive this Ph.D. degree home. Dr. James Chen, thank you for allowing me access to your lab’s plentiful resources and co-sponsoring my NIH F31 fellowship. John Abrams, thank you for all of your experimental and professional support. You listened to my concerns, and always pointed me in the right direction. And

James Amatruda, thank you for being such a receptive and understanding committee chair. To all of you, thank you.

All of this would not be possible without my undergraduate research training which I received from Dr. Jean Y.J. Wang and Dr. Gabriel Pineda at UC San Diego. Thank you for supporting my efforts in getting into graduate school whole heartedly, and provided me with the requisite training and skills needed to be a successful student. With your help, I was able to hit the bench running from day one. In the same regards, I also want to thank Dr. Nancy Street for giving me the opportunity to come to UTSW. I know I was not the best student on paper, but you believed in me and gave me a shot when others did not. You were always there when I needed guidance, be it emotional or otherwise, you played a big part in getting me in and through graduate school in one piece.

I would also like to give a huge thank you to the entire Department of Molecular Biology and the Genes, Development and Disease family, especially Drs. Thomas Carroll, Ondine Cleaver, Michael Buszczak, and Peter Douglas. I want to thank all of you for your support in sharing invaluable life/career advice with me. I also want to thank all of my colleagues at UTSW who made my graduate school experience truly special. Thank you sharing your science, and making these past five years ones to remember. I could not have done it without your support and friendship.

I would be remiss if I did not give a huge shout out to Dr. Michael Dellinger for being a source of immense scientific wisdom that I could tap into anytime I needed to. Thank you for all of the good times, jam sessions, skate sessions, for treating me like a scientist, and for just being a such a great person that I could always rely on. Thank you, my friend.

I also want to thank my entire family back home in California. Thank you for giving me strength during these past five years. And to all my Dallas friends, thank you for making my time in Texas special. In the toughest of times, I knew I could count on you guys to get me through the day. You were there for the good times and the bad. My time in Dallas would not have been the same without you. Sincerely, thank you for your friendship.

Lastly, I want to give the biggest thanks to my one and only partner in crime, Mary Topalovski. Thank you for sharing your life with me. These past five years have been such a whirlwind, and with you by my side, they have been the greatest of my life. Thank you for always being there, for being such an integral part of this whole process from start to finish, for truly understanding me as a person, and for us, the story of our lives has only just begun.